Doctoral School in Environmental Engineering

The influence of redox dynamics on nitrogen cycling and nitrous oxide emissions from soils

Simonetta Rubol

UNIVERSITÀ DEGLI STUDI DI TRENTO
Dipartimento di Ingegneria Civile e Ambientale

2010

Doctoral thesis in Environmental Engineering, XXI cycle

Faculty of Engineering, University of Trento

Academic year: 2008 - 2009

Supervisors:
Prof. Alberto Bellin, Università degli Studi di Trento
Prof. Gianni Andreottola, Università degli Studi di Trento
Prof. Whendee Silver,University of California, Berkeley, USA

Cover photograph:
The Waggon Tracks, Miró 1918.

Università degli Studi di Trento

Trento, Italy

March 2010

In memory of my mom Fiorella Raffaelli Rubol,
to my family and
to the Ray of sun which every day enlightens my window.

Acknowledgements

The present work has been done under the supervision of Prof. Alberto Bellin, Prof. Gianni Andreottola and Prof. Whendee Silver. I am really grateful to each one of them. Their help and support was crucial for the development of this dissertation. Each one of them, in different stages of my work, has been source of inspiration and an example from the professional and the human point of view.

In particular, I want to thank my former advisor Prof. Alberto Bellin for challenging himself in a topic which is border line with his research line. He encouraged me in the dark moments and his kindness and gentle manners helped me keep motivated. It has been a pleasure to have the possibility to learn form him during these years!

I am also thankful towards Prof. Gianni Andreottolla, for helping me with better understanding of the nitrogen cycle and for being always optimistic. His never ending curiosity motivated and inspired me to learn more.

I am especially grateful to Prof. Whendee Silver, at the University of California, Berkeley, who opened me her laboratory and her house as I were a family member and accepted to advice my work. Berkeley is a magic place and Whendee made me feel welcomed and part of the her group during all my staying. I will never forget this experience and her example, as a strong and energetic person in life and science, while at the same time being a very sweet and caring person. Whendee give me the possibility to discover and learn so much, that I will never be able to express in words my gratitude!

I am also thankful to Dr. Elizabeth Baggs, who guest me in her laboratory at the University of Aberdeen, UK to perform diffusion and gas samples analysis and providing useful hint to my research.

I am also grateful to all in the Whendee Silver's laboratory during my stay in 2007-2008: Thanks to Becca Ryals, Wendy Chou, Daniela Cusack, Tana Wood, Marissa Lafler, Daniel Lipzing, Erika Marin Spiotta, Steven Hall. In particular, I would like to thank Andy Thompson, Yit Arn Teh and Wendy Yang which, with lots of patience guiding me through the lab, the calculation, the use of the mass spectrometer and the Lachat! I will never forget how much you all did for me! These people helped me a lot with the experimental part. It was not easy coming from an engineering background and to learn so many new things from ecologists. Also, I want to thank Todd Dawson for letting me attend the isotope course in Berkeley and Stefania Mambelli for being so protective and nice to me during my staying in Berkeley!

I am grateful to Prof. Mary Firestone, Prof. Dennis Badocchi, Prof. Gary Sposito, Prof. James Hunt, and Prof. Celine Pallud for the valuable conversations in my research. My

sincere acknowledgment goes to Prof. Michael Riemer, for being interested in my work and being extremely kind to help me in some soil analysis! I am very thankful to Don Herman: He never get mad at me when I had trouble with Lachat. I thank him for always being very patient and kind in explaining the pool dilution technique and the use of the mass-spectrometer. Also, I would like to thank all the nice persons I met at ESPM (University of California, Berkeley) and especially to: Sarah Placella, Steven J Blazewicz, Jennifer Petty Ridge, Rodrigo Vargas, Oliver Sonnentag, Ben Runkle, Joe Verfaillie, Federico Maggi, Matteo Detto, Silvano Fares, Alessandro Montaghi, Karelyn Cruz Martinez, Cahtee Pham and Chlow Lewis. I want also to thank the IISA and the Italian community I met in Berkeley.

I am very thankful to all the professors, researcher and PhD student I met and in NitroEurope and which provide me useful information about literature review and N-cycle in soil.

I am very thankful to Dr. Stefano Manzoni and Prof. Amilcare Porporato for the help and exchange of idea in developing the modeling part. It is very exciting for me to have the opportunity to work with them!

I am thankful to Prof. Joshua Shimel, Prof. Erik Davidson, Prof. Jam Galloway Prof. Franz Meixner, Prof. Jirka Simunek and Prof. Timothy Clough, Prof. Riccardo Ceccato and Dr. Lorenzo Tognana for their comments and suggestions.

I am especially thankful to Mauro Bortolotti and to Nicola Tondini: They helped share the Berkeley experience from a Trentino perspective! Mauro was a fantastic friend and housemate. I want also to thank my house-mates in Trento, Cristina Mattiucci and Alessandra Marzadri, for sharing bad and good moments and all the Bellin group, in particular to Oscar Cainelli. I am very thankful also to the PhD students of the XXI and XXII and XXIII cycle who were close to during these years and all the person which in different moment helped me; in particular, I want to thank Marco Ranzato, Federica Maino and Franceso Orsi.

I want to thank Lorenzo Forti for the construction of the column, Laura Martuscelli for her efficiency, all the professors of DICA, my office-mates and Elena Huber for creating a very conformable working environment.

I am thankful to Corrado Pellachini, a true friend and to my ”fake” sisters Simona Corrado, Carla Tranquillini and Carlotta Borghetti and their families for always being close to me despite distances.

My special acknowledgement goes to Felipe Pereira Jorge de Barros, a true angel, for his love, help, support, for always putting me before his work and for pushing me to ”go for

it!" when I was about to break down. If very hard to express in few words how important it was having him close to me.
My thoughts also goes to my father Adriano and to my brothers, Roberto and Lorenzo which have been a true support in the sad moments, bringing me back to "real" life.
Finally, I want to thank the European Science Foundation for granting my visiting period at the University of California, Berkeley, and at the University of Aberdeen.

Contents

List of Figures

List of Tables

Abstract

Soils are a dominant source of nitrous oxide (N_2O), a potent greenhouse gas. The complexity of drivers of N_2O production and emissions has hindered our ability to predict the magnitude and spatial dynamics of N_2O fluxes. Soil moisture can be considered a key driver because it influences oxygen supply, which feeds back on N_2O sources (nitrification versus denitrification) and sinks (reduction to dinitrogen). Soil volumetric water content is directly linked to dissolved oxygen and to redox potential, which regulate microbial metabolism and chemical transformations in the environment. The relationship between soil moisture and N_2O is usually based on incubations of soil at different soil moisture levels. Few studies have focused on the interaction between soil moisture and nitrogen dynamics in the vadose zone.

In this thesis soil column and chamber experiments were performed in order to investigate the relationship of soil moisture dynamics to redox sensitive nitrogen dynamics in the organic matter layer of a pasture peatland in Sacramento, Bay Delta area, California.

Field data has been canalized and statistics has been used to evaluate the influence of irrigation practices on spatial pattern of measurements.

The relationship of nitrous oxide versus water content was reproduced by using a lumped model which include oxygen dynamic. Data indicate that organic peatland might be an important source of nitrous oxide emissions.

The comparison of rainfall, saturation and deposition shown that trace gases emissions, dissolved nitrate and ammonium changed considerably along the soil column profile as a response of the microbial community to the high variability in redox, soil moisture, oxygen experienced by the soil at different depth. Water movement favored the formation of zones at different redox condition, redistributed the nutrient along the soil profile, and considerably changed mineralization, nitrification and dissimilatory reduction to nitrate (DNRA) rates. It was observed a asymmetrical behavior between nitrogen and ammonium profiles. Experiments shown that this assimetry is a function of the degree of saturation (as well as its duration). Also the fraction of the total N_2O that is actually emitted to the atmosphere depends heavily on the structure and wetness of the soil.

The nitrous oxide dynamic is therefore a function of the antecedent wetness condition, the nutrient content of the peat-land, the physical characteristics of the peat-land and the vertical stratification of layers at different redox and oxygen condition, which may affect the annual N budget. In addition, the combined use of soil column and chamber experiments

suggest a negative correlation between soil moisture and N_2O in dynamic condition and a functional dependence of N_2O emissions from the oxygen concentration. We found that the time scale of water dynamic was faster than the biological scale of trace gas emissions. Finally, a lumped model has been developed to reproduce the bacteria response to changes in soil moisture. Preliminary results suggest that by accounting for oxygen dynamic, it is possible to reproduce the functional behavior observed in the experiment and that the latter is depending on the physical and biological properties of the soil.

Keywords: water dynamic, nitrous oxide emissions, dissimilatory nitrate reduction to ammonium, feammox, denitrification,soil heterogeinty, oxygen, redox.

1 Introduction

Nitrogen compound and fertilizers are widely used in the agricultural and the industrial sectors. They are also major sources of eutrophication in water bodies and nitrous oxide (N_2O) emissions (Reay, 2003). Understanding how nitrous oxides are formed and transported in the unsaturated zone is a challenge and of importance to many environmental issues. The challenge rises given the complexity of the driving forces and biogeochemical activity that produces N_2O fluxes. In addition to this, processes that take place in the unsaturated zone are highly non-linear.

It is known that soil moisture can be considered a key driver in emitting N_2O. This is because soil moisture influences oxygen supply, which feeds back on N_2O sources (e.g. nitrification versus denitrification) and sinks (reduction to N_2). Soil water content is directly linked to dissolved oxygen and to redox potential, which regulates microbial metabolism and chemical transformations in the environment. Moreover, precipitation generally drives rapid changes in soil moisture and this change consequently affects the redox-sensitive nitrogen transformations. The importance of soil moisture in the nitrogen cycle (henceforth denoted as N-cycle) has already been investigated in the past from several authors. Among those, several works have been done by using static chambers (*i.e.* jar incubation) in order to separate N_2O produced during nitrification and denitrification (Stevens et al., 1997), to measure the ratio N_2O - N/NO_3 - N and the ratio of N_2O -N/N_2-N at different water content by using different types of soil (e.g., Maag and Vinther, 1996). However only few studies have focused on the N-cycle - soil moisture interaction trying to measure the changes in total emissions given by changes in water content (Meixner et al., 1997; Skiba et al., 1999; Schindlbacher et al., 2004). The effect of re-wetting in jars has been investigate in the work of Ruser et al. (2006).

All the above mention works provided useful steps in order to understand the N_2O formation, however the incubation experiments do not allow to account for realistic water dynamics and soil heterogeneity. There are some works which account for soil spatial variability trough soil column experiments in which the biological reactions are measured along

a profile (Khdyer and Cho, 1983). Also the ebullion and entrapment of N_2O at a given soil moisture (Clough et al., 2005), the changes in hydraulic properties given by bacterial growth (Soares et al., 1991) and the role of oxygen on trace gasses (McKenney et al., 2001) has been investigated, but none of the above mention work accounted for water dynamic. Only some works in hydrology field (e.g., Cainelli, 2007) attempted to account for a realistic rainfall regime in a soil column where therefore the biological activity was not included.

In order to fill the previous gaps, a soil column was designed and constructed in which a realistic rainfall input can be investigated and flooding event can be reproduced. To the author's knowledge, this has not been done before. Both the liquid and the gas phase has been monitored in order to measure nitrate, ammonium and trace gasses along the profile. Also, reaction rates at different depths, corresponding to different water contents has been measured. Among the results, evidence of dependence on nitrate ammonification from water content and the possible occurrence of anaerobic ammonium oxidation iron mediated (pathway denoted as *Feammox*)has been found.

Thus the main objective of this dissertation is comparing the effects of rainfall, saturation and deposition on trace gases emissions. Furthermore, we measure the reaction rates of gross mineralization, gross nitrification and nitrate ammonification at different water contents.

This dissertation is divided into two parts. The first one consists of an experimental component. A soil column and chamber experiments were used to investigate the relationship between soil moisture and nitrogen dynamics. For the chamber experiment, soil was incubated under ambient conditions. In this experiment, we are interested in the effects of aggregate disruption on N concentrations and fluxes. As for the column experiment, we study how different physical conditions affect the processes under investigation. Dissolved NO_3^-, NH_4^+ and trace gases were collected during the following scenarios: (i) Drought that represents dry soil condition, (ii) rainfall events (iii) flooding events and finally, (iv) nitrogen deposition. Once the experiment is performed, we are able to observe N-cycle dynamics to include in trace gas models. As for the second component of this dissertation, we develop a conceptual model that incorporates all the major biogeochemical processes necessary to understand the interaction between soil moisture and N-cycle. This allows us to investigate a wide range of conditions and verify whether simulated results are in agreement with the experimental observations. A comparative analysis between the new and enhanced model, developed in this dissertation, and the model of Porporato et al. (2003) is performed in order to quantify the effects of the newly added processes.

The combined experimental-modeling characteristics of this work will add the fundamental knowledge necessary to create accurate N budgets and improve existing denitrification models. The current state-of-the-art mechanistic models mainly predict N_2O soil emissions from denitrification (Porporato et al., 2003; Manzoni and Porporato, 2007; Maggi et al., 2008), while ecological models, which account for many pathways, use empirical relationships and require many parameters (Li et al., 1992). We believe that the approach used in this dissertation provide a step towards capturing important pathways that produce N_2O emissions by using a reasonable amount of parameters. Hence, understanding the importance of these pathways through a combined modeling and experimental work is needed to better quantify future climate change and stratospheric ozone depletion. Moreover, an interesting novelty in the current thesis is the soil under investigation. The soil used in this study is a peat located in the San Joaquin-Sacramento Bay Delta area (Sherman Island, Northern California, USA). The physical characteristics of this soil have not undergone deep study and many of its parameters are not found in the literature thus justifying our experimental analysis. This region in California is of concern to the state government given its critical role as the water supply for most of the state.

The structure of this dissertation is as follows: Chapter 1 presents the introduction and motivations of the work. Chapter 2 provides the state-of-the-art in the nitrogen cycle in peatland soils and site characterization of the field. Chapter 3 will describe all the experimental procedure and details of the instruments used. In Chapter 4, results and discussion from the incubation and column experiments are given. Chapter 5 provides results at the field scale. Chapter 6 describes the conceptual mathematical model. Hypothesis and assumptions are provided. In the end of Chapter 6, simulation results are shown. These results are linked with the observations described in Chapter 4. Finally, Chapter 7 summarizes the main findings of this dissertation as well as suggestions of future research extension of the current work.

2 Nitrogen Cycle and Peatland Soils: Fundamentals and Insight

2.1 Global Changes, Nitrogen Cycle and Nitrous Oxide Emissions

Reactive nitrogen (Nr) includes all biologically, chemically and physically active N compounds in the atmosphere and biosphere of the Earth. Nature converts N_2 to Nr by biological nitrogen fixation (BNF), while humans convert N_2 to Nr by fossil fuel combustion, and cultivation-induced BNF. The massive use of fuel, fertilizers and the intensification of industrialization started during the last century, dramatically increased the anthropogenetic input of reactive nitrogen (Nr) to ecosystem, changing the natural balance between trace gas production and consumption and leading to multiple environmental issues (Galloway et al., 2003, 2008). Among those, a significant increase of atmospheric terrestrial temperature (Pachauri, 2009) has been recorded in the last century (Figures 2.1,2.2 and 2.3).

Global terrestrial temperature is increasing (Pachauri, 2009)(see Figure 2.1) due to atrophic activities. This affect the hydrologic cycle frequency increasing intensity and duration of rainfall, flooding and droughts (Porporato et al., 2004; IPCC, 2007). These modification within the water cycle alters the spatial and temporal distribution of soil moisture with impacts on the biology and biogeochemistry of the terrestrial and aquatic habitats enhancing biotic and abiotic processes responsible for the production of trace gases (mainly nitrous oxide, methane and carbon dioxide), and thus increasing of the terrestrial temperature (see Figure 2.2), trough a complicate and still poorly mechanisms which may evolve as a chaotic system (IPCC, 2007).

Since 1970, trace gas emissions increased of 70% (EEA, 2007) (see Figure 2.3), with the consequent increase of 0.74°C in temperature. Predictions indicate that if emissions will not be reduced, atmospheric temperature will increase between, 1.1 and 6.4°C by the end

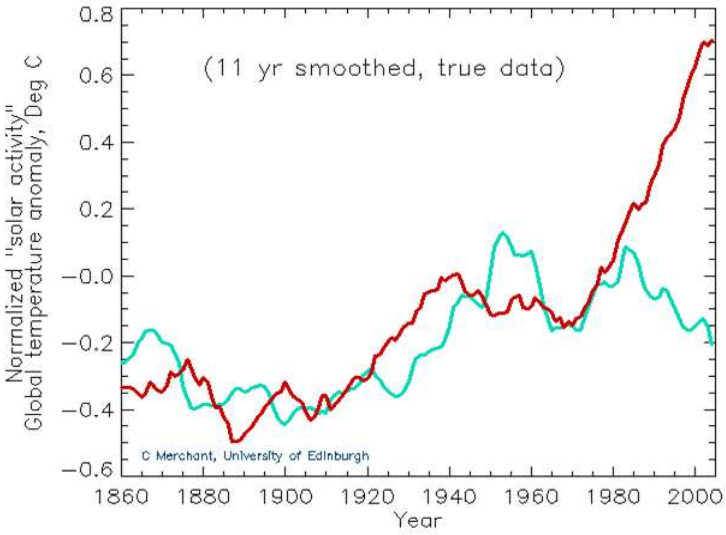

Figure 2.1: Changes in terrestrial temperature since 1860. Red line indicates the surface temperature, while blue line indicates the averaged soil radiation, Source Chris Merchant.

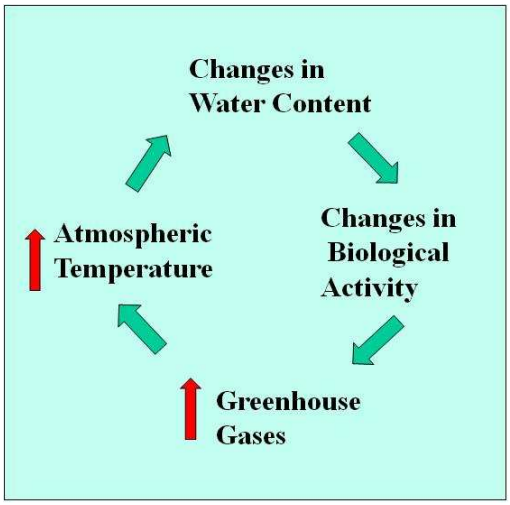

Figure 2.2: Proposed scheme of link between climate change, water cycle, biological activity and trace gases emissions.

of the century, with catastrophic consequence for humans and the environment (Pachauri, 2009).

In the past scientific community and media focused on carbon dioxide emission, but in the last decades the potential impact of nitrous oxide emissions and methane has been enlighten (Galloway et al., 2008). Among trace gases, indeed, nitrous oxide has a GWP 310 time higher than CO_2, so even relative small concentration may cause a significant environmental impact (e.g., Prather et al., 2001; Ramaswamy et al., 2001; IPCC, 2007). Being tropical forests and agricultural fields the major emitters of nitrous oxides (Skiba et al., 1999; Stehfest and Bouwman, 2006), the understanding and prediction of the biogenic emissions from soil is crucial in order to understand the consequence on global change. This challenge is raising given the complexity of the N-cycle and the nitrogen cascade process (Galloway et al., 2003), which indicate the ability of a singular molecule of nitrogen to be recycled in different environments, procuring multiples source of pollution (EEA, 2007). The impact of these processes affect flora, fauna and human health, e.g.(Squillace et al., 2002). High concentration of nitrate, for instance, lead to pollution of aquifers, eutrophication of water bodies and anoxic condition for fishes and micro-organisms (Lowrance et al., 1997).

In addition, even though the role of microbes in emitting nitrous oxide emissions is known e.g. Reay (2002), the biological complexity of soils make hard to identify bacteria responsible of a particular pathway, especially in case of fluctuating redox conditions, where bacteria cope to environmental challenges in different way than the ones used to static conditions (e.g., Pett-Ridge et al., 2006; Templer et al., 2008). Also, many processes are far to be fully understood, as for example the complex interaction between the carbon and the nitrogen cycle (Braden et al., 2009).

Nevertheless, at the same time, in the last five years, potential for new pathways in the N-cycle has been discover (Francis et al., 2007; Colman et al., 2008; Shrestha et al., 2009) as a consequence of the progress in knowledge and in analytical and isotopes techniques. The understanding of new pathways might lead to new vision of the N-cycle (Burgin and Hamilton, 2007) and change the current view of modeling emission of trace gases (see Chapter 6)both in terrestrial (Francis et al., 2007) and aquatic ecosystems (Burgin and Hamilton, 2007).

Nitrogen is a key element for the formation of vital organic compounds as proteins and amino acid. Among the nutrient cycles, the one which describe nitrogen (N-cycle) is one of the most complex, since it involves solid, liquid and gaseous forms and oxidation numbers which range from +5 of nitrate ion (NO_3^-) to -3 of ammonia (NH_3).

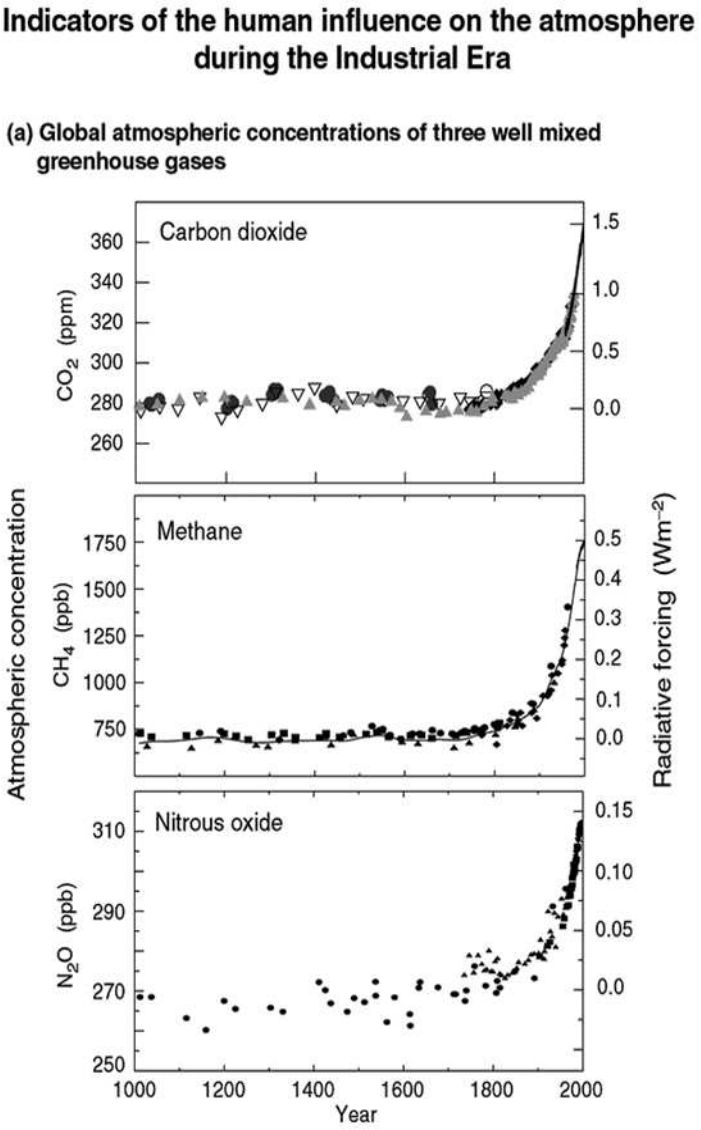

Figure 2.3: Emissions of carbon dioxide (CO_2), nitrous oxide (N_2O) and methane (CH_4) in the last millennium. Source, IPCC (2007)

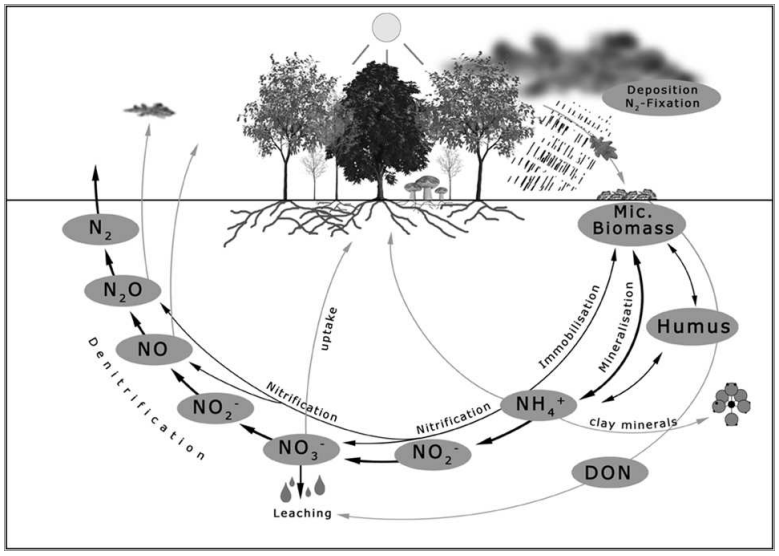

Figure 2.4: Nitrogen cycle pathways. Source: Second Nitro-Europe Summer School, Edinburgh 2008.

Figure 2.4 shows a picture of the N-cycle, which underline the complexity of the fundamental cycle, in which both biotic and abiotic processes may transform nitrogen compounds. A complete description of the nitrogen cycle can be found in Sylvia et al. (1998). The main pathways of nitrogen cycle in soils are:

• Mineralization (e.g., Manzoni and Porporato, 2009): Conversion of organic matter to ammonia and ammonium (NH_4^+);

• Nitrification (e.g., Wrage et al., 2001, 2007): Conversion of ammonium (NH_4^+) and/or ammonia (NH_3) to nitrate (NO_3^-);

• Denitrification (e.g., Tiedje et al., 1984): Conversion of nitrate (NO_3^-) to nitric oxides (NO), nitrous oxide (N_2O)and dinitrogen (N_2);

• Immobilization (e.g., Sylvia et al., 1998): Assimilation of mineral nitrogen by bacteria.

Also wet and dry deposition (e.g., Sutton et al., 1994), plant uptake, leaching (e.g., Porporato et al., 2003) and abiotic processes (e.g., Venterea and Rolston, 2000) has been investigate with renew interest in the last years, given the future projection of nitrogen deposition (Galloway et al., 2008) and the possible role of abiotic processes in nitrate reduction Colman et al. (e.g., 2008). To these reactions, has to be added the recently discover partway which include the dissimilatory nitrate reduction to ammonium (DNRA) also known as nitrate ammonification and the interaction between nitrogen and iron cycle

(*i.e.* feammox and iron wheel).

DNRA (Tiedje, 1988; Silver et al., 2001) is a dissimilatory pathway as denitrification, but contrary to it retains N in soils. As denitrification is favored by carbon, nitrate and low oxygen conditions (e.g., Silver et al., 2005). Latest research suggests that DNRA can occur during short term anaerobic event and may not require super low redox (Silver personal communication).

Recently has been discovered that some forms of iron (mainly Fe^{2+} and Fe^{3+}) might interact with ammonium (Clement et al., 2005; Whendee et al., 2009) and nitrate (e.g., Straub et al., 1996) to produce nitrite and molecular nitrogen. Nitrite is an intermediate product of nitrification and denitrification processes, which is very toxic for organisms and highly reactive. Nitrite usually does not accumulate in soil (except in particular soil condition, see (Venterea and Rolston, 2000). Therefore this pathways are important since nitrite produced, may be denitrified to N_2O/ N_2, converted to nitrate (nitrification) or to ammonium (nitrate ammonification) leading to potential danger for the environment, especially in soil rich in iron and nitrogen, or where fertilizers base on these compound has been used. At the current stage is still unknown if anaerobic ammonium oxidation mediated by iron (known as feammox) is mainly driven by biotic or abiotic processes. In fact while Fe(II)-oxidizing nitrate-reducers has been identified (Kappler et al., 2008), ammonium-oxidizing Fe(III)-reducers to the knowledge of the author has not been isolated so far. Finally the conversion of ammonium to dinitrogen, known as anammox (anaerobic ammonium and archeal ammonium oxidation) has been speculated but never found in soil (Francis 2007). The implication of these new pathways on the production of trace gases are still unknown. Feammox seems to be favored in anoxic soils rich in nitrogen (Silver *personal communication*). In fact, even though the potential impact of N_2O emissions on ozone destruction is known since Crutzen et al. (2007), modeling and predicting them is still a challenge, since some processes are still poorly understood. For instance, even though is known than N_2O can be produced by both nitrification (e.g., Venterea and Rolston, 2000) and denitrification (e.g., Reay et al., 2003; Davidson and Seitzinger, 2006), and that biotic production of N_2O can significantly contribute to global change (Reay et al., 2003), the production of nitrous oxide is much more complicated and involves, in addition to the potential new reactions mentioned before, other reactions : nitrifier denitrifcation (e.g., Wrage et al., 2007), heterotrophic nitrification (e.g., Robertson and Kuenen, 1990) and chemo-denitrification (e.g., Venterea and Rolston, 2000). However, furthermore it can come via aerobic denitrification (e.g., Robertson and Kuenen, 1990). Modeling these

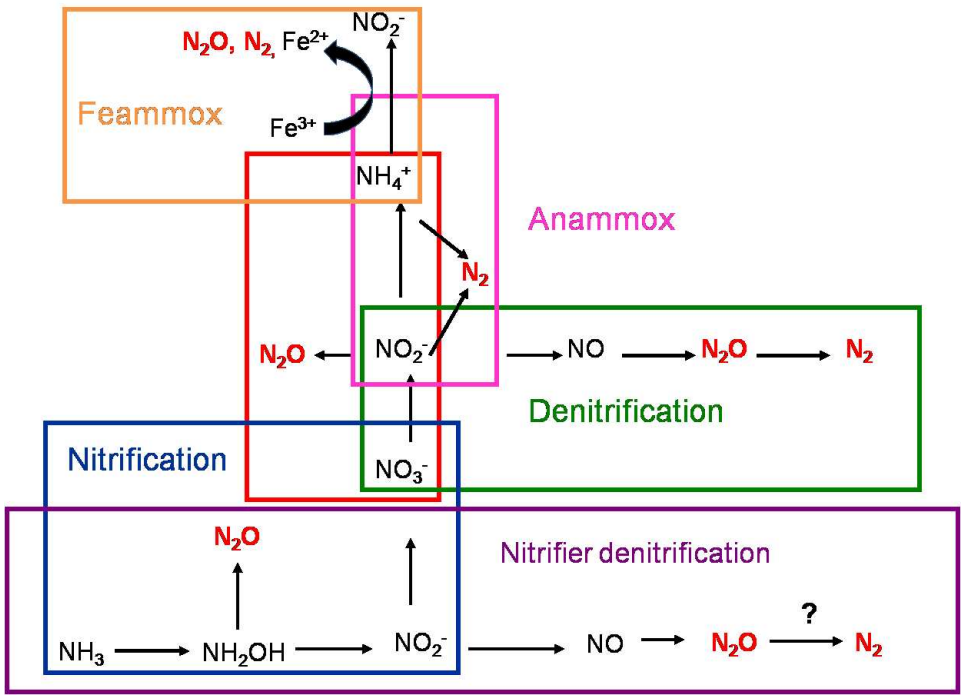

Figure 2.5: Possible mechanisms of N_2O production in soils.Anammox has only been speculated in soils (Francis 2007), while Feammox has been recently discover (Silver et al. 2009).

pathways is still very challenging, since the keys factors which control them are still far form a full comprehension. Of these processes, nitrification, nitrifier denitrification and chemo-denitrification are not heterotrophic (*i.e.* not depend on organic C; but at least the first two depend on CO2). Figure 2.5 reports our modified scheme based on Wrage et al. (2007)and Baggs (2008) of the possible pathways of N_2O production.

2.1.1 Technology improvement

In the last decades improvement of technologies lead to better understand the N-cycle (Baggs, 2008). Isotopes are largely used to understand elementary cycles. In particular ^{15}N, ^{18}O and ^{17}O are the one used for the N-cycle. In this section we report some main consideration concerning the use of isotope in the N-cycle and the novelty in the sector. A detailed description of the use of isotopes can be found in Hoefs (2008), Kendall and McDonnell (1998). A review of isotopes in the nitrogen cycle and future challenges in their use can be found in Baggs (2008).

^{15}N research in natural and managed ecosystems generally focuses on two techniques:

isotopic enrichment and natural abundance studies. Many application exists in which ^{15}N is used to describe the nitrogen cycle pathways at a plot, field, landscape, and even global scale.

^{15}N has a greater atomic weight than the conventional ^{14}N atom. Being different in atomic weight, ^{15}N isotopes behave identical to ^{14}N atoms in biochemical reactions but can be detected separately. Concentrations of ^{15}N are usually measured as the ratio of $^{15}N/^{14}N$ ($R^{15}N$) or in term of delta value, being delta the ratio of $((R^{15}N)_{sample}$-$(R^{15}N)_{standard})/(R^{15}N)_{standard})$(Kendall and McDonnell, 1998). The use of enriched ^{15}N is particularly useful to study the movement of nitrogen through the fundamental processes of the nitrogen cycle. For example net mineralization can be measured simply from the changes in the NH_4^+ pool, but this does not account for losses through ammonium immobilization and nitrification. Gross mineralization can be best studied employing the pool dilution technique (Davidson et al 1984, Hart et al. 1991).

These techniques involved the addition of $^{15}NH_4^+$ to the indigenous $^{14}NH_4^+$ pool and changes in $^{14}N/^{15}N$ are measured over specified period taking into consideration the nitrification and immobilization. Natural abundance techniques can also be used to measure gross nitrogen transformations, particularly in combination with other techniques such as $\delta^{18}O$ and $\delta^{17}O$ analysis. The cost of ^{15}N labeled substrates and analytical cost remain the confounding issue for these techniques. Problem of uneven distribution of applied enriched ^{15}N substrate is particularly challenging at field scale. Preferential use can also occur before establishment of equilibrium between ^{14}N and applied ^{15}N which is problematic for isotopic dilution. In addition to this application of ^{15}N in N-limited systems can lead to over-estimation of gross-mineralization as NH_4^+ consumption can be stimulated upon substrate addition. This can be overcome by using natural abundance techniques but these too are limited. In natural ecosystems indeed there are many co-occurrence N pools and simultaneous transformation between the pools which make difficult the use of natural abundance techniques. The main problems are relating to fractionation, which occurs during chemical reactions when the abundances of the heavy isotopes in the substrate are different from the ones in the product and mixing, a process that combines different substrates into the products. Also fractionation factors associated with a single process vary,since (i) processes are limited by substrate availability, (ii) there are multiple substrate for the same product (e.g. N_2O ,NO) and (iii) multiple fate for each substrate (e.g. NH_4^+ ,NO_3^-).

Quantification in fractionation rates has emerged as challenge in recent research work. Use of ^{15}N techniques must be careful to avoid interpreting the data in isolation; often

other techniques are required to differentiate sources and pathways effectively. Currently the field of isotope is very active, facing new challenges. These mainly concern the identification and understanding of new pathways and the appliance of new technologies. New pathways involve denitrification of ammonium to nitrate (DNRA) and the feammox reaction. Innovative technologies include the use of bacteria to convert NO3- to easily measurable N_2O, the use of isotopomers (measuring site preference within molecules), the use of Nano Sims (see Figure 2.6) which can scan isotopic surface for the samples and is able to capture assimilatory processes at cell level and the use of N_2/ Ar chambers to measure N_2 fluxes (Yang *personal communication*). Also Butterbach-Bahl et al. (2002) developed a gas-flow core method to determine simultaneously N_2 and N_2O fluxes with high accuracy. ^{15}N stable isotope techniques are indispensable for comprehensive understanding of microbial mediated pathways of N cycling both in natural and managed ecosystems, but in general additional techniques are recommended to compliment analysis this work. Cross disciplinary studies and technologies improvement are therefore needed to better understand new processes, the link between functional groups and processes and the scaling issues from gene to landscape.

2.1.2 The Role of Water on Nitrogen Emissions

The hydrological control on N_2O emissions is exerted through the effects of oxygen availability and redox potential, which regulate microbial metabolism (e.g., Brady and Weil, 1974; Stark and Firestone, 1995; Hunt et al., 1995; Davidsson and Leonardson, 1997) and chemical transformations in the soil (Daly and Porporato, 2005). Several studies are available that have investigated the relationship between volumetric water content (VWC) and N-gas emissions in using laboratory incubation experiments where the water content was maintained constant (e.g., Stevens et al., 1997; Reay et al., 2003; Ridolfi et al., 2003b). An approximate dependence of the emissions from VWC has been compiled by repeating the experiment with several different VWCs; these experiments have also been conducted using a range of static VWC. For example, measurements of the ratio N_2O-N/NO3-N and the ratio N_2O -N/ N_2-N in incubation (jars) experiments with different VWCs were performed by Maag and Vinther (1996), while Schindlbacher et al. (2004) and van Dijk and Meixner (2001) measured total gas emissions under similar experimental conditions. Furthermore, the effect of re-wetting in jar experiments has been investigated by Ruser et al. (2006). These studies contributed to improve our understanding of the mechanisms controlling gas emissions from the soil, which have a strong influence on the earth's climate. However, under natural conditions, soil moisture is generally dynamic, changing on

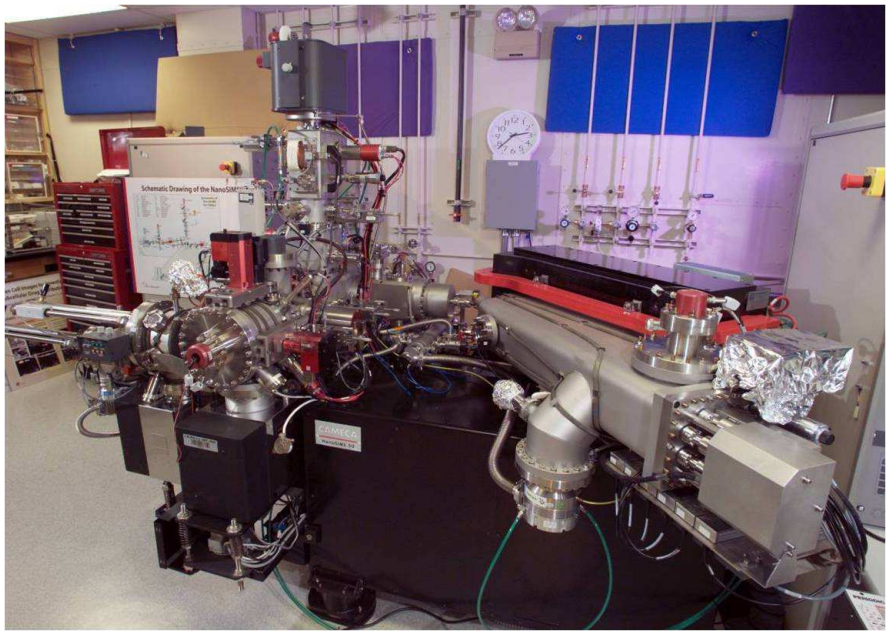

Figure 2.6: Picture of the Ion-Secondary ion mass spectrometry from the Livermore National Laboratory, California (LNLL). Primary beam scans sample surface to produce secondary ions. Secondary ions detected to produce quantitative digital images with simultaneous detection of 5 species, Courtesy of Jennifer Petty Ridge.

the scale of hours to days. The effects of dynamic soil moisture on N cycling and N_2O emissions is less well understood. An important aspect that has not been taken into account so far is the interplay between gas emissions and soil water dynamics. Soil moisture affects the partitioning of N_2O and N_2 controlling physical transport of gases in the soil.

Understanding the water dynamics in the unsaturated zone thus helps to better quantify the amount of contaminant mass arriving in the saturated zone. In vadose zone, N-cycle reaction rates are a non linear function of the volumetric water content (VWC) and infiltration is the main mechanism which regulate the transport (Rostagno, 1989). Water movement modifies soil moisture dynamics and soil structure (Zejun et al., 2002), affecting trace gases production, consumption and emissions (Clough et al., 2005). Surface soil moisture is a key factor in controlling the energy fluxes between atmosphere and soil surface. Soil structure, also influence transport phenomena. Pachepsky and Rawls (2003) studied as soil structure and texture influence soil water flow, availability and storage. Smith et al. (2003) investigated the interaction of soil physical factor and biological processes in exchange of greenhouse gases between soil and atmosphere and underlined the role of soil structure in defying the quantity of trace gases emitted to the atmosphere. The transport of nutrients in the vadose zone, redistribute nutrients (Skopp et al., 1990) along the soil profile (see Figures 2.8 and 2.7) modify the ratio of aerobic versus anaerobic zone (e.g., Potter et al., 1996; Franzluebbers, 2002), untimely affecting the intensity and temporal dynamics of nitrous oxide emissions. In order to provide a quantitative description of nitrous oxide dynamics, is thus important to better understand the transport of N-compounds within the soil profile.

In particular, in organic rich soil, flow and transport processes are strongly influenced by organic material which can absorb the moisture from the soil and increases porous spaces facilitating the movement of the water (Franzluebbers, 2002). Soil organic matter is a key attribute of soil quality that impacts soil aggregation and water infiltration. The organic material can be decomposed by bacteria to become organic glues that help the formation of macro-aggregates and affect hydraulic properties. The changes in hydraulic properties given by bacterial growth were studied by Soares et al. (1991), Thullner et al. (2002), Thullner et al. (2005), Yarwood et al. (2006), and the role of oxygen on trace gasses is reported in Khdyer and Cho (1983), McKenney et al. (1997) and McKenney et al. (2001). In addition, natural soils, present irregular heterogeneity which precludes in many cases the use of averaged parameters to predict the transport. Several authors try to model solute transport by accounting for heterogeneity and soil moisture dynamic. Among those, Russo et al. (2006), Russo and Fiori (2008), Ryu and Famiglietti (2006),

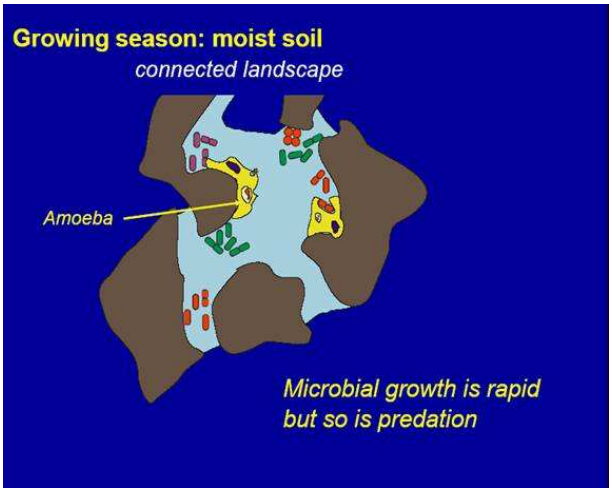

(a) Figure a.

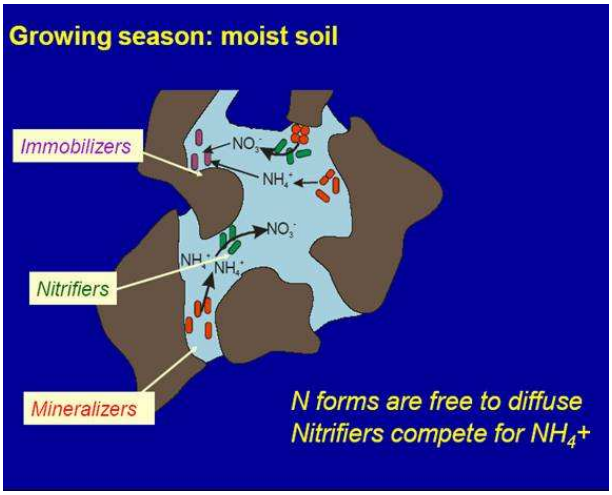

(b) Figure b.

Figure 2.7: Effect of connected landscape on microbial communities, predators and nutrients, when soil is wet. Unpublished Pictures, courtesy of Joshua Shimel.

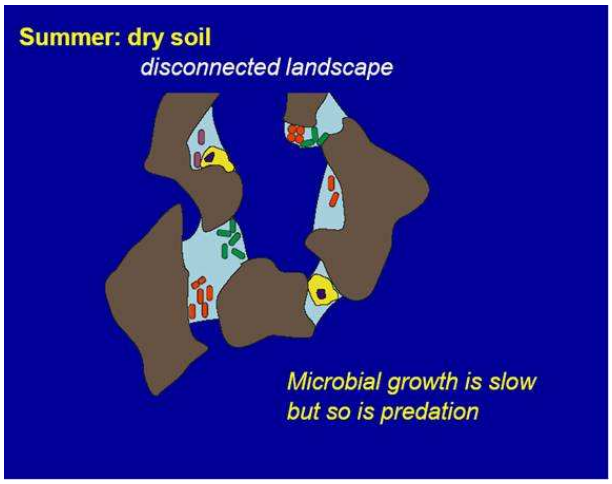

(a) Figure a.

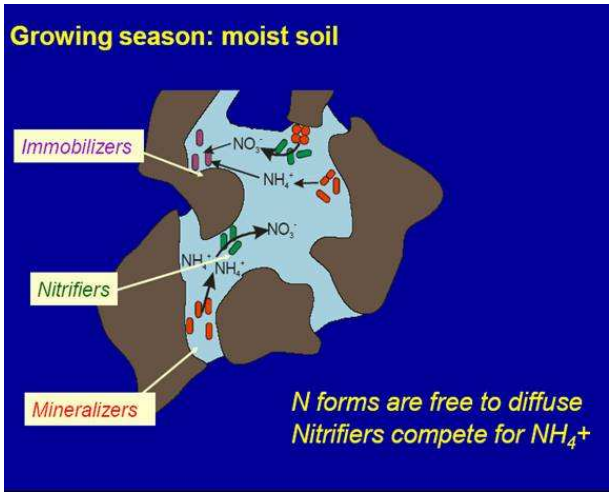

(b) Figure b.

Figure 2.8: Effect of disconnected landscape on microbial communities, predators and nutrients, when soil is dry Unpublished Pictures, courtesy of Joshua Shimel.

and Vereecken et al. (2007) give a quantitative description of the problem, but no one specifically focused on the nitrogen cycle and on biological aspect. Experimentally, there are some works which account for soil spatial variability through soil column, in which the biological reactions are measured along a profile (e.g., Khdyer and Cho, 1983). The ebullion and entrapment of N_2O at a given VWC value has been investigated by Clough et al. (2005). A review of N_2O diffusion within the soil profile has been done by Heincke and Kaupenjohann (1999) et al. in 1999. Nevertheless, these works do not account for soil moisture dynamics.

Further research investigations are therefore needed to better understand the combined effects of soil heterogeneity, VWC, realistic precipitation and flooding events at a column scale experiment in nitrous emissions (see Chapter 4). These aspects are particularly relevant in the top soil layer (top 0-5 cm). At this depth range, the soil experiences fast variation in soil VWC, which depends on the interplay between rainfall infiltration and evapotranspiration.

This complex interaction between water dynamic and N-cycle thus cannot neglect the variation of soil moisture in time and in space. Evidence in our experiment (see Chapter 4) shown the macro-scale N-cycle is the results of micro-scale processes whose interaction with substrate is regulated by soil heterogeneity and in particular by hydraulic conductivity and connectivity.

For instance Shiemel in: "The biogechemistry of drought", talk given given at Biogeomon 2009 (Helsinki), explained the shift from dry to wet season considering that in moisture soils, pore are better connected, allowing microbes, their resources, and their predators to move over relatively long distances (e.g., Harris, 1981). As soil dry out, microbes may lose the bridges that connect one soil particle to another (e.g., Vargas and Hattori, 1986). According to this hypotheses changes in N-cycle from the dry to the wet season are driven by changes of the hydrological connectivity on the microbial landscape (see Figures 2.8 and 2.7).

2.1.3 Nitrous Oxide Emissions from Peatland

There are only few studies looking at the potential of nitrous oxides emissions from peat land (e.g., Guthrie and Duxbury, 1978; Muller et al., 1980; Verhoeven, 1986; Regina et al., 1999; Maljanen et al., 2009) and Teh et al. (2010),under review. Contrary to natural peat, which in general acts as a sink for N_2O, peat soils with high nitrogen content are potential sources of nitrous oxide (e.g., Von Arnold et al., 2005). High N_2O value has also reported in **artic** peatland (Maljanen et al., 2009). Some works (e.g., Goodroad and

Keeney, 1984; Martikainen et al., 1993) reported that drainage has an impact in enhancing emissions of N_2O from some peat soil. One possible explanation is because of increased nitrification activity in the uppermost aerobic peat profile. Zimenko and Misnik (1970) observed an increase in nitrification after a water table draw-down in a few wetlands. Also after drainage of a peatland, the availability of oxygen and mineral nitrogen increase, this favors N_2O production (e.g., Martikainen et al., 1993). Finally Guthrie and Duxbury (1978) recovered up to 98% of the dissolved N_2O in the leaching of an organic soils column. The increased nitrification in the surface peat may lead to nitrate leaching in the anaerobic layer and subsequent enhancement of denitrification. Regina et al. (1999) underlined how this process may continue for many decades given the availability of a large nitrogen pool which is gradually but continuously tapped. Further research efforts are therefore needed to understand the role of rich organic peatland to climate change (see Chapter 5). In the following section we describe the main issues concerning the patland used to perform our analysis (peatland soil collected in the Bay Delta area, California). In this case, nitrous oxides emissions may also be affect that salinity. In general N_2O is more soluble in acid solution than in alkaline ones (Heincke and Kaupenjohann, 1999).

2.2 Understanding the Importance and Complexity of the Environmental Issues in the Bay Delta Area, Sacramento, California, USA.

2.2.1 Relevance

The Bay Delta is located at the confluence of the San Joaquin and the Sacramento Rivers. It is blanketed by peat and peaty alluvium deposited where streams, originating in the Sierra Nevada, Coast Ranges, and southern Cascade Ranges enter the San Francisco Bay system. The region has been of great concern to the California state government given its critical role in the water supply of the region (Drexler et al., 2009). In order to obtain soil suitable for agricultural purposes, a system of sleeves has been build to prevent frequent flooding (see Figure 2.10). Drainage ditches prevent the island from flooding internally and maintains groundwater levels deep enough for agricultural crop to grow. Currently islands in the Delta are below sea level and are maintained by a 2200 km network of levees. The use of soil for reclamation and agriculture has led to the subsidence of the land surface, which ranging from 1 to 8 meters below the sea level in the central part of the Delta.

Land subsidence is mainly relating to the oxidation of the organic carbon in the peat soil. Figure 2.11 depicts the mechanism of oxidation of soil exposed to air (see Figure 2.11). As subsidence increases, the levees need to be reinforced in order to support the increasing strengths on their banks. The fragility of the levees is an environmental issue, since salt water intrusion might affect the water quality an the biodiversity of the area. Conseguens include the loss of nutrients and soil fertility, the loss of habitat for many animal and plant species and the spread of invasive plants.

The Sacramento-San Joaquin Delta is indeed the source water for more than 20 million people and habitat for several endangered species. In addition, is an exceptionally rich agricultural area (over $500 million crop value as of 1993) and is also important for many socio-economic activities (fishery, recreational, etc.)

The conflicting interests of farmers and water municipalities has lead to a big debate over the last few decades to solve a large set of issues including the levee fragility, climate change, flood plain development, upstream diversions and new strategies for diverting water out of the Delta. For this purpose, the Governor has convened several forums including the *Delta Vision* and the *Bay Delta Conservation Plan* to develop a comprehensive plan for the Delta. The decision-making project CALEF has been created in order create a common vision to improve the Delta region. The plan includes the participation of local, governmental agencies, environmentalists, farmers, stake-holders and industry representatives. This program favored the creation of a robust science program to study the Delta and to create a vast knowledge base in which ecological decisions could be made.

Among these works, Deverel and Rojstaczer (1996) studied the water flow from the San Joaquin River towards the island center and drainage ditches, finding that the primary source of drain flow from the period May to November is groundwater, while during the December to April, the shallow-zone flow is the primary source.

Moreover, recent works Muller et al. (e.g., 1980); Gorham (e.g., 1991) focused also on global change in the Bay Delta area and in particular on the role of water management in carbon (C) storage and trace gasses emissions since the State of California has a political mandate to reduce greenhouse gas emissions to 1990 levels by 2020.

These studies are important, since fresh-water peatlands, with saturated soils and high carbon content, are also significant sources of carbon, in the form of methane, an important greenhouse gas (Conrad, 1996). In anaerobic settings, hydrogen (H2) and acetate are produced by fermenting bacteria. These compounds then serve as electron donors for the metabolism of methanogenic bacteria (Conrad, 1996; Schimel, 2004). The net emission of methane, however, is complicated. It is a function of the rate of methane production, cou-

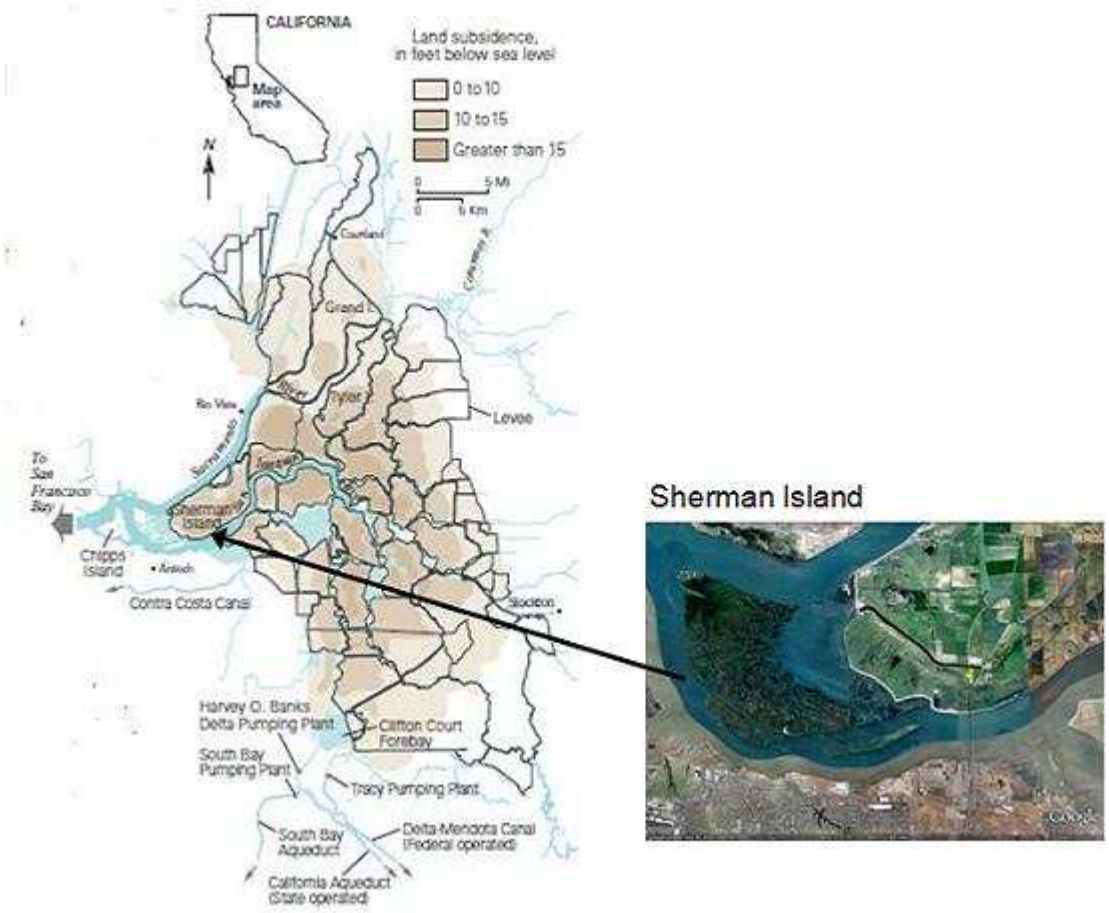

Figure 2.9: Bay Delta Area, California, USA. Different colors in the map measures the land subsidence, in feet below sea level. *Source:* USGS (2007).

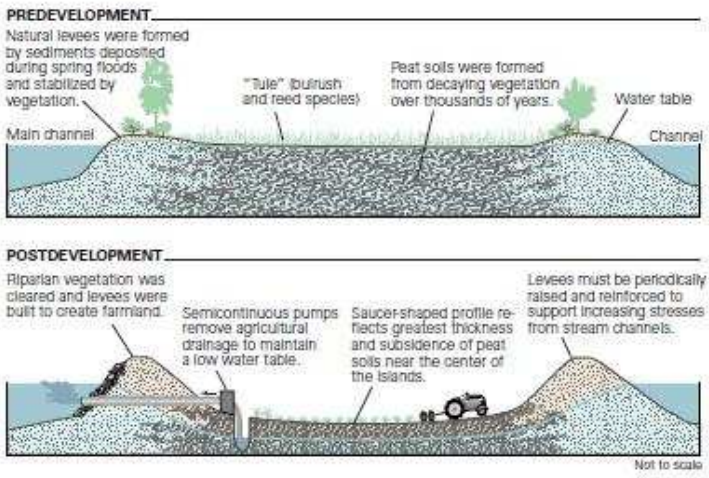

Figure 2.10: Land use changes in the Bay Delta area and its implication on carbon oxidation. Source: USGS (2007).

Field studies (Deverel and Rojstaczer, 1996) determined that the increased flux of carbon dioxide gas from the drained peat soils was sufficient to explain most of the carbon loss and measured subsidence. The dissolved organic carbon pumped from the islands in agricultural drainage could account for only about 1 percent of the carbon loss. The studies also showed that rates of carbon-dioxide production increase with increasing temperature and decrease with increasing soil moisture.

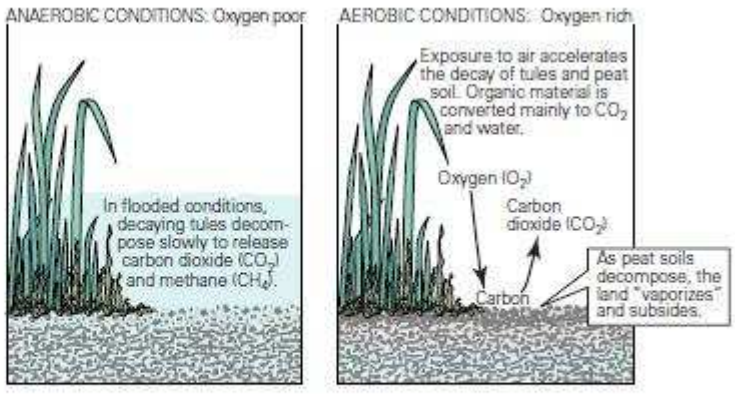

Figure 2.11: Same as in Figure 2.10. Details concerning anaerobic and aerobic conditions. Source: USGS (2007)

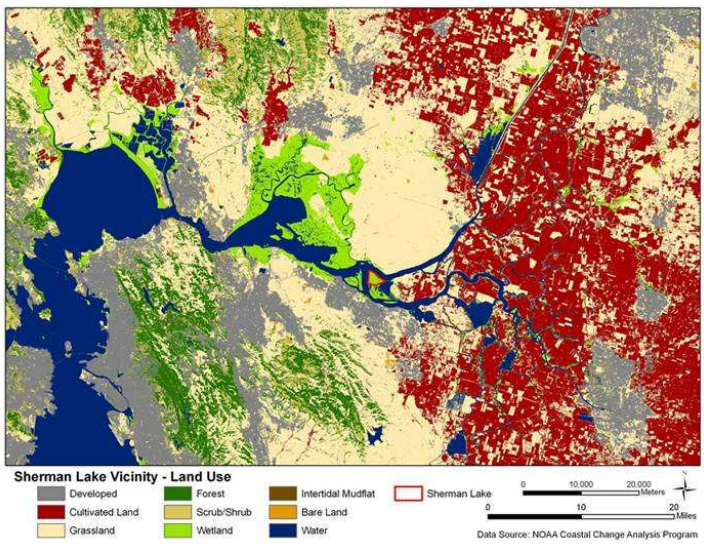

Figure 2.12: Bay Delta Area, California, USA. Different color in the map, indicate different land use Source: Matteo Detto.

pled with the methane consumed by methanotrophic bacteria as methane diffuses across aerobic zones in the soil and into the atmosphere, or is shunted past the soil aerobic via xylem transport and ebullition (e.g., Conrad, 1996; Whalen, 2005; Teh and Silver, 2006). The metabolism of a peatland can be best understood by studying the exchanges of carbon dioxide, water vapor, methane and energy between peatlands and the atmosphere in tandem because they are intrinsically linked. A recent comparison of a peat soil in the Sherman island (Guha A. and H., 2009) and a peat soil used to rice cultivation in the Twitchell Island, in the Bay delta area, shown that the rice crop, at a cost of more water usage, was able to sequester great quantities of CO_2 with minimum losses in terms of ecosystem respiration and methane emissions compared to an semi-abandoned field. Methane emissions from the rice were double than from the aerated peat soil, but still low comparing to CO_2 fluxes (less than 5% in term of GWP100) and with more uncertainty. (Figures 2.13, 2.14)

2.2.2 Site Characteristics

As described in the previous section of current chapter, only few works focused in studying nitrous oxide emissions from temperate peatland. Nitrous oxide is of particular interest to biogeoscientists and policy makers because it is a active trace gas whose greenhouse warming potential is more than 310 times greater than CO_2 on a *per* molecule basis (IPCC,

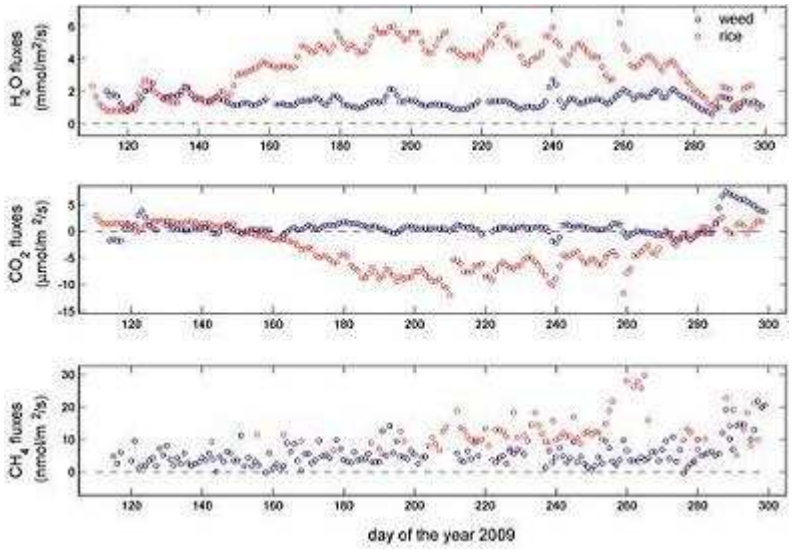

Figure 2.13: Comparison of multi-tower eddy-covariance daily averaged fluxes of water vapour, carbon dioxide and methane for peatlands with pepperweed and rice coltivation, cortesy of Matteo Detto.

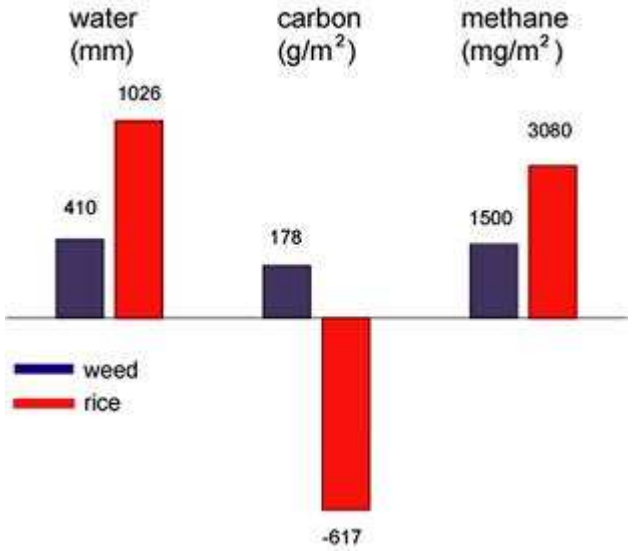

Figure 2.14: Fluxes: Growing season GHGs budget for peatlands with pepperweed and rice cultivation, courtesy of Matteo Detto.

2007).

In order to investigate the role of N_2O from rich organic peatland, soils (at 0 to 5 centimeter depth) were collected from an irrigated peatland pasture (see Figure 2.15) soil on Sherman Island (Figure 2.12), in the San Joaquin-Sacramento Bay Delta area of Northern California (lat: 38.0373N; long: 121.7536W; Elevation -12.1 m). The prime field site is an irrigated pasture over peat soils more than 7 m thick (Deverel and Rojstaczer, 1996) which is often near the maximum salinity intrusion line (*i.e.*, 1000 parts of chloride per million parts of water, 1.5 hours after high tide, Runkle (2010)). The site under investigation is part of an ongoing study to explore the effects of water management on greenhouse gas emissions (Teh et al., 2010). The field is dominated by a discontinuous canopy of perennial pepper-weed (Lepidium Latifolium) but also includes the nonnative annual C3 grass Hordeum murinum. The soil texture is a silty clay loam (sand: 23.1-29.2%, clay: 21.7-28.5% and silt 42.3-55.1%) with a near surface bulk density in the range 1.09-1.3 g/cm3 and a porosity which varies from 45 to 76% in the first 60 cm, (data from Runkle), but can reach up to 88% in the organic top layer, comparable to values (Deverel and Rojstaczer, 1996) of soil bulk density (0.85) and organic matter content (28.0%) measured on Sherman Island in the years 1990 and 1991. The site is characterized by a mean annual precipitation of 217 mm and a temperature of 9°C. The water table normally oscillates around 0.7 m below the surface (Deverel and Rojstaczer, 1996), but subsurface irrigation, via a network of spud ditches, periodically raises the water table to the surface, causing flooding conditions. This periodic irrigation activity provides a unique opportunity to study changes in the water table, evaluate their effect on gas fluxes at the field scale and finally, compare them to the behavior shown by the column (mainly focusing on mitrous oxide emissions), as described later in this dissertation.

Figure 2.15: Field site, Sherman Island in the San Joaquin-Sacramento Bay Delta area. Simonetta Rubol and the UC Berkeley group during soil sampling campaign in 2008.

3 Experimental Apparatus and Field Data Acquisition

3.1 Overview

In this chapter we describe the experimental set up used to perform the experiments which include the soil column device, the incubation chambers and the field measurements. The soil column represent a system which allowed to account for a more realistic rainfall regime than the incubation chambers, but which is under experimental control (since it is performed in a laboratory), contrary to to the field, where many variables can contribute to the actual flux measurements. Chambers, therefore are needed in order to measure the N-cycle reaction rates, as described later in this chapter (Figure 3.1).

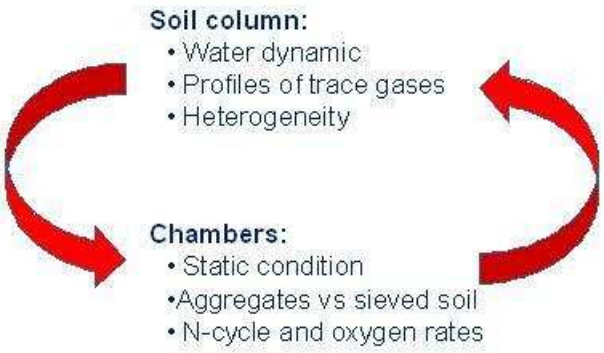

Figure 3.1: Synergic effect of chambers and soil column.

Lab Measurements	*Temporal Scale*
Abiotic	
VWC	Continuously
Soil Temperature	Continuously
Soil ectroconductivity	Continuously
Atmospheric Oxygen	Continuously
Redox	Continuously
Biotic	
Gas samples	According to changes in VWC and riequilibration time of silicone tube
Liquid samples	According to application of rainfall/saturation
Headspace Fluxes	Daily (starting form the Julian day 313)
Reaction rates	Twice (Julian day 272 and 334)

Table 3.1: Abiotic and biotic parameters measured during the experiment.

3.2 Soil column

The experiment was conducted using a 1.5 m high (internal diameter of 0.15 m) column constructed of polyvinyl chloride (PVC) (Figure 3.2). Sensors were installed along the length of the column, and concentrated near the top 0.5 m of the column where we expected a rapid variation of VWC. Table 1 summarizes the parameters measured in each section of the column (Table 3.1). Sensors were installed to compare biotic and abiotic parameters at the same height along the column (Figure 3.3).

We measured N_2O fluxes into the headspace of the column, i.e. the space between the top of the soil and the head used to simulate rainfall (Figure 3.2).

Along the column we measured the following: VWC, trace gases concentrations (N_2O, CO_2 and CH_4), dissolved NO_3^- and NH_4^+, and dissolved N_2O. In addition, the monitoring program included the measurement of bulk electro-conductivity (EC), soil temperature, soil O_2 and redox potential.

The column was set over a base where a perforated disk (see Figure 3.5) allowed water outflow and the base was covered by a geo-synthetic fabric membrane, a porous material that allowed water to flow through, but not soil. The water outflow was collected in a small chamber and routed through a tube which could be used for both draining the column outflow (in case of top infiltration experiments) and feeding the column from below (in case of bottom infiltration experiments).

Rainfall was simulated through a head attachment that created a uniform rainfall

Figure 3.2: Column device used to perform experiments.

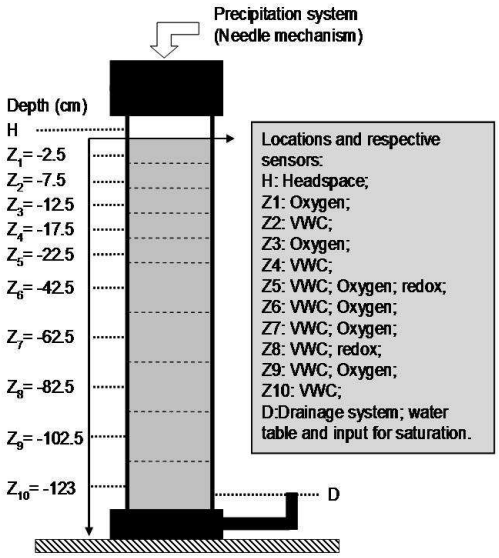

Figure 3.3: Scheme of the experimental column along with the sensors.

distribution across the inlet section of the column. The head attachment was designed according to the one proposed by Cainelli (2007), and used in a series of infiltration experiments with varying rainfall intensity. In essence, the head attachment was composed of a chamber where a peristaltic pump ensured inflow from the top, while water was delivered to the column soils through 250 needles which simulate rain droplets (see Figure 3.4). Each needle acts like a capillary tube; according to Poiselle's flow, a uniform pressure head on top of the needles produce a uniform outflow with each needle contributing the same amount of water. In order to achieve uniform pressure distribution over the needles, it was necessary to place the head in a horizontal position. We measured the degree to which we achieved equal water distribution with various head inflow rates following the procedure of Cainelli (2007)and determined that there was < 5 % error.

In order to limit as much as possible air entrainment the head chamber was feed by using a Venturi tube. The tube was connected to tap water in order to create a depression in the head chamber which sucked water from a reservoir underneath. Air entrapment in the head should be minimized because otherwise air bubbles may form in the needles, thus creating a meniscus which may impede the water flowing through them. Preliminary experiments showed that the Venturi tube was effective in limiting to a few the number of non contributing needles. The resulting rainfall is therefore uniform over the inlet of the column.

The column was equipped with gas and water ports to sample the soil matrix along

Figure 3.4: Head rainfall maker of the column.

Figure 3.5: Drainage system of the column.

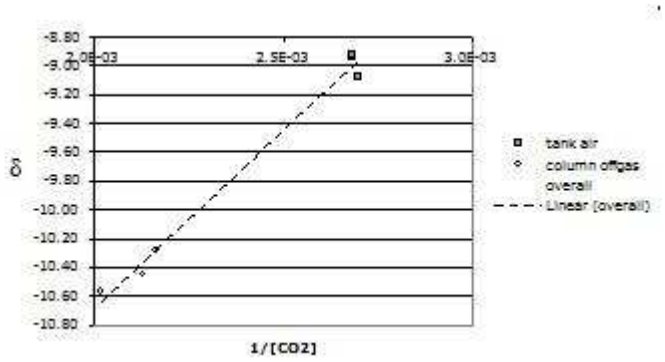

Figure 3.6: Carbon dioxide signature.

the column (Figure 3.3). The gas ports were composed of a silicone tube (1cm i.d. Tygon tubes) connected through fittings (Swagelog 63.5 mm) and septa to a copper tube previously installed along the column. Each liquid port was equipped with a microlysimeter (Volumetric Water Content Equip. Corp.) 100 mm long and with a diameter of 2.5 mm connected to fittings in order to obtain airtight conditions. Mycrolysimeters have no deadh volume, so that liquid samples reflect the soil column composition present in the soil at the moment of collection. VWC was measured by using capacitive probes (EC5 and ECTE, Decagon; with the latter measuring also the temperature and the soil electro-conductivity). We measured soil O_2 concentrations by using Apogee sensors (Apogee Instruments, Roseville, CA) and redox by using OPR Decagon sensors (Decagon Devices, Pullman, WA). All ports were airtight and waterproof.

Sensors were CO_2 signature less depleted than air. This implies that the free atmosphere in the PVC tube yield a CO_2, concentration larger than that of the background (laboratory) air (i.e., of 470 ppm, against 373 ppm of background laboratory air) (Figure 3.6).

VWC, oxygen and redox sensors were set to measure continuously using a data-logger (Campbell Scientific CR100) and a multiplexer (Campbell Scientific, Logan, UT). Deionized water (DI) was used to simulate rainfall and saturation events. The column experiment was run from Julian day 273 to 331 (59 days) and included a sequence of typical hydrological conditions.

Within this period the dissolved N-species and the N_2O gas samples were collected during 7-8 sample periods according to the duration of the event simulated and in respect to the re-equilibration time required by the silicone gas tubes, to be in equilibrium with the surrounding soil air (estimated to be 2 days). Samples were collected according to the

Figure 3.7: Oxygen probes calibration for humid condition.

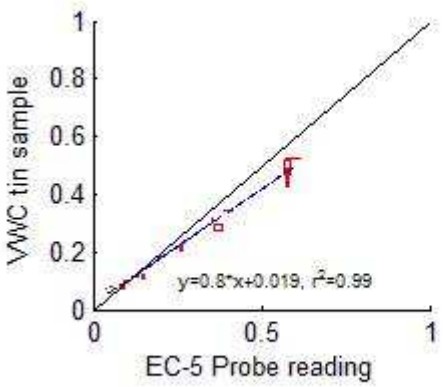

Figure 3.8: Example of soil moisture calibration for the peatland soil of Sherman Island, Bay Delta area, Califonia, used to perform the experiment.

schedule shown in Table 2, while data from sensors were recorded at the time step of 5 minutes, which was reduced to 1 minute during water addition.

Sensor were calibrated one by one. For the oxygen and the OPR (redox) probes measurements were corrected by the offset value. Oxygen sensors were calibrated in humid ambient (Figure 3.7), while OPR probes off-set value was measured using as standard reference a solution of saturated KCl Ag/AgCl. VWC probes were calibrated with the same soil used for the column. Expression were derived for each sensors through the regression curve of the row data vs VWC measure in sub-samples at different water content (Figure 3.8).

Figure 3.9: Example of soil chamber incubation.

3.3 Chamber Incubation Experiment

We performed two soil incubation experiments to determine gross N cycling rates and associated $^{15}N_2O$ fluxes. For the initial incubation experiment, we used well mixed soil collected at the same time and location as the column experiment. For the final incubation experiment samples were taken at three depths in the column to explore the effects of vertical zonation within the column. For the first incubation experiment five replicates were split in two and half were enriched with $^{15}NH_4Cl$ resulting in a concentration of 0.13 mg/g (final soil enrichment of 12 atom % $^{15}NH_4^+$), while the remaining 5 samples received $^{15}KNO_3$, corresponding to 0.64 mg/g (final soil enrichment of 4 atom % $^{15}NO_3^-$). For the final incubation, 3 set of samples consisting of 6 replicates each were collected at 20, 50 and 120 cm. For each set 3 replicate were labelled with ammonium with and 3 with nitrate. In particular (based on the background concentrations) the first two sets received $^{15}NH_4Cl$ and $^{15}KNO_3$, resulting in concentrations of 0.01mg/g and 0.12 mg N/g soil, respectively. The third set was enriched with $^{15}NH_4Cl$ and $^{15}KNO_3$, resulting in 0.27 mg N/g soil and 0.011 mg N/g soil, respectively for a final enrichment for all the sets of 60 atom % $15NH_4^+$ and 30 atom% $^{15}NO_3^-$. Each sample was incubated in a 225-mL jars under ambient conditions at a temperature of 25 °C. The enrichment level was chosen according to the background concentration. In both enrichment experiments, gas samples have been collected after 15 minutes and 3 hours of incubation. (Figure 3.9)

3.4 Field Measurements

Field measurements include fluxes measured through the eddy covariance towers and chambers data collected along 5 transect as describe in chapter 4. Data has been collected as a part of a larger-scale project on the Bay Delta by Yit Arn Teh, Matteo Detto and Benjamin Reade Kreps Runkle during years 2007, 2008 and 2009. Figures 3.10 and 3.11 show

Figure 3.10: Gas samples collection with chambers in the pasture peatland of Sherman Island, Bay delta area, California.

the Eddy Covariance tower used to measure carbon dioxide, methane and water vapor fluxes, and the gas samples from the filed chambers.

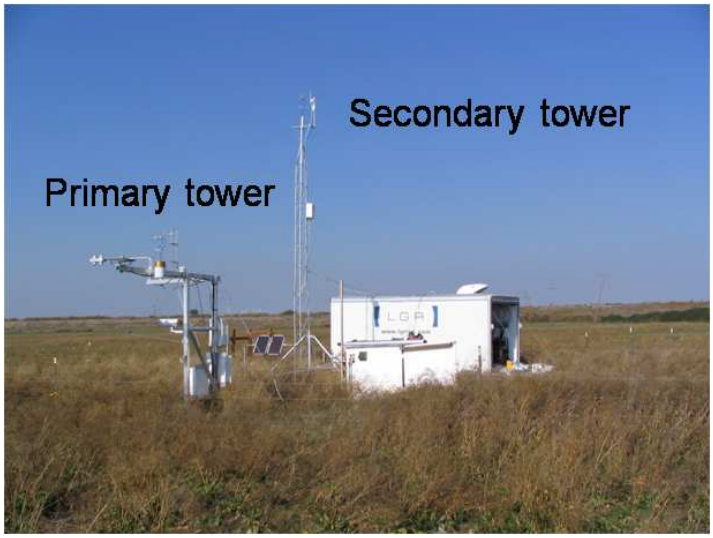

Figure 3.11: Eddy covariance tower in the pasture peatland of Sherman Island, Bay delta area, California.

3.5 Analysis

Saturated hydraulic conductivity was measured using a constant head permeameter and water content at field capacity was determined as the amount of VWC held in the soil after excess water has drained by gravity. Initial C and N were measured on a CE Elantec

elemental analyzer at UC Berkeley. Initial nitrate (NO_3^-) and ammonium (NH_4^+) was determined after extraction in 2M KCl on a Latchat autoanalyzer (Loveland, CO).

Gas fluxes from the head space of the soil column and in the field were measured by following the procedure described in Matthias et al. (1978). Samples were collected at 0, 5, 10, 20 and 40 minutes. To calculate the fluxes equations 3.1 and 3.2 are used, where C_o is the trace gas concentration of gas, C_a is the air concentration, D is the diffusion of the trace gas, L is the depth and H is a factor accounting for the shape of the chamber.

Fluxes per unit area at $t = 0$ were measured by equation (5.1), after data were fit with equation to determine the value of C_0 and the D/l ratio through an iterative process (Matthias et al., 1978).

$$C(x,0,t) = C_o - (C_o - C_a) \cdot e\left(\frac{D \cdot t}{L \cdot H}\right) \tag{3.1}$$

$$F = (C_o - C_a) \cdot \frac{D}{L} \tag{3.2}$$

Gas samples along the profile were immediately measured on Schimadzu GC 14 gas chromatograph (GC) for methane (flame ionization detector), nitrous oxide (electron capture detector) and carbon dioxide (thermal conductivity detector). Liquid samples collected in the micro-lysimeter were measured for dissolved NO_3^- and NH_4^+ on a Lachat Colorimeter (Lachat Quik Chem flow injection analyzer, Lachat Instruments, Milwaukee, Wisconsin) and for dissolved nitrous oxide according to the procedure described by Reay et al. (2003). We determined NO_3^- and NH_4^+ concentrations from KCl extracts colorimetrically (Colorimeter: Lachat Quik Chem flow injection analyzer, Lachat Instruments, Milwaukee, Wisconsin). Extracts were prepared for isotope analysis by diffusion (Herman et al., 1995), and N isotope ratios were measured using an automated nitrogen carbon analyzer coupled to an isotope ratio mass spectrometer (ANCA-IRMS; PDZ Europa, Limited, Crewe, UK). We determined N_2O by gas chromatography using a 63Ni detector (Europa Scientific, Cheshire, UK), and determined N-gas isotope ratios using a trace gas module coupled to an IRMS. We calculated rates of dissimilatory NO_3^- reduction to NH_4^+ (DNRA) as the difference in the $15NH_4^+$atom % between sampling periods, multiplied by the mean NH_4^+ pool size during the interval, and corrected for the mean residence time (MRT) of the NH_4^+ pool. This was then divided by the mean $^{15}NO_3^-$atom % during the interval to account for the isotopic composition of the source pool (Silver et al., 2001). We used individual MRT values generated from each treatment. Gross mineralization, nitrification, and NH_4^+ and NO_3^- consumption were calculated according to Kirkham and Bartholomew

Figure 3.12: Soil extraction with 2MKCl to measure nitrate and ammonium concentration from the soil column, Whendee Silver's laboratory, UC Berkeley, USA.

(1954). VWC was determined gravimetrically after oven drying sub-samples at 105 °C to a constant mass. Finally, ^{15}N abundance was measured as described above after extracting 30 g of soil with 150 ml of 2 mol/l KCl, while Nitrification potential was measured according to Hart et al. (1994). Total iron (Fe) was measured following extraction in 2 M KCl extractions were measured for total iron using on the atomic absorbance method spectro-photo-meter. This was done in accordance with the Standard Method Soil Science Handbook (Van Loon, 1980).

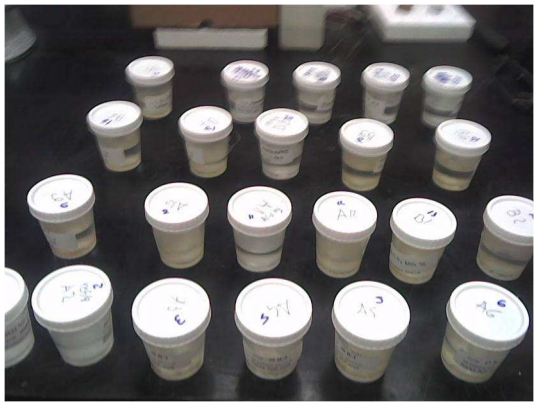

Figure 3.13: Specimen cups used to diffuse enriched 2MKCl soil extraction to measure N-cycle rates, Whendee Silver's laboratory, UC Berkeley.

4 Micro-site Scale: Soil Column and Incubation Experiments

4.1 Overview

As described in previous chapters, soils are a dominant source of nitrous oxide (N_2O), a potent greenhouse gas. The complexity of drivers of N_2O production and emissions has hindered our ability to predict the magnitude and spatial dynamics of N_2O fluxes. Soil moisture can be considered a key driver because it influences oxygen supply, which feeds back on N_2O sources (nitrification versus denitrification) and sinks (reduction to dinitrogen). Soil volumetric water content (denoted by VWC) is directly linked to dissolved oxygen and to redox potential, which regulate microbial metabolism and chemical transformations in the environment. Few studies have focused on the interaction between soil moisture and nitrogen dynamics in the vadose zone. Column and chamber experiments were used to investigate the relationship of soil moisture dynamics to redox sensitive nitrogen dynamics in the organic matter layer of an irrigated peatland in Sacramento, Bay Delta area, California.

The experiment was run from Julian days 272 to 334, for a total of 62 days. The column experiment included a sequence of typical hydrological conditions (Table 4.1). During this period the dissolved N-species and the N_2O gas samples were collected during 7 to 8 sample periods (Table 4.2). Dissolved NO_3^-, NH_4^+ and trace gases were measured during the following hydrological conditions:

Monitoring Chronogram								
Time (Julian calendar)	272	273-278	279	288	290-302	322	326-328	334
Event	Column packed	Monitoring period	Rainfall event	Rainfall event	Flooding event	Rainfall event	Deposition event	Column destructed

Table 4.1: Experimental Chronogram.

Measures	Timing of acquisition
Gas samples	Julian days: 274, 278, 283, 318, 322, 326, 331, 334
Liquid Samples	Julian days:279,288,302,322, 326, 328, 331
VWC, EC, T ,O2 and redox	1 during the events , 5 min otherwise

Table 4.2: Timing of data acquisition.

1. Low VWC, which represented the typical dry soil conditions during seasonal drought (from day 272 to day278);

2. Intense rainfall events (days 279, 283, 322), corresponding respectively to 8 minute (Julian day 279) and 5 minute rainfall events (Julian days 283, 322) with a constant intensity of 80 mm/h ;

3. Flooding event (from day 290 to day 302) when the water table rose from 130 cm to 82.5 cm depth and;

4. Nitrogen deposition (from day 326 to day 328), when the column was saturated from below with a solution of NO_3^- equivalent to 30 Kg/Ha yr, followed by drainage. Incubation experiment were performed on Julian days 272 and 334, as described in Table 4.1.

Given the climate forcing and the system of internal ditches which regulate the water table, both rainfall and fluctuation events characterizes the Bay Delta area, and are therefore interesting to investigate (see Chapter 2).

The target os these experiments is to better understand the mechanisms which regulate trace gas production conditions in a controlled environment under static (chamber incubation) and dynamic (soil column experiment) moisture conditions. Results and discussion are presented in the following sections.

4.2 Experimental Pre-Run

A preliminary experiment was conducted in May 2008. The experiment was done by keeping the room temperature constant at 9 °C (see Chapter 5), which is the average annual temperature for the field site. The soil used was homogenized (a *cooler device* with

30 kg of soil was lightly mixed for 30 minutes by hand) and analyzed for initial chemical properties. The experimental pre-run indicated that:

- The PVC tube has a CO_2 signature less depleted than air. This implies that the free atmosphere in the PVC tube yields a CO_2, concentration of 470 ppm relative to the 373 of background (lab) air.
- The dissolved N_2O was very high (the CG was saturated) and it was possible to detect a peak of $^{15}N_2O$ at natural abundance level.
- The water contained detectable nitrate and ammonium.

After this preliminary experiment, we decide to use enriched isotopes, given the high amount of gas needed (100 ml) to perform natural abundance analysis, which required multiple collections from gas ports, with the problem of fraction action effect (Hoefs, 2008).

4.3 Comparison of Static and Dynamic Conditions

4.3.1 Initial Condition of the Soil

The soil used in the experiment was dominantly organic matter with almost no clay component and had an initial N concentration of 1.2 % and 18.8 % C, yielding a C:N ratio of 18. At the time of collection, the peat soil had a saturated hydraulic conductivity of K_s= 2.6×10^{-6} m/s, and field capacity θ_{fc}= 0.23. There were 14 μg N/g of NO_3^--N, and 0.8 μg N/g of NH_4^+-N (with VWC equal to 0.35).

4.3.2 Soil column

Rainfall Events versus Changes in Water Table

The column was kept airtight from Julian day 273 to Julian day 278 when reareation of the system was inhibited. When the top was opened to the atmosphere, O_2 diffused quickly through to the bottom, where the concentration increased from 5% to 12 %. During the drainage process, O_2 also increased in the deeper layers (Figure4.2).

The soil column experiment allowed us to monitor the response of the soil to rapid changes in water content resulting from rainfall events and changes in water table elevation. On Julian days 279, 283 and 322 a 8 minutes and 5 minutes (for days 283 and 322) rainfall event with a constant intensity of 80 mm/h were applied to the column. Soil moisture

increased by 50% of its initial value during the first rainfall event and 30% in the second and third event. The water reached 50 cm depth after 10 minutes of the beginning of the events, while the bottom of the column was reached respectively 6 days later for event on Julian day 279, 1.5h and 7.5h later for events on Julian days 283 and 322, as detected by soil moisture sensors (Figure 4.1). Changes in water table level were performed twice:

- On Julian days 290-302, the water table was raised from 130 cm to 82.5 cm;
- On Julian days 326-328, a deposition event was performed. This event is composed by the saturation of the column from below with a solution of nitrate equivalent to a fertilization of 30 Kg/Ha yr, followed by drainage (Figure 4.7).

A closer inspection of Figure 4.7 reveals that at the end of the rainfall event, VWC is 10% higher than its initial value before the event started and it does not decline with time until the start of the saturation experiment. In particular, after the third rainfall event, soil moisture stayed elevated to a slightly higher value for 50 hours while, after the deposition event, VWC went immediately back to 0.25. An increase in soil O_2 concentrations and the redox potential were observed at 82.5 cm depth (Figure 4.2) during the rainfall event on Julian day 279. Later rainfall events resulted in a decrease of O_2 and redox (Figure 4.2 and 4.3). For instance on Julian day 322, redox decreased for both sensors of 20 mV and oxygen of 1% (average value along the column depth). Saturation from below caused a more severe depletion of O_2 and redox potential than the rainfall events. We observe a quick drop in the redox potential followed by a rebound when the column drained. At the end of the deposition event, and the redox potential increased with respect to its initial value at the depth of 22.5 cm and became more reduced at the depth of 82.5 cm. Also oxygen concentration after the saturation of Julian days 290-302, went back to the same value only on day 320 (Figure 4.2).

The water dynamics of the soil column thus showed a different behavior for rainfall events than for changes in water table. Soil moisture time series indicate that rainfall events may trap water into soil, while after oscillation of the water the table, soil does not retain water. This different behavior is linked to the holding capacity of the soil aggregates within small pores. Aggregates filled with water during the rainfall experiment because of their high capillary pressure do not drain in the successive period, which precedes the saturation experiment (Or et al., 2009; De Gennes et al., 2004).

At the beginning of the deposition event, at day 326, a fraction of the pores was not accessible and did not participate to the following saturation/drainage cycle. Consequently, drainage could empty only the pores that were not already occupied at the beginning of

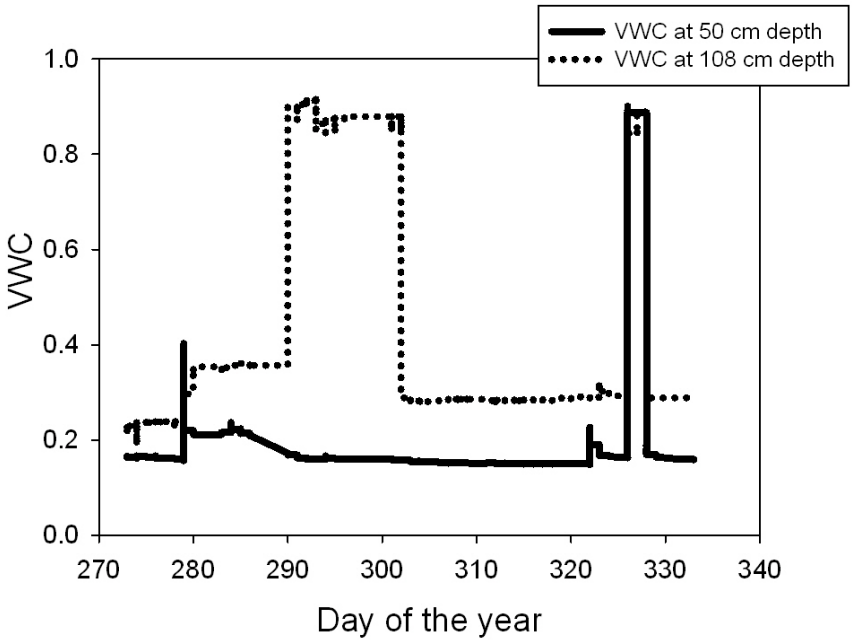

Figure 4.1: Time series of volmetric water content (VWC).

the deposition experiment, thus explaining why at the end of drainage stage, VWC was the same as at the beginning of the saturation phase, but larger than the VWC before the rainfall event. This is confirmed by the oxygen concentration at both the depths of 73 and 108 cm, which does not recover to its initial value after the rainfall event, and before dropping because of the saturation (see days from 323 to 326). Overall, we observe that variation in water content, such as those caused by the short and intense rainfall at Julian days 278 and 322, triggered variations of oxygen concentration and redox potential acting on time scales much larger than that of the VWC variation.

Nitrous Oxide Emissions versus Soil Moisture, Oxygen and Redox.

Figures 4.4 and 4.5 show N_2O fluxes versus VWC at several depths from day 318 to day 333 and day 318 to day 325, respectively. The first period includes the intense rainfall event, while the second includes the deposition event. Notice that only in the second case we reached fully saturation. As expected, emissions during the deposition event are larger as a consequence of the higher NO_3^- concentration.

Nevertheless, N_2O emissions show a much complex behavior with respect to VWC. In particular, we evidence the counterintuitive result that the highest emissions are observed

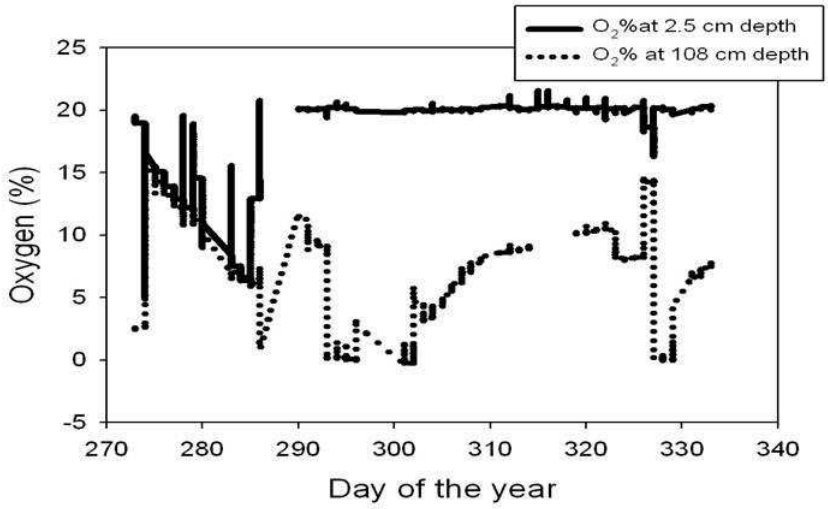

Figure 4.2: Time series oxygen (O_2%).

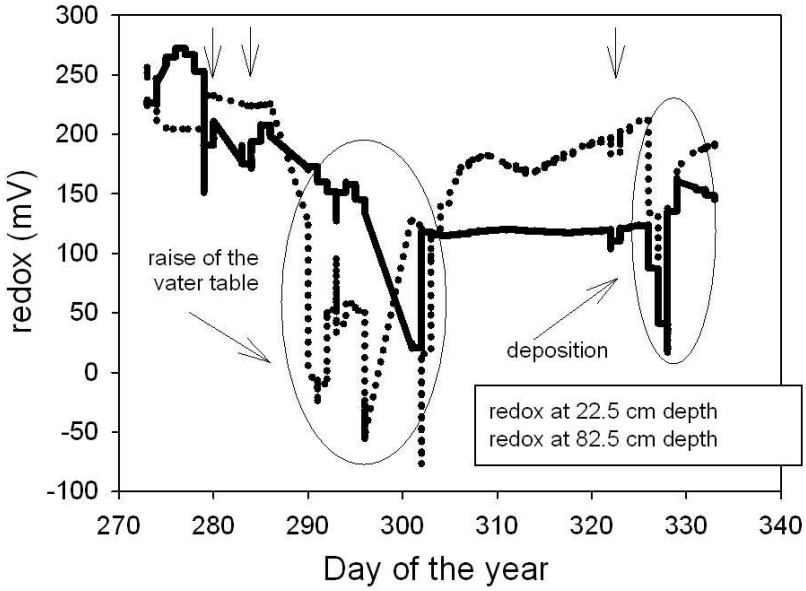

Figure 4.3: Time series of redox (mV).

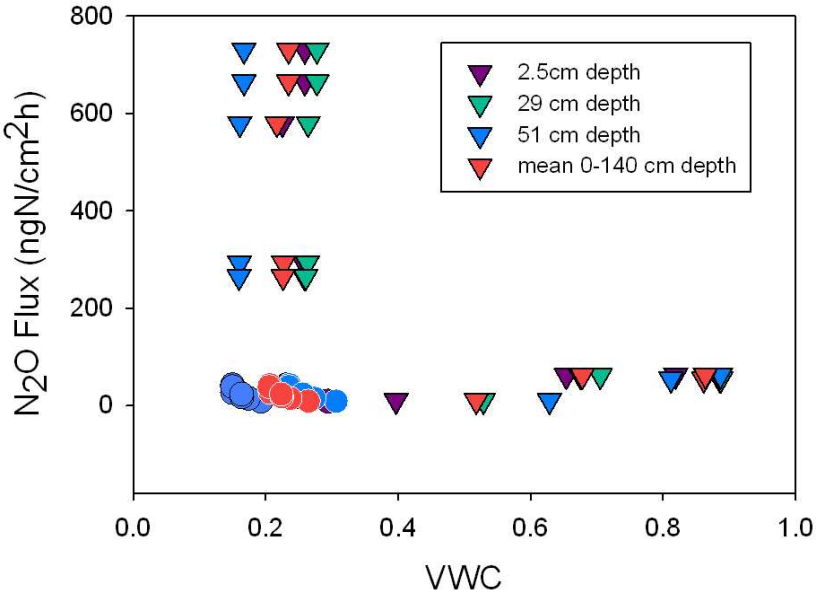

Figure 4.4: Fluxes of nitrous oxides (N_2O ngN/cm^2/h) versus volumetric water content in dynamic condition. Triangles refer to depostion event, while dots refer to rainfall event.

for the lowest VWC. The two limbs of the deposition experiment seem to belong to different data groups. During drainage, N_2O emissions are higher for lower water content, while the opposite is observed for the saturation limb. During the rainfall experiments VWC shows smaller variations with respect to the deposition event, and contrary to what was expected emission reduces as VWC increases, possibly due to delay of the microbial activity with respect to VWC variations.

To further investigate this behavior, N_2O emissions were plotted as a function of O_2 (Figure 4.14) and redox (Figure 4.6) concentrations. Low oxygen concentrations values, during the drainage limb of the deposition experiment, lead to high emissions, while intermediate emissions are observed at the intermediate oxygen concentrations typical of the saturation limb. Rainfall events are characterized by higher oxygen concentrations, and thus they result in smaller emissions, as shown by the open circles in the Figure 4.14. Altogether, the data suggest a functional dependence of N_2O emissions on oxygen concentration, with most of the experimental data grouped around the exponential regression curve.

In this case we find a consistent behavior with the emissions which are larger for

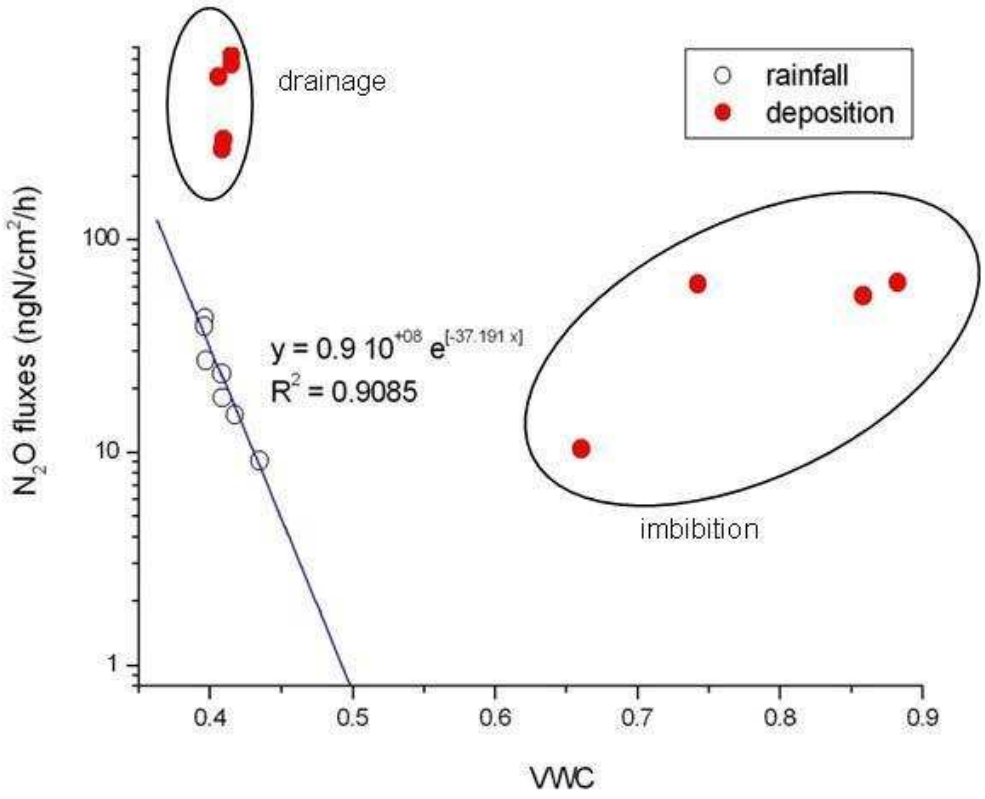

Figure 4.5: Regression, fluxes of nitrous oxides (N_2O ngN/cm^2/h) versus volumetric water content in dynamic condition.

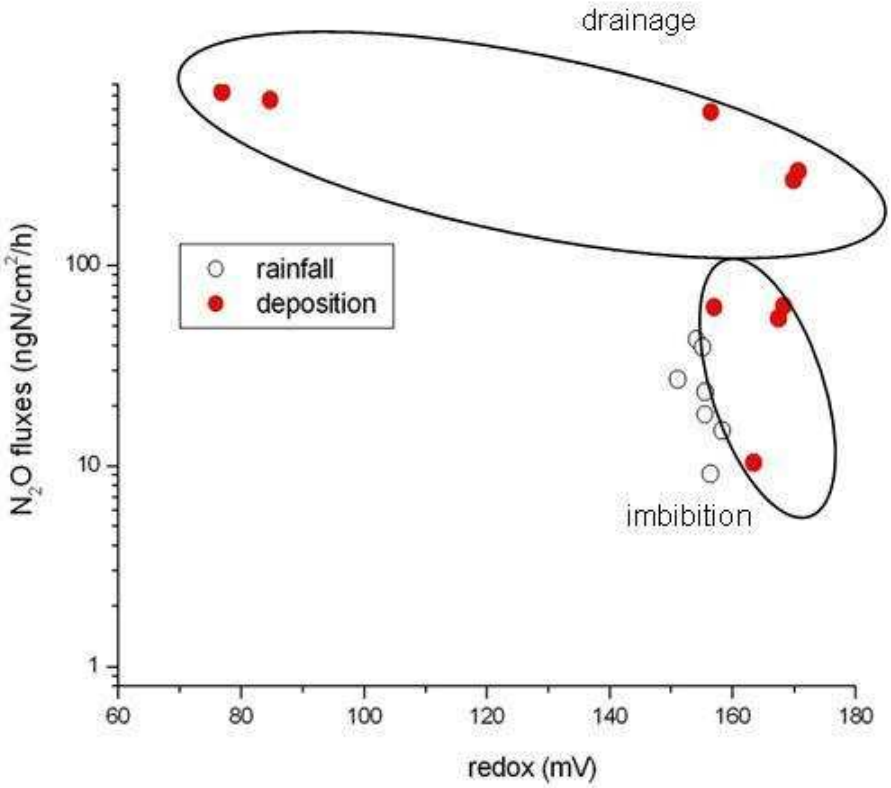

Figure 4.6: Regression, fluxes of nitrous oxides (N_2O ngN/cm^2/h) versus redox in dynamic condition.

smaller O_2concentrations. Consequently, emissions were preferentially produced when oxygen concentration was low, thereby favoring the emissions from anaerobic sites. The data do not suggest possible functional relationship of N_2O emission with redox (Figure 4.6).

Regression correlation coefficients (Table 4.3) shown that both N_2O and CO_2 trace gas missions has a high negative correlation with oxygen concentration. Similarly, correlations are observed between both N_2 and CO_2 trace gas emissions and VWC. Correlations with all the measured quantities does not inform much about the system's dynamics.

On Water Dyamics and Nitrous Oxide Emissions

The column experiment unveiled a complex and nonlinear relationship between the nitrogen cycle and VWC dynamics triggered by the external meteorological forcing, but that also depends on the hydraulic properties of the soil. The rising of the water table

Ranking correlations	**VWC** -	**O_2** [%]	**redox** [mV]	**N_2O** [ngN/cm^2/h]	**CO_2** [μgC/cm^2/h]
VWC -	1	0.946 dep.	0.786 no dep. -0.632 deep sensor	-0.946 no dep. -0.836 dep.	**-0.654**
O_2 [%]		1	0.632 dep.	**-0.751**	-0.876 no dep.
redox [mV]			1	-0.566 deep sensor	-0.861 no dep.
N_2O [ngN/cm^2/h]				1	0.610 no dep. 0.8013 dep.
CO_2 [μgC/cm^2/h]					1

Table 4.3: Matrix of Ranking Correlation for volumetric water content (VWC), oxygen (O_2), redox, nitrous oxide emissions (N_2O) and carbon dioxide (CO_2) (No dep. indicates days 318-325, dep. includes days 326-33, while "deeper sensor" refers to the redox sensor at 82.5 cm depth).

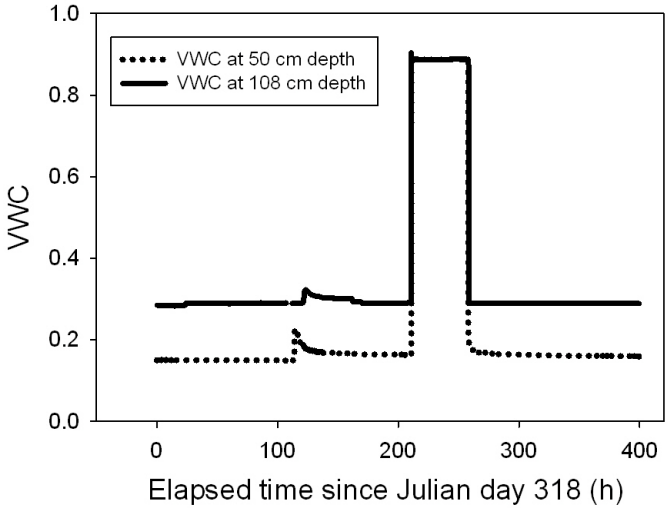

Figure 4.7: Time series of volumetric water content (VWC) comparing rainfall versus deposition.

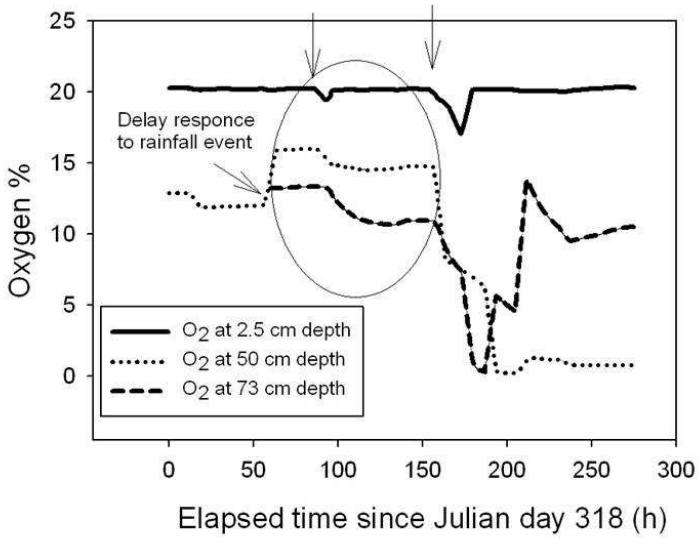

Figure 4.8: Time series of oxygen (O_2%) comparing rainfall versus deposition.

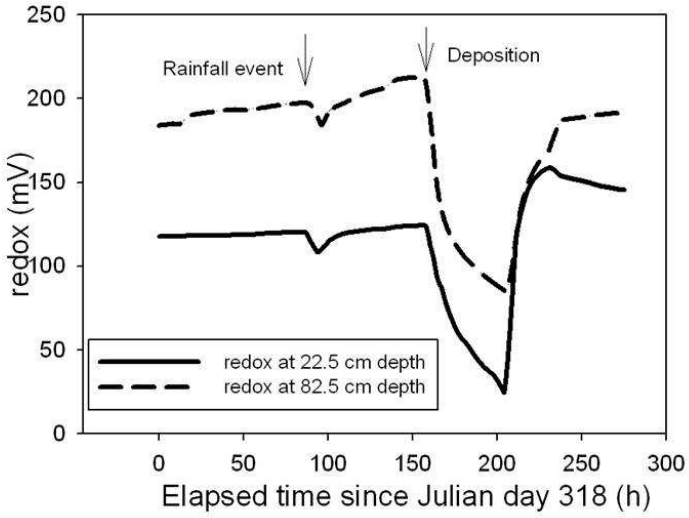

Figure 4.9: Time series of volumetric redox (mV) comparing rainfall versus deposition.

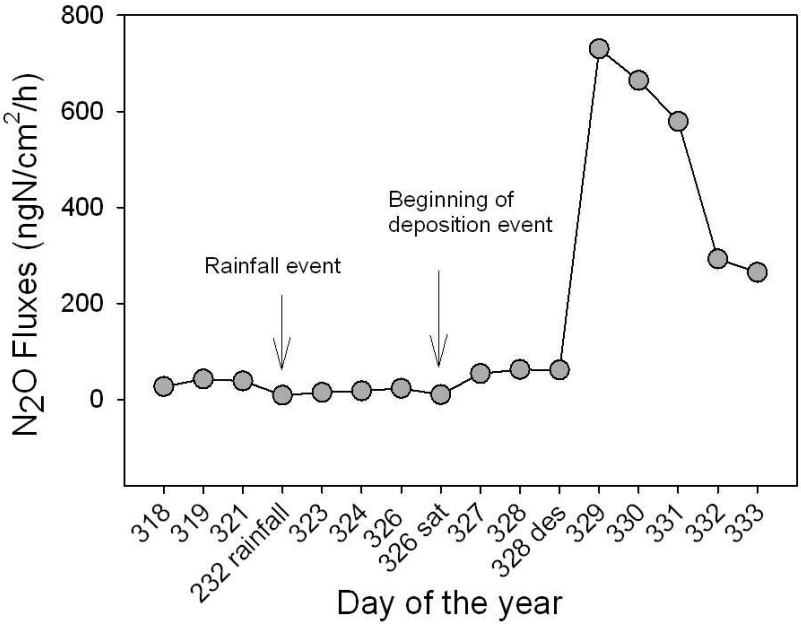

Figure 4.10: Time series of nitrous oxide emissions (N_2O ngN/cm^2/h) comparing rainfall versus deposition.

mobilizes nitrate and ammonium that were transported close to the column surface from the deep of the column. Here they encountered different oxygen, redox and biological conditions, which resulted in higher gas emissions than in the case of infiltration from above, due to rainfall (Figure 4.10). This complexity contrasts the apparently simplicity of the relationship between N_2O emissions and VWC described by the Davidson's diagram and extensively used in modeling N_2O emissions (Davidson, 1991, 1993). Davidson (1991) devised a theoretical scheme in which N_2O emissions depend only on the *Water Filled Pore Space* (WFPS), which is given by the ratio between VWC and porosity. The author assumed that when WFPS is less than 0.5, the soil does not emit N_2O. The emission of N_2O increases rapidly for larger relative saturations, peaking at WFPS equal to 0.75 and then finally decreasing again to zero at WFPS equal to 1, when fully saturated conditions are reached (see Figure 4.11). This diagram depends on soil and biological characteristics of the ecosystem and is typically obtained by performing incubation experiments in jars equilibrated to a given VWC, thus after the soil "adapt" to water content conditions (Schindlbacher et al., 2004).

The striking result here is present in Figure 4.4. We observe larger N_2O emissions for lower VWC, a result that seems to contradict the Davidson (1993) scheme which is based

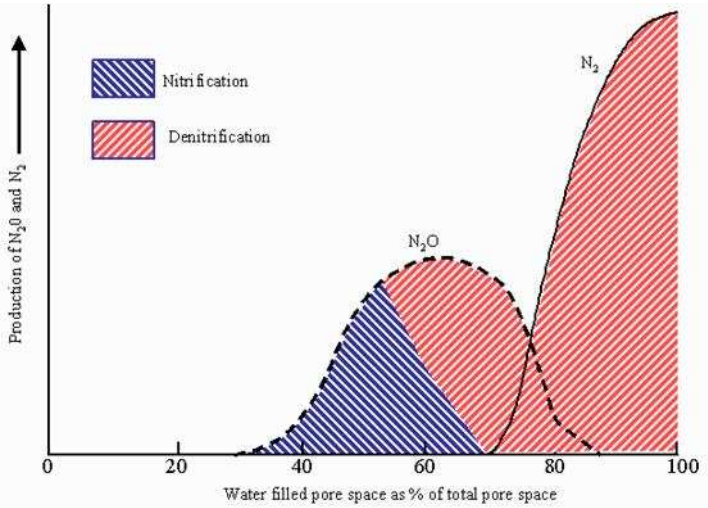

Figure 4.11: Relationship between water filled pore space (WFPS) and nitrous oxide emissions (N_2O) proposed by Davidson (1993).

on the results of incubation experiments conducted in equilibrium conditions, *i.e.* a point in the Davidson's graph is obtained by measuring N_2O emissions in an incubation (jar) experiment conducted at constant VWC. This behavior is mainly due to the fact that in hydrologically realistic situations such as those reproduced in our column experiments oxygen variation is delayed with respect to the pulse of VWC, thus resulting in a delayed N_2O emission (Figure 4.12).

In other words, the time scale of VWC is shorter than the characteristic time scale of trace gases, and of N_2O in particular. The time required by the soil to drain is much less than the time required by bacteria to produce trace gases and the time needed to the nitrous oxide to be emitted. Therefore, assuming that emissions can be computed by means of the empirical relationship between N_2O emissions and VWC obtained from jars experiments, whenever accurate they are, may lead to inconsistent results. Furthermore, due to the complex nonlinear relationship between N_2O emission and VWC, the results cannot beneficiate from averaging over longer time steps, for example by using mean daily values of VWC.

The critical assumption concerning this approach is that the time scales of biotic and abiotic processes are nearly the same, such that the dependence of the emissions from VWC can be obtained by means of incubation (jar) experiments. In each incubation experiment, VWC is kept constant and the flux of N_2O is measured as the ratio between the total cumulative emission per unit surface and the duration of the incubation. The

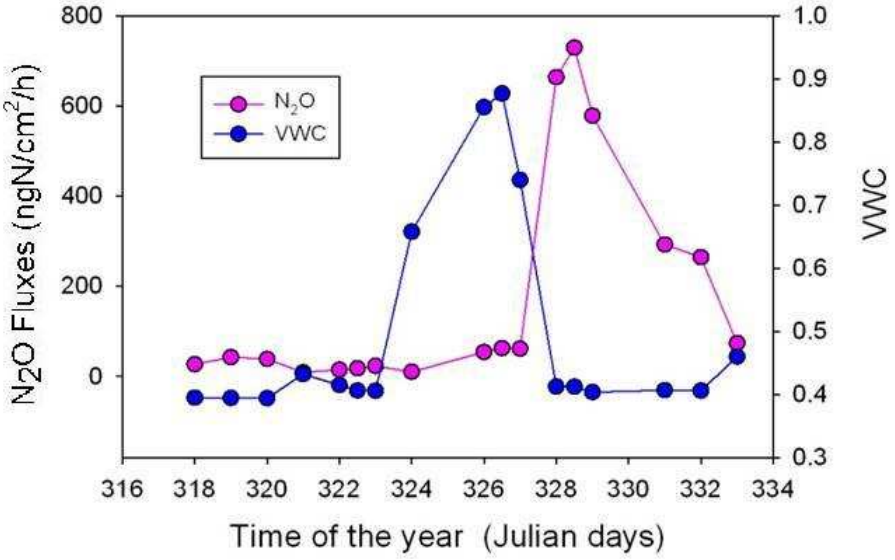

Figure 4.12: Time series of weight mean values of oxygen (VWC) and nitrous oxide emissions (N_2O) in ngN/cm^2/h.

dependence of the emission from VWC is therefore obtained by repeating the incubation experiment with different VWC. Since the typical duration of an incubation experiment is of several hours, one should recognize that it does not represent field conditions where significant variations of VWC occurs over much shorter time scales. Therefore, strictly speaking the Davidson's diagram, obtained from long term incubation experiments, can be applied to field scale studies only if the relationship between N_2O emission and VWC can be approximated as linear and this is mainly dependent of the physical and biological properties of the soil.

Delayed Oxygen Response

Although VWC is nearly constant between the surface and column depth of 73 cm, near the surface, oxygen concentrations are much higher and less influenced by VWC content than at depth (see Figures 4.1 and 4.2). This can be due to the fact that the pores at 2.5 cm from the surface are open to the air in the void between the soil and the top of the column. The delay in oxygen consumption with respect to water content increases is likely a result of the physical properties of the soil which control the propagation of water in the soil corresponding to the external climatic forcing and also to the bacteria activity.

Also, this delay might be related to the coupling of microbial respiration and physical destruction of protected organic matter during cycles of wetting/drying. (Schimel et al., 2007), found that after water addition, a flux is release with additional carbon than the one contained in the biomass. The delay in oxygen may thus be related to the use of this carbon by bacteria as shown in Figures 4.13, or more simply by the time required by bacteria to switch from nitrification to denitrification (which has been measure to be about 1 day).

In addition, Figure 4.14 show a clear, although noisy, dependence of N_2 O emission from O_2 concentration. The data referring to the increasing and decreasing limbs of the deposition experiments, when the column is first saturated with water rich of nitrate, and successively drained are shown with closed red symbols in Figure 4.14. We can conclude that emissions resulting from rapid floods events, *i.e.* a rapid saturation followed by a rapid drainage, can be better reproduced by considering their relationship with oxygen concentration, rather than with VWC. A high correlation is observed between N_2 O emissions and VWC during rainfall events, though the data suggest a negative correlation between the emissions and VWC, rather than a positive correlation as assumed in most applications, owing to the reduction oxygen concentration when equilibrium is obtained (constant water content). Probably, the delay of the oxygen reduction following an increase of VWC is responsible of what can be considered as a counterintuitive behavior of N_2 O emission with respect to VWC. Overall, the dependence of N_2 O emissions from the oxygen concentration is the only showing predictive capabilities over a wide range of VWCs.

4.3.3 Chamber incubation

Jars incubation experiments are mainly dependent on the condition of the soil at the moment of the sampling. For that reason, we perform incubations at both the beginning and the end of the soil column experiment (Table 4.1). The objective of this experiment was to measure the overall effect of water dynamics on the cumulative emissions of N_2O and the N-cycle rates (*i.e.*, mineralization, nitrification, DNRA, average residence time and pool size), during our experiment which includes a short and intense rainfall event and saturation from below (*i.e.*, flooding conditions) with deposition. These two situations are typical in the Bay Delta peat land area. Chambers also provided an idea of the temporal scale required by the mesocosm to move from aerobic to anoxic condition, which indirectly reflected the predominance of denitrification vs nitrification conditions. Based on these values we decided to extend the saturation period from Julian day 290 to Julian day 302,

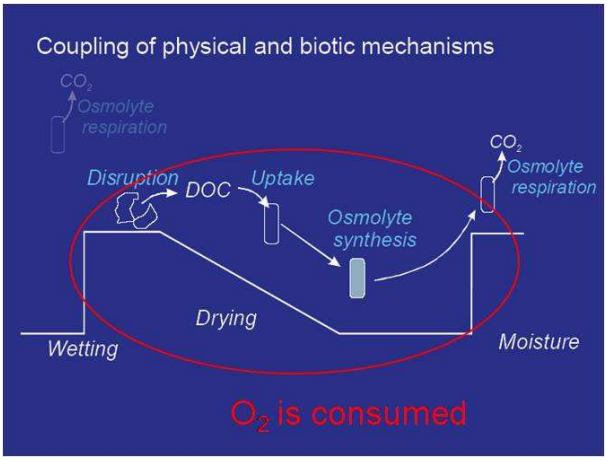

Figure 4.13: Wet/dry cycle, multiple destruction of protected organic matter, and oxygen consumption. Modified Shimel, 2007.

in order to create prolonged anaerobic conditions and a two days saturation period for the addition of water with nitrate (deposition experiment on Julian days 326-328), to measure the effect of irrigation with water rich in nitrate. N_2O emissions vary as a consequence of rapid variations in VWC due to the meteorological forcing, a situation which represents field situation much better than jar experiments.

Incubation Experiment on Julian Day 372

The column has been prepared on Julian day 272 by inserting the soil, sensors, gas and liquid ports in the column. During this process, soil samples with VWC = 0.35 has been collected and incubated according to the procedure described previously in this dissertation. Nitrate pool (see Figure 4.15) was large in the pre run extraction (36.12±1.59 μg N/g soil) and increased at the beginning of the incubation experiment while ammonium pool measured in the pre-run was relatively small (4.51±0.44 μg N/g soil) and similar to that at the beginning of the incubation.

Both $^{15}NH_4^+$ and $^{15}NO_3^-$ pools declined during the 3h incubation time; the former from 0.64± 0.06 μg N/ g soil to 0.16±0.03 μg N/ g soil, and the latter form 2.59±0.14 μg N/ g soil to 1.77±0.32 μg N/ g soil. Gross mineralization rate was 45.3±5.2 μg/g/d, gross NH_4^+ consumption was 54.37±13.9 μg/g/d, while the mean resident time was of 0.1 d. The emissions of nitrous oxide were low (see Figure 4.17), but higher emissions were detected after the addition of ^{15} NH_4^+ than $^{15}NO_3^-$. This indicates that the nitrification or nitrifier denitrification could be an important source of nitrous oxide emission from this soil. In

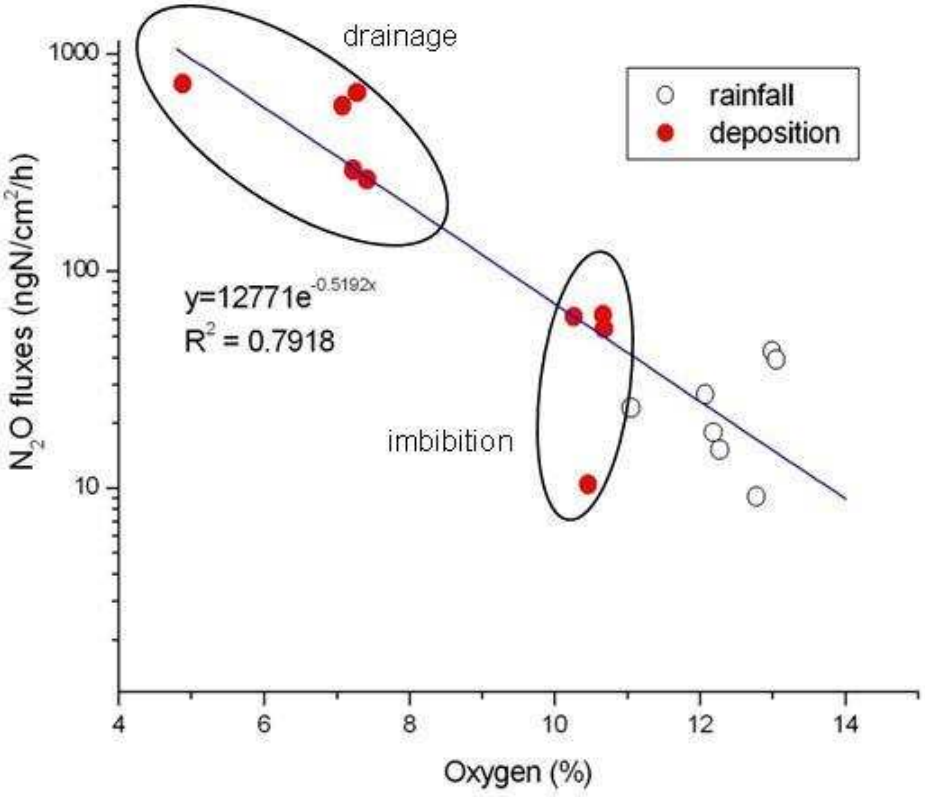

Figure 4.14: Regression, fluxes of nitrous oxides (N_2O ngN/cm^2/h) versus volumetric water content in dynamic condition.

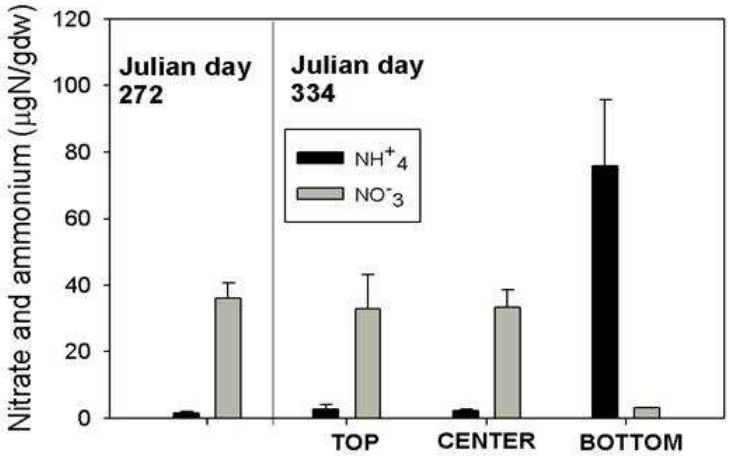

Figure 4.15: Comparison of nitrate (NO_3^-) and ammonium (NH_4^+) extracted with 2MKCl at the beginning of the soil column experiment on Julian day 272 and at the end on Julian day 334, when a gradient of VWC was present.

particular, we measured 0.007 μg/g/d and 0.002 μg/g/d of $^{15}N_2O$ after ammonium and nitrate addition, respectively. Thus for the soil collected before the rain season started (VWC average 0.35), we measured fast pool changes given by potential mineralization and nitrification rate, while in this condition DNRA was not significant. We repeated the jars experiments after sieving the soil obtaining larger emissions in wet conditions and lower emission in dry conditions (data not sown here). Therefore, soil structure in addition to texture and VWC, influences tracer gas emissions.

Finally, the rate of atmospheric oxygen consumption in the headspace over time in dry and wet conditions was measured under both unsaturated (aerobic) and saturated (anaerobic) conditions, the latter has been obtained by letting the water to pond on the surface after saturation from below. We found a consumption of 4.17% of the initial value per hour in anoxic condition and a consumption of 1.6% of the initial value in aerobic condition, indicating that bacteria activity was enhanced in flooded condition.

Incubation experiment on Julian day 334

The incubation process was repeated on Julian day 334 with soil collected at 2.5 cm, 60 cm and 120 cm depths according to the VWC and oxygen gradient registered by the sensor after the deposition event what follows we denote these three sampling points as top, center and bottom. Sensors, on day 329, indicated a VWC gradient along the profile moving from: 0.27 at the depth of 2.5 cm to 0.88 at the depth of 110 cm, while the

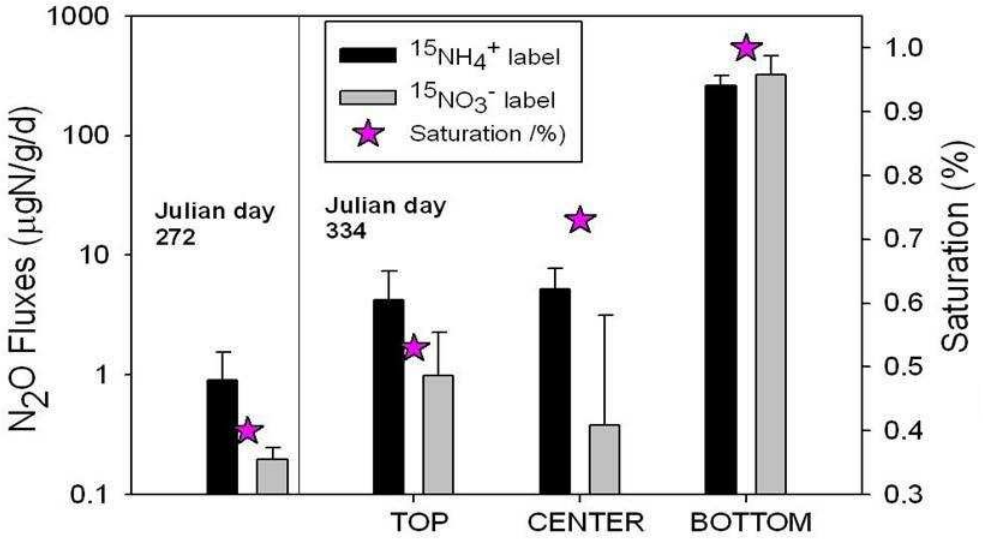

Figure 4.16: Comparison of nitrous oxide emissions (N_2O in $\mu gNg^{-1}d^{-1}$) measured at the beginning of the soil column experiment on Julian day 272 and at the end on Julian day 334, when a gradient of VWC was present.

atmospheric oxygen was 20% at 2.5 cm depth, 10% at 50 cm depth and finally, 1% at 108 cm depth (the soil ad the depth of 108 cm is often in nearly saturated conditions).

Pre-pool dilution run analysis evidenced a different behavior of the soil from surface to the depth of 80 cm and the underneath soil from 80 to 140 cm as a response of the soil to the cycles of VWC, oxygen and redox. Figures 4.15 and 4.16 evidence that at the bottom soil sample (*i.e.*, the sample taken at the depth of 120 cm) undergoes a significant reduction of both nitrate and ammonium concentrations, accompanied by high N_2O fluxes. At day 334, top and center samplers have a small ammonium pool (3.2±0.9 μg N/g soil for the top and 2.4±0.2 μg N/g soil for the center) and a large nitrate pool (32.9±10.2 μg N/g soil for the top and for the center 33.4±5.3 μg N/g soil), while at the bottom of the column the ammonium pool is extremely large (49.0±9.6 μg N/g soil) and nitrate pool (3.2±0.03 μg N/g soil) is one order of magnitude smaller than that measured in the range 0-80 cm (Figure 4.15).

On day 334, after 3 hours of incubation $^{15}NH_4^+$ decreased in all samples with a relative reduction with respect to the initial value that ranges from 45%, to 58% and 63% moving from top, to center and bottom samplers, respectively.$^{15}NO_3^-$ also decreased. Mineralization rates and NH_4^+ consumptions at the top (34.2±3.4 μg/g/d and 35.9±3.8 μg/g/d) and center (39.8±6.9v and 40.3696±5.9 μg/g/d) of the column were similar to those measured

	Gross Mineralization	*Gross Nitrification*	*DNRA*	N_2O fluxes $^{15}NH^+_4$ label	N_2O fluxes $^{15}NO^-_3$ label	Saturation Degree
Top	34.2	614	0.01	0.99	4.2	0.53
Center	39.8	335.7	0.02	0.38	5.2	0.73
Bottom	1187.4	3.7	0.39	323	363	1

Table 4.4: N-cycle rates in μgN/g/d and nitrous oxide emissions (N_2O) in ngN/g/d, and saturation degree measured on Julian day 334

on Julian day 272 before starting the column experiment, while both rates consistently increased at the bottom (1187.4±460 μg/g/d and 1222.3±519 μg/g/d). Furthermore, MRT was 0.02d at center and top samplers and 0.08 day at bottom.

Table4.4 shows that at the Julian day 334, gross nitrification and nitrate consumption were both higher in the upper part of the column (*i.e.*, from surface to the depth of 80 cm) than in the deeper part (*i.e.*, from 80 cm to 140 cm). Similarly, DNRA rates increase with depth, see Table 4.4. This indicates that the saturation of the soil at the bottom of the column lead to an asymmetrical behavior of the upper part, which results in high potential for nitrous oxide emissions and for leaching. We detect indeed supersaturated dissolved N_2O concentration as high N_2O values in gas samples. These differences in rates are also reflected in N_2O emissions (Figures 4.16 and 4.17). Jars incubation with soil collected from the top and the center of the column, where O_2 concentrations was higher, showed small N_2O emissions, while at the bottom the fluxes were much higher (for nitrate label: 0.99±1.2 μg/g/d in the top, 0.38±2.7 μg/g/d in the center and 323±138 μg/g/d in the bottom; for ammonium label:4.2±3.13 μg/g/d in the top, 5.2±2.6 μg/g/d in the center, 363.5±54 μg/g/d in the bottom). Also, $^{15}N_2O$ fluxes were three times higher for ammonium than for nitrate label (Figure 4.17. VWC measured in the jars filled with soil collected at the bottom, indicated that this soil was in saturated, or in near saturation condition. Undoubtable, the reaction rates values of gross mineralization and nitrification measured higher than the values reported in the literature. Extra analysis are required to understand the reason of the values given in the current dissertation. However, the interest here is to illustrate how the prolonged saturated condition at the bottom of the column produced significant changes in the N-cycling comparing to the upper part of the column, which experienced dynamics variation of the VWC values as well as the gradient (in other words, the relative change rather than the absolute values) of the reaction rates.

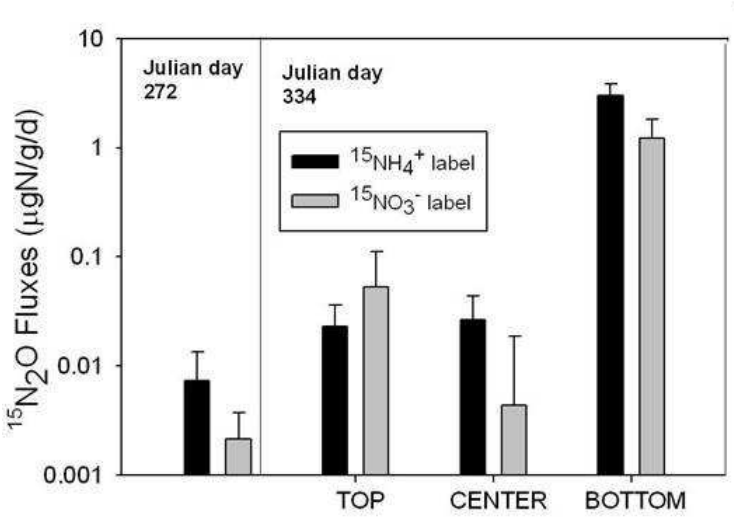

Figure 4.17: Comparison of nitrous $^{15}N_2O$ emissions (μgN $g^{-1}d^{-1}$) measured at the beginning of the soil column experiment on Julian day 272 and at the end on Julian day 334, when a gradient of VWC was present.

On the Role of Water Dynamics on Chambers Incubation

Chamber results indicate that water dynamics may induce trends in biotic and abiotic properties, thus creating conditions favorable to N_2O emissions. Jar experiments showed that at the beginning of the experiment all the parameters controlling the nitrogen cycle where the same along the column, such as N_2O emissions and the pools of ammonium and nitrates. However, the repetition of the same experiments at the end of the column experiment (at day 334), showed a clear stratification. The upper part of the column (up to a depth of 80 cm) showed no significant alterations with respect to the properties measured immediately before starting the column experiment. On the other hand, the bottom layers (depths from 80 to 140) showed lower nitrate and high levels of ammonium and N_2O emissions, indicating that the changes given by the presence of the water table and the transition zone from saturated to unsaturated conditions, constitute the favored ambient towards the production of N_2O. In addition, this zone depicted the presence of DNRA and iron reduction. This underlines the importance on the transition zone on the surface fluxes. The decrease in nitrate in Julian days 290-302 can be explained by the prolonged saturated condition with the water table at 130 cm since Julian day 283, which created an anoxic environment that favored denitrification of nitrate to N_2O and N_2 both in the liquid and in the gas phases.

Notwithstanding, the observed accumulation of ammonium at the bottom was not ex-

pected. At these depths, high ammonium levels might be related to a combination of high mineralization and nitrate ammonification rates, possibly in combination with leaching of ammonium from above soil layers, as supported by the previous data (see Table 4.4). The incubation experiment of Julian day 334, with soil collected at 120 cm depth, resulted in a consistent decrease of ammonium and nitrate during the 3h incubation time. The conditions present at the bottom nevertheless does not favor nitrification, so a steep drop in the ammonium pool was not expected. One possible explanation is that soil was contaminated by ambient oxygen before the experiment and therefore fast cycling of nitrification and denitrification happened during the incubation time. However this is in contrast with the low rate of gross nitrification and nitrate consumption rates measured at the bottom (3.7 ug g-1d-1and 18.4 ug g-1d-1), the formation of N_2O instead N_2 in saturation condition and the higher $^{15}N_2O$ measured by ammonium label vs nitrate label. Since N_2O is potentially produced by different factors (see Section 2.1 of Chapter 1), one hypothesis is that part of the N_2O was produced trough Feammox, a reaction of ammonium with iron which produce molecular nitrogen and nitrite (Yang and Silver, *personal communication*) that can then form nitrous oxides. In this case a reducing condition and the high ammonium value provided the ideal ambient for the reaction. This is supported by the analysis of dissolved iron in the 2MKCl extraction, which showed an increase of total iron from the samples at the bottom (4 ug/g soil) comparing to top and center and a decrease of ammonium (2 μgFe/ g soil). Since pH was in the range of 4-5.5 and given the low solubility of iron III (Fe^{+3}) it is reasonable to assume that the increase in the total iron is mainly an increase in iron II (Fe^{+2}). However the iron reduction could be totally independent form the ammonium decreasing process. Ad hoc experiments are required to isolate different N_2O production, but this analysis is behind the scope of the present work.

It is interesting to note how, on a two months time scale, the prolonged anoxic conditions in the bottom part enhanced the mineralization rates and the nitrous oxide productions. The top 80 cm showed nitrate and ammonium concentration and rates similar to the beginning of the experiment, even though we could depict DNRA in this zone at the end of the experiment. This imply that prolonged saturation condition have a strong impact on the N-cycle on a monthly timescale. This is in agreement with the work of Guthrie and Duxbury (1978),Terry et al. (1981) which showed how organic soil has a large potential to release nitrogen through the process of mineralization. In addition, the incubation with jars, recorded the maximum N_2O fluxes for the saturated condition (see Figure 4.16, 4.33), while in non-equilibrium condition, the movement of the water is so fast, that the peak appears when the soil has already drained (see Figure 7). Notice that both results

contradict the behavior described by the Davidson's diagram and suggest that the trace gases emissions cannot be modeled as directly proportional to the mean VWC. However, our experiments showed that N_2O is inversely related to oxygen concentration and that a relationship can be established between N_2O emissions and oxygen concentration. This calls for modeling activities which are able to capture jointly the spatial variability of VWC and oxygen concentration, in order to properly simulate N_2O emissions, thus resulting in a much higher complexity in the hydrological component of the model. The real dynamics at the bottom of the column is more realistic given by a combination of biotic and abiotic processes which are hard to distinguish. In Chapter 6, we propose a model which account on the joint effect on oxygen dynamic and water dynamic on nitrous oxide emissions.

4.4 Soil profiles and the Significance Soil Heterogeneity on N_2O Formation

4.4.1 Profiles along the Soil Column

Results shown that the first rainfall event applied to the soil lead to the diffusion of ammonium and nitrate and high emissions along the profile (4.19). We also found that N_2O gas samples collected at different depths during the rainfall events were lower than the ones measured during the draining phase of the deposition experiment (see Figures 4.19, 4.28). Also, dissolved N_2O samples collected after changes in water table level (saturation/deposition) were one order of magnitude higher than the ones collected after rainfall events (Figure 4.29) This reflected also in the N_2O fluxes (4.33,4.10). In particular, our results also indicate that nitrous oxide dynamics is related to:

1. The antecedent wetness condition (e.g. we observed different N_2O emissions after deposition and rainfall as shown in Figures 4.33,4.10);

2. The nutrient content of the peat-land (organic soil has high value of carbon and nitrogen which favored the N-cycle process ,see Figure 4.15);

3. Physical characteristics of the peat-land (e.g. the role of high organic content level on N_2O production, see Figure 4.12);

4. The vertical stratification of layers at different redox and oxygen conditions (Figures 4.2,4.3).

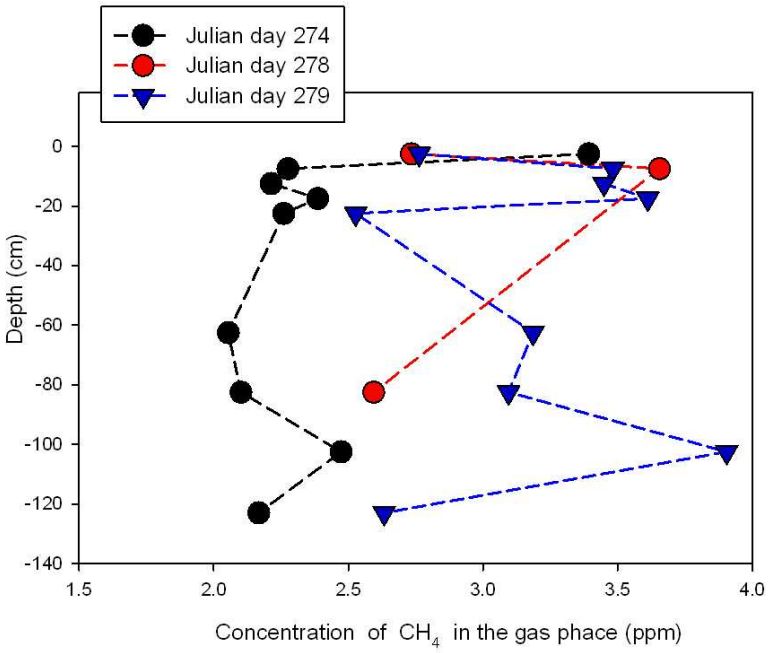

Figure 4.18: Profile of methane emissions on Julian days 274, 278 and 279.

Monitoring Week

The column was packed on Julian day 272 with soil collected at the end of the dry season. The bacterial activity at the beginning of the experiment was assumed to be relatively uniform along the column, as soils were well mixed prior to filling the column. No external input were applied and the apparatus was kept airtight during the entire monitoring week (Julian days 273-278). Thus, changes in the trace gas production or consumption were related to the difference in the oxygen level and/or the soil compaction. Values for VWC, temperature and soil electro-conductivity were constant. Oxygen was consumed uniformly along the profile and dropped from 20% to 12% over 5 days and redox sensors produced a symmetrical behavior. In particular, the sensor at 22.5 cm depth showed larger values than the one at 82.5 cm depth.

Trace gas concentrations increased with time potentially, as showed in Figure4.19, where N_2O profile measured on Julian day 278 showed higher concentrations than the one measured on Julian day 274. On Julian day day 278 (open circles in Figure 4.19) we could not depict gas below 20 cm depth.

The high value at the top of the column was not expected since the oxygen at 2.5 cm depth was 20% The height N_2O values in the top recorded during might be related

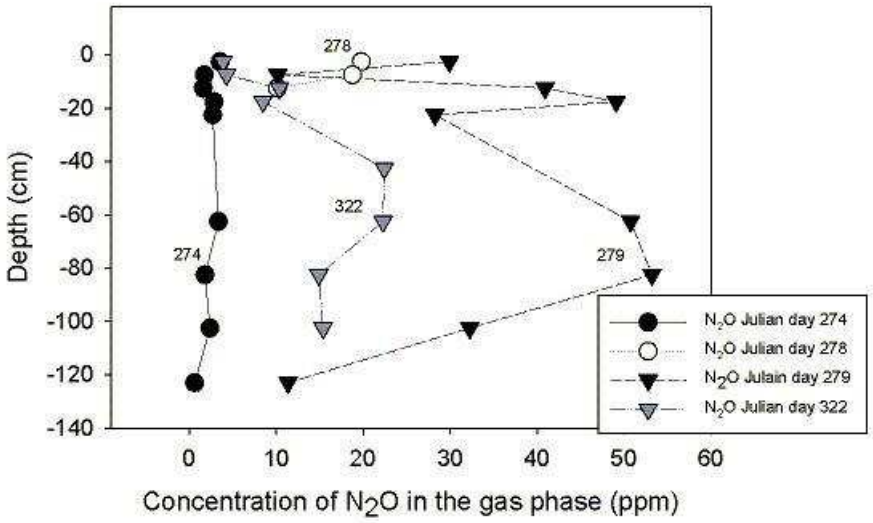

Figure 4.19: Profile of nitrous oxide emissions on Julian days 274, 278 and 279.

to gas diffusion or displacement near the surface, where the soil was less compacted than at depth because of the smaller weight of the soil above. In particular, diffusion from the central part of the column to the top may explain the lower N_2O concentration in the lower part of the column. Also, denitrification has already been depicted in well-aerated structured soil trough the decomposition of particulate organic matter and to the development of anaerobic conditions in hot-spots or soil aggregates e.g.(Schramm et al., 1999). Thus N_2O may have been produced in these spots. The absence of gas below 20 m depth, on Julian day day 278 (open circles in Figure 4.19) might indicate that in the lower parts of the column, gas consumption or displacement via compaction was greater. Furthermore, methane production occurred under dry soil conditions. We also monitored methane production under dry condition. These data suggest that methanogens were tolerant or well protected from O_2 contamination, and that methane oxidation may be differentially inhibited over methane production under these conditions (Figure 4.18).

Rainfall Events

During all the rainfall events, water drained quickly up to 51 cm depth, but during the first rainfall event (on Julian day 279) the infiltration process at depth 51-140 cm was very slow, since the soil was dry and reareation was inhibited. Also, the addition of water increased the EC of one order o magnitude. In particular,during the first event we recorded the highest values of soil electro-conductivity at 29 cm and 51 cm depth, where the highest

N_2O concentrations were measured. Oxygen was low around 8% and was affected on a daily scale by the rainfall events. Nitrate increased along the profile as expected (data not shown).

During the second and third rainfall event, water moved much quicker in the soil . In this case, the top of the column open to the atmosphere and the water table kept at 130 cm depth favored the movement of the water front to the bottom. Comparing to the first rainfall event, water leached out of the system. Nevertheless, the third rainfall event, performed with the same boundary conditions of the second, produced a slower infiltration process. EC increased immediately up to two order of magnitude (ranging form 0.2 ds/m to 4 dS/m) when soil get in contact with DI water.

The concentrations of nitrous oxide following water addition were higher than the dry week as expected and showed correspondence with oxygen levels. Rainfall event after dry period has indeed show to cause an immediate response of bacteria to dormant condition with consequent high N_2O emissions.The low value in the bottom can indicate that the anoxic condition is favoring the formation of N_2 (Figure 4.19).

Saturation event

DI (deionized) water has been added (on Julian day 290) from the bottom of the column raising the water table of 47.5, from 123 cm to 82.5 cm depth. The water table was then drained to the original depth (123 cm) on Julian day 302. The saturation process was fast (about 60 min) and produced an immediate drop in the redox values and increased the soil electro-conductivity. Rinsing the water table mobilized water and compounds previous at different redox state which were moved superficial to the peat surface, affecting substantially the micro habitats.

Water samples were collected and analyzed for dissolved nitrate, ammonium and nitrous oxide. It is interesting to observe that prolonged saturated condition in the depths range 82.5-140 cm increased ammonium concentration and decreased nitrate concentration (Figures 4.20,4.21). On the contrary, in the unsaturated zone (up to 82.5 cm depth) nitrate and ammonium behave similarly since they both increase. In addition, it was observed that the high N_2O of dissolved nitrous oxide occurred in the saturated zone and the concentration value was the higher than recorded during the entire experiment.

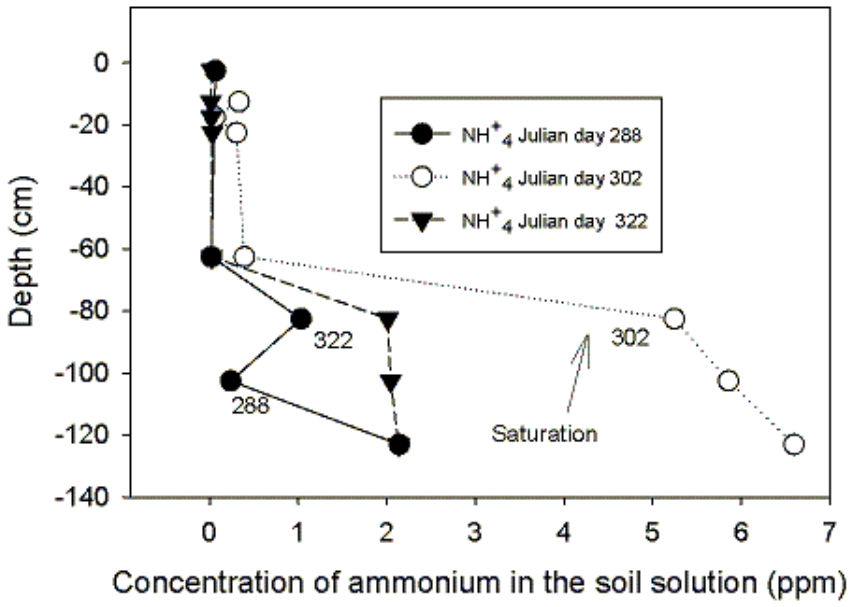

Figure 4.20: Dissolved ammonium in the soil solution (ppm) on Julian days 283, 302 and 302.

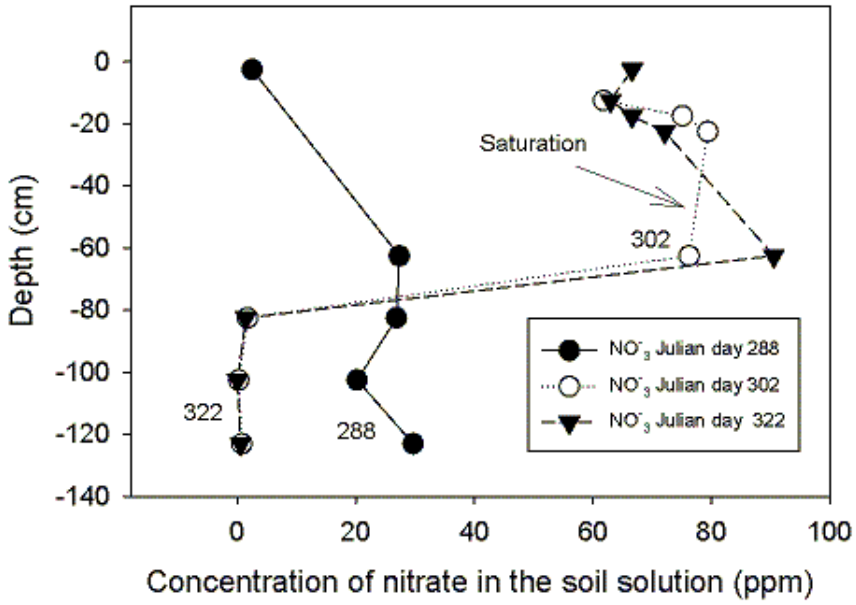

Figure 4.21: Dissolved nitrate (ppm) in the soil solution on Julian days 283, 322 and 302.

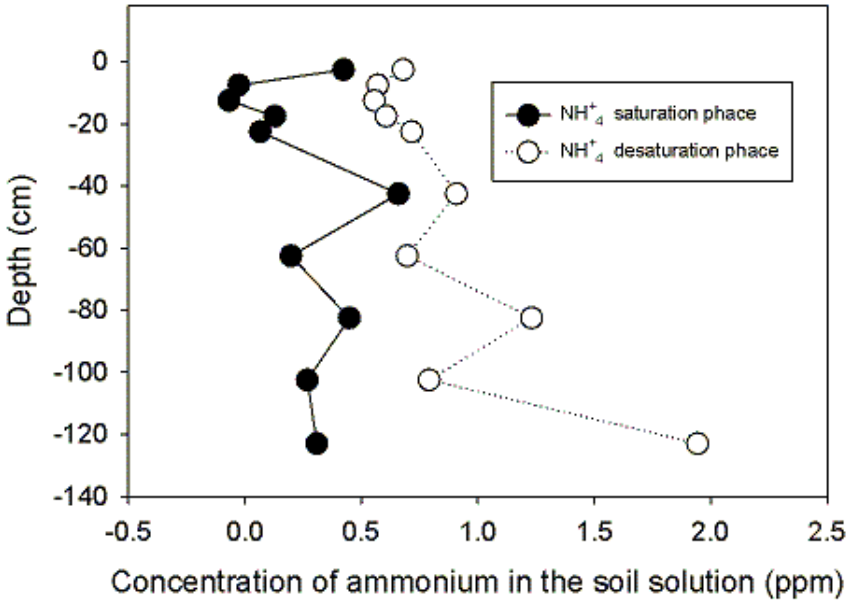

Figure 4.22: Shift in profile of dissolved ammonium,(NH_4^+ in ppm), during the deposition event (Julian days 326-328).

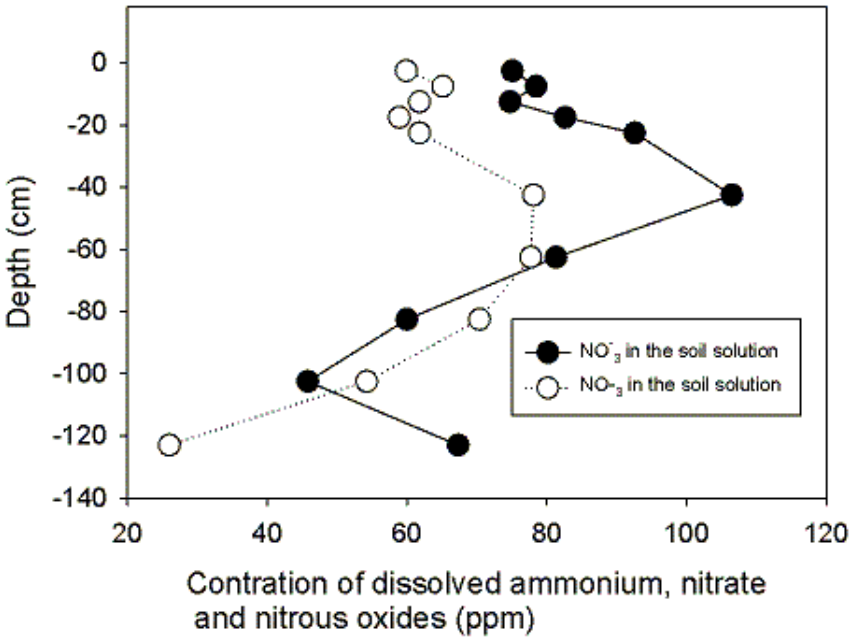

Figure 4.23: Shift in profile of dissolved nitrate, (NO_3^- in ppm), during the deposition event (Julian days 326-328).

Deposition Event

On Julian day 326 gas samples were collected, then the column was saturated from the bottom to the top with a solution of nitrate equivalent to a concentration of 30 Kg Ha yr and soil solution was sampled along the profile. As for the saturation with water, we registered a decreasing in oxygen content within a few hours of the saturation and a decreasing in the redox levels. Column was kept saturated until day 328, when it was drained, and gas samples along the profiles were collected within the following 48h. In this case, by comparing the saturation and desaturation profiles (see Figures 4.24 and 4.25), we observed along the entire profile an increase in ammonium concentration and a decrease in nitrate. The decrease was higher in the bottom part where anoxic conditions were maintained for a longer period (given the previous saturation process and the presence of the water table).

Nitrate were present in the top 60 cm, where microbes could still use the oxygen as electron donator, while along the remaining part of the profile, the lower oxygen concentration favored the nitrate consumption. In the same figure we show also the N_2O concentration in the gas phase, which was measured before starting the saturation and two days after the drainage. We observe a peak of N_2O at 20 cm depth. No gas samples could be collected below 60 cm depths (see Figure, where we measured high level of dissolved N_2O, indicating that at depths 60-140 cm gas was present only in the liquid phase and/or anoxic conditions favored the production of N_2. Figures 4.22,4.23 shows the shift in the profiles of dissolved ammonium and nitrate on Julian form Julian day 326 day 328. The shift is similar to the one observed in the saturated part of the column during the partial saturation with water (see Figures 4.20,4.21).

Profiles Correlation

Figures 4.26,4.27,4.28 and 4.29 show a summary of the profiles of dissolved nitrate, ammonium and nitrous oxide. Also concentration of N_2O in the gaseous phase are reported. Also, statistical analysis shows that profile of nitrous oxide, ammonium and nitrate were correlated within the Julian days 322,326 and 328 (331 for the N_2O in gas phase). It is interesting to point out that there was a negative correlation between ammonium profiles and nitrous oxides , while there was a positive correlation between nitrate and nitrous oxide. Also, during the rainfall event the correlation were very close in value amongst each other (0.2), the raise of the water table with water rich in nitrate, lead to a decrease of the ammonium correlation, and an increase of the nitrate correlation in time, the oppo-

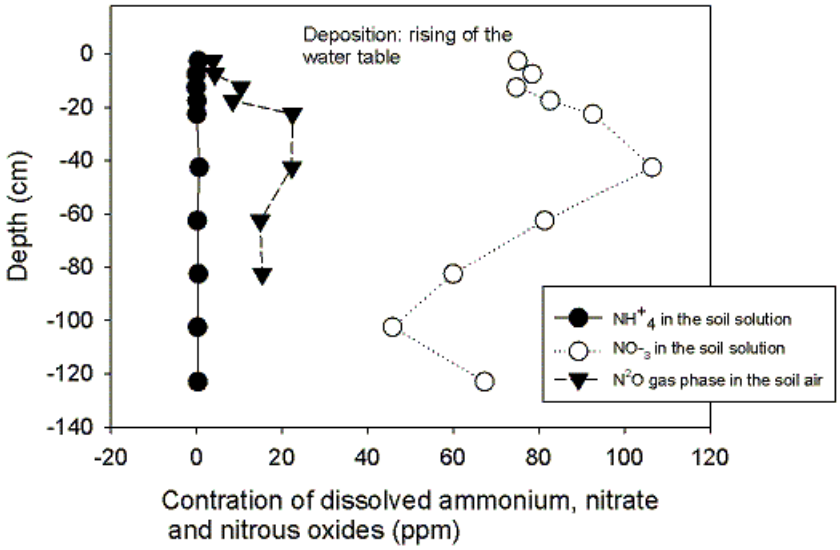

Figure 4.24: Profiles of dissolved ammonium (NH_4^+), nitrate (NO_3^-) and nitrous oxide(N_2O) on Julian day 326.

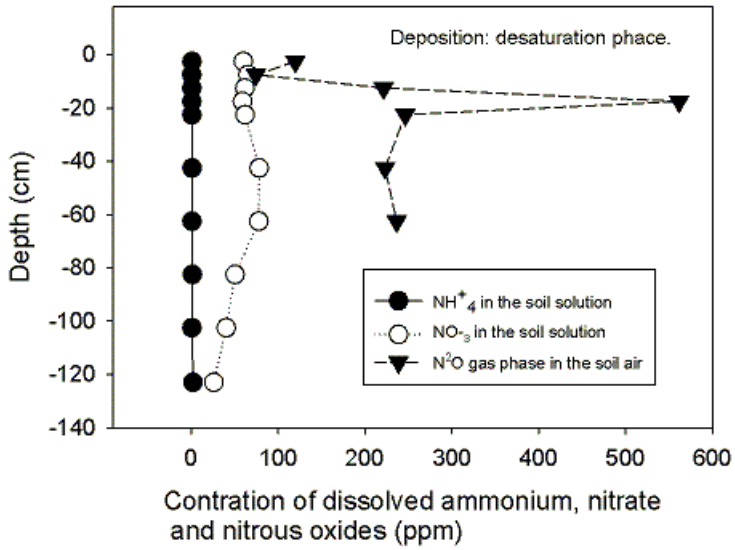

Figure 4.25: Profiles of dissolved ammonium (NH_4^+), nitrate (NO_3^-) and nitrous oxide(N_2O) on Julian day 328.

site happened during the desaturation phase on Julian day 328 (321 with N_2O in the gas phase). Also carbon dioxide and nitrous oxides (gas phase) profiles were highly correlated (Figures 4.30 and 4.31). We measured a correlation of 0.75 on Julian day 326, 0.905 on Julian day 322 and 0.952 on Julian day 331.

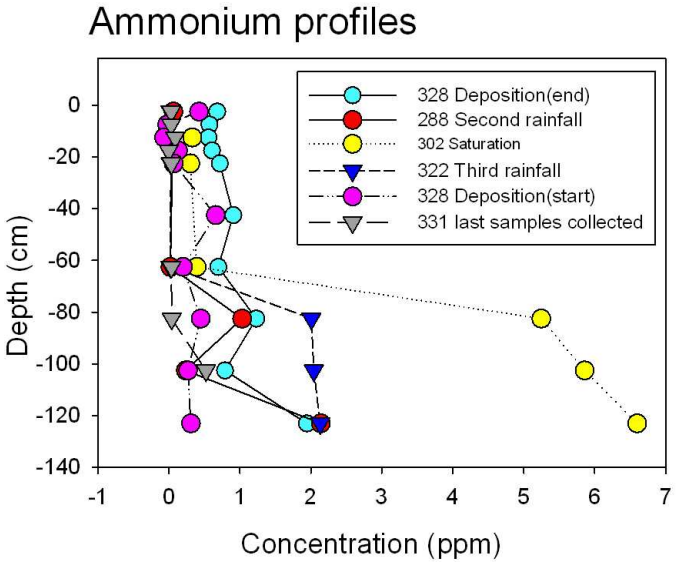

Figure 4.26: Profiles of dissolved ammonium (NH_4^+) collected during the soil column experiment (see Table 2).

4.4.2 Spatial Variability

One important aspect often neglected when estimating trace gas emissions at the soil surface is soil spatial heterogeneity. Although this is not the primary focus of this work, we kept the heterogeneous nature of the aggregates in the experimental column in order to investigate this matter. In our experiment, we were able to determine zones in which the gas dynamic was more enhanced. To illustrate this, we monitored oxygen, VWC, temperature, redox and electro-conductivity at different depths (e.g.Figures 4.2,4.1 and 4.3). For each time series, we evaluated the coefficient of variation (CV), which is given by the ratio between standard deviation and mean in order to quantify the oscillation of the signal with respect to its mean. The coefficient of variation along the depth of the column for oxygen, VWC (ECTE probes) and temperature are shown in Figure (Figure 4.32). Notice that a increment in water content results in a reduction of O_2, as it was expected. Furthermore, the larger variability of O_2 is shown between 10 and 40 cm depth and at 120 cm (see Figure 4.32).

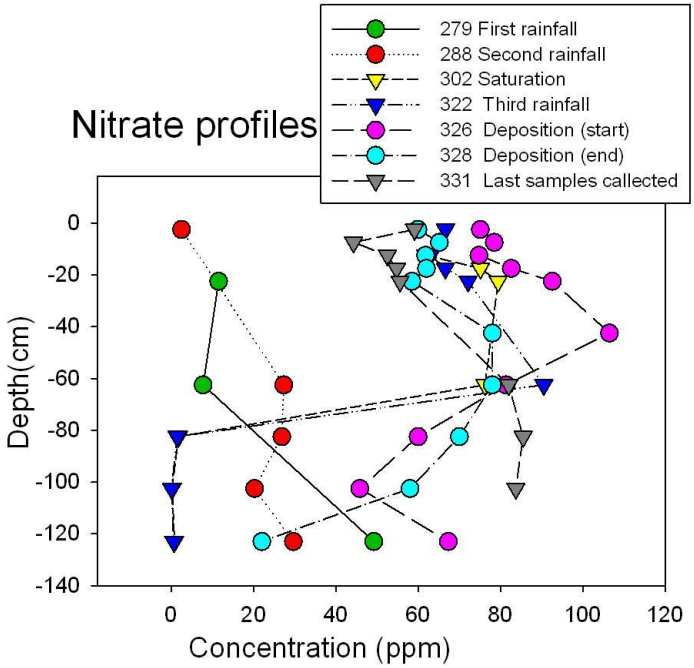

Figure 4.27: Profiles of dissolved nitrate (NO_3^-) collected during the soil column experiment (see Table 2).

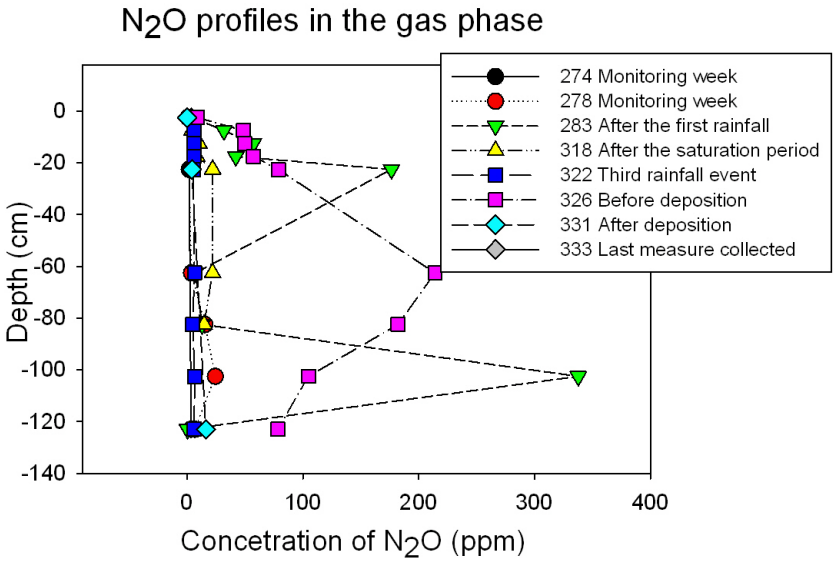

Figure 4.28: Profiles of gaseous nitrous oxides (N_2O) collected during the soil column experiment (see Table 2).

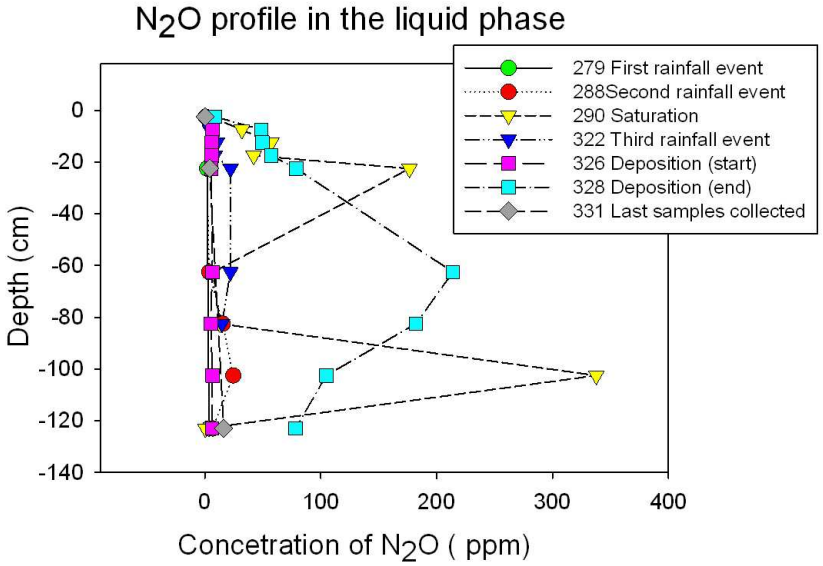

Figure 4.29: Profiles of dissolved nitrous oxides (N_2O) collected during the soil column experiment (see Table 2).

In our work, soil heterogeneity explained the variation we had in the soil profile and in the trace gas emissions. The movement of water has changed the ratio of micro and macro-aggregates, modifying the N-cycle, since gases are mainly transported in the macro-pores and mainly produced by microbes in water-filled micro-pores. A larger value of the coefficient of variation reflects intense variability between the values in the time series (for example: a time series with erratic shape and large derivatives from its mean). Moreover, it's important to note that the large coefficient of variation in the top 20 cm for O_2 is due to the fact that it represents a lumped effect of soil in heterogeneity in the bottom part of the column. In other words, what is been measured in the gas phase is not only the O_2 captured at that specific location of the sensor, but also the O_2 coming from deeper layers of the column (where the value of VWC is different) and traveled a tortuous path to reach the sensor. This was observed by performing a statistical data analysis using *R* software by plotting histograms, box-plots and time series at different depths the column (not shown here). This result has strong implications in modeling. Therefore, to accurately predict trace gas fluxes, through the use of mathematical models, one must account for the heterogeneity of the soil below the point where the gas is been predicted. In addition, we deem important not only to consider the availability of water as a key controlling factor in gas trace emissions but also its combined effect with spatial heterogeneity. The former is crucial in dictating the distribution of water in the natural environment (low

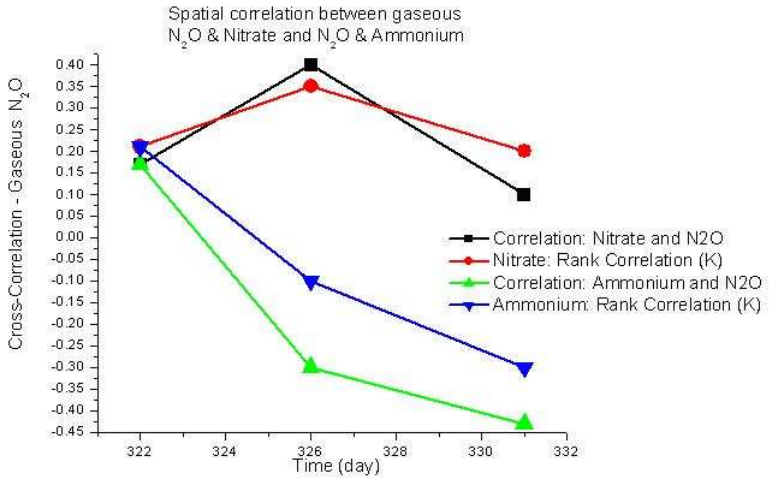

Figure 4.30: Correlation between profiles of nitrate(NO_3^-), ammonium (NH_4^+) and nitrous oxide emissions (N_2O), see Table 2.

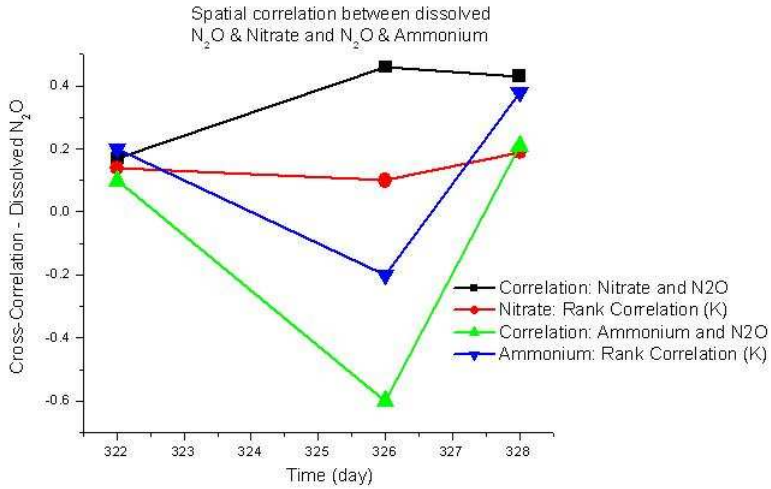

Figure 4.31: Correlation between profiles of nitrate(NO_3^-), ammonium (NH_4^+) and dissolved nitrous oxide emissions (N_2O), see Table 2.

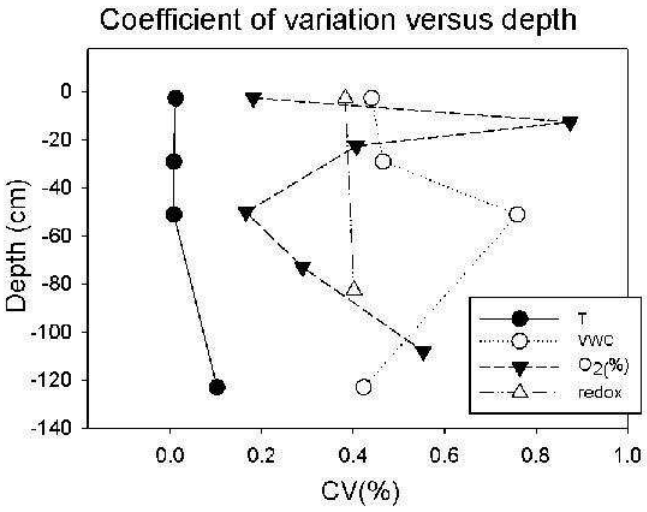

Figure 4.32: Coefficient of variation (CV=σ/μ) for the time series along the soil column.

hydraulic conductivity, K_s, dead end pores, clogging, etc). Here, the term heterogeneity does not only imply the connectivity between the pores, but also its joint effect with the fluid's property (K_s) Hydraulic conductivity vary with time in the column. Our tests showed decreasing value of K_s in subsequent replicates given the decrease in porosity of the medium. We measured as first value 0.069 cm/sec and last value measured was 0.015 cm/sec. There are only few studies looking at the potential of nitrous oxides emissions from peat land (e.g., Muller et al., 1980; Verhoeven, 1986; Goodroad and Keeney, 1984; Regina et al., 1999; Maljanen et al., 2003; Maggi et al., 2008).

4.5 Nitrous Oxide Fluxes, Water Dynamics and Management

Our work showed a high potential for N_2O emissions from organic peatland layers. In particular we found that the N_2O peak magnitude and duration were different after rainfall and changes in water table. The peak of N_2O emissions after rainfall event appeared after 3 days, while the peak given by saturation and deposition event appeared 2 days after and was higher in concentration (see Figures 4.33 and 4.10). Also, in this case, it took about one week to go back to background concentration. Denitrification is likely to occur in anaerobic or micro-aerophillic micro-sites within the soil. As the O_2 concentration drops, the frequency of anaerobic micro-sites increases. Results indicate that the oxygen

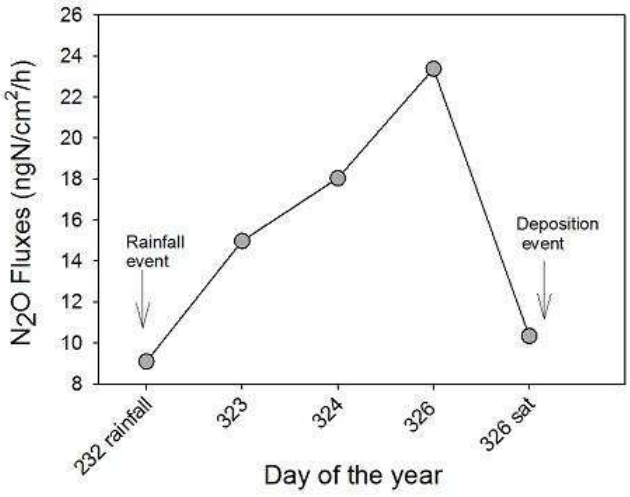

Figure 4.33: Fluxes of nitrous oxides (N_2O) in ngN/cm^2/h from the head space of the column o Julian days 322-326. Note that the peak of N_2O compare there day after the rainfall event of Julian day 322.

depletion was slow when comparing to the infiltration/drainage time scale and this can explain a delay in the maximum peak of N_2O emissions whose extent depend on both the changes in the diffusivity and soil properties (Smith et al., 2003). Changing in size and type of population (bacteria) indeed modifies the properties of the porous media and increase the capacity of the porous medium to hold water (Allton et al., 2007). The delay is thus a combination of biological factor (denitrification), physical factors (entrapment, preferential flow paths, broking down of protected organic matter) and a combination of the two (biomass increase changes hydraulic properties e.g. clogging) (Zejun et al., 2002). We therefore believe that these contributions should not be underestimated or ignored since their contribution need to be accounted in the annual N budget.

Contrary to natural peat, which in general acts as a sink for N_2O, peat soils with high nitrogen content are potential sources of nitrous oxide (e.g., Regina et al., 1999; Saquet, 2003; Von Arnold et al., 2005). High N_2O value has also recently found in arctic peatland (Repo et al., 2009). We found that cycle of saturation/desaturation produced high fluxes due to the increase of the anaerobic front and of air displacement form the deeper layers. For that reasons, repeating fluctuations in the water table would lead to larger emissions and should thus be avoid by the farmers as irrigation procedure. The delay in the N_2O peak after deposition is due to the soil initially being too wet to permit N_2O to diffuse out of the soil surface. It may be reduced to N_2 or it may simply be accumulating until there is

enough air-filled pore space to allow diffusion. Assuming no N_2O production/consumption hot-spots in the profile, the delay in N_2O flux will be a function of (a)peat texture (pore size) - the finer it is the greater the tortuosity, and (b) VWC - the wetter it is the fewer pores there are for gas diffusivity and it may take days for N_2O to emerge and during this time it may be transformed to N_2 - which then takes days to emerge.

In reality, the mechanisms are more complex since soil heterogeneity (see previous section) play a key role on the dynamic of the soil solution and trace gases displacement. Therefore a better understand of the role of soil heterogeneity is required to better understand the functions of the soil solution, which can act as a barrier (water may occlude space for gases to move), as a storage reservoir (entrapment of gas in soil) and as a transport medium (high level of N_2O can move with the dissolved water be diffused) for N-cycle compounds as exhaustively explained by Heincke and Kaupenjohann (1999). In particular, it took six days for the N_2O peak (emitted after the deposition event) to reach the background concentration.(see Figure 4.10). Concerning the rainfall event, is known that filling of small pores on the soil surface with water reduces the ability of capillary forces to actively move water in the soil. Raindrop impacts breaks large soil clumps into smaller particles and seal the surface This particles clog the surface pores reducing the movement of water into the soil and retarding the trace gas emissions.

One possible explanation is because of increased nitrification activity in the uppermost aerobic peat profile. (Zimenko and Misnik, 1970) observed an increase in nitrification after a water table draw-down in a few wetlands. Also after drainage of a peatland, the availability of oxygen and mineral nitrogen increase, this favors N_2O production e.g.Maljanen et al. (2003). The works of Goodroad and Keeney (1984), and Martikainen et al. (1993) reported that drainage has an impact in enhancing emissions of N20 from some peat soil. The high N_2O fluxes and concentrations both in the liquid and in the gas phase are in similarity with the works of Guthrie and Duxbury (1978); Terry et al. (1981) which found extremely high concentrations of N_2O dissolved within the soil solutions of organic soil. They indicated a large potential of these soils for the release of nitrogen through the process of mineralization.

Thus in a organic peatland the number of precipitation and the water table fluctuation will affect the annual budget of trace gases. We also found that the rich organic peatland soil considered in the present work has significant N_2O emissions when the soil drain. This aspect need to be accounted in peatland management considering that their contribution to the total atmospheric N_2O load is consistent (Maljanen et al., 2009). For instance, organic soils drained for agriculture are responsible for 25% of the anthropogenic N_2O

emissions in Finland (Klemedtsson et al., 1997), even though they cover less than 10% of the total arable land area. Thus, we expect that, in the organic soil of California, the infiltration process, the variability in saturated conductivity and the soil water retention curve may be the keys factor which determine not only the connectivity properties of the field, and thus the diffusion of nutrient toward bacteria, but also the changes in soil structure with possible entrapment and ebulliement which determine the variability in the surface fluxes.

4.6 Chapter Summary

From our results, we observed that changes in VWC in unsaturated media affect both physical and biological properties. The behavior of water dynamics can indeed lead to preferential flow path or entrapments of both air and water, which have a crucial role on physical displacement of trace gases. Effects are intimately related to the way in which water changes. We have found that rainfall and water table fluctuations alter the physical properties of the unsaturated soil (i.e. compactation) and its micro-fauna in different ways: rainfall infiltrates into soil, modifying the soil structure (porous structure) in a non-uniform way creating zones of aerobics and anaerobes and thus leading to possible entrapment of the pore space air, while increases in the water table level creates a uniform front which moves upwards. This upward movement causes mixing of dissolved elements from levels which have different redox condition and possibly causing the movement of air from lower layers to top layers.

The delay in the infiltration process during the rainfall event on day 322 comparing to the one on day 283 indicate that the pore structure at this time was more connected which may be related to clogging of the surface layers due to raindrop impacts on large soil clumps. The difference of ammonium and nitrate profile below the water table during the saturation event can be a consequences of enhanced mineralization and denitrification as the nitrate ammonification (also known as denitrification nitrate reduction to ammonium) given in presence of low oxygen and high C and nitrate. This zone has high potential for N_2O emissions. This in agreement with the works of Regina et al. (1999); Kasimir-Klemedtsson et al. (1997) and Bateman and Baggs (2005) which shown as temporary saturation may cause large emissions of denitrifier N_2O from the soil. Finally although it is known the asymmetric behavior between ammonium and nitrate, we showed that is also dependent on saturation. The former has a definite role in defining the magnitude of the emissions (see Figures 4.20, 4.21, 4.22, and 4.23). The reason may be related to the more

uniform distribution of water during saturation process and the extent of the anaerobic front.

Rapid changes in VWC on short time scale as water table fluctuations or short rainfall events are often neglected in modeling. Their effect on trace gases, known as "pulse event", is often not captured by the mathematical models. We found that these non equilibrium processes might affect bacteria on a longer time scale and significantly contribute to N_2O production and nutrient mobilization. At cell level the changes in VWC and the associated variation in water potential alter the microbial activity. In particular, increases in VWC lead bacteria to release substances that might change the community and consequently, alter the N reactions rate. For that reason, we believe that changes in rainfall intensity and frequency may change nitrous oxide emissions and required better investigations.

On a longer time scale, our results indicate that water dynamics alter the initial condition, here assumed homogeneous in the experimental setup. In particular, at the end of the experiment we could determine two different zones: (i) The first one including the top and central layers and (ii) the other the bottom layers of the soil column

Moreover, we also want to emphasize that the results reported in this paper are highly depended on the type of soil peat (organic matter) and by soil heterogeneity. The values of saturated conductivity and the porosity has been varied according to the external input given to the system (rainfall, saturation and deposition) and relating to the initial condition in which the material has been packed (not to mention displacement of soil aggregates and microbial growth).

Trace gas emissions, dissolved nitrate and ammonium changed considerably along the soil column profile as a response of the microbial community to the high variability in redox, VWC and oxygen both on short and long timescale. We therefore believe that more investigations concerning are required to better understand the role of the unsaturated zone in the global N budget.

In summary, the key message of our work is that in order to understand the role of redox dynamics on N_2O emission it is crucial to include the role of soil heterogeneity and account for non-equilibrium processes. Emissions depend indeed on the timing and the way in which water is applied to the system. Neglecting these aspects may result in a wrong estimation of the annual N-budget. We also shown that in organic rich pasture peatland fluctuation of water table and the use of fertilizer might potentially produce high nitrous oxide emissions.

5 Field Scale Observations

5.1 Effect of Water Dynamics on Field Site

The soil used to perform the experimental work described in this dissertation has been collected in the Sherman Island, Bay Delta area, San Francisco, California (CA), USA. The field has been monitored for over a year (Teh et al., 2010) and gas samples has been collected along five transects, corresponding to different landform. Measurements have been taken at five locations along each transect, as shown in Figure 5.1.

In addition, water vapor, methane and carbon dioxide has been measured using eddy covariance towers (see Figure5.2(b)). This integrated approach is needed to capture the behavior of the peatland. Unequal distribution of water and nutrient between adjacent landform indeed, favor the expansion of some microform types and the contraction of other, leading to the emergence of distinctive vegetation structure ($\sim 10^{-1}$-10^{2}m scale) and hydrologically distinct peatland units (($\sim 10^{2}$-10^{3}m scale)). In turn, larger scale structure set the boundary for processes occurring at the elemental component part of the ecosystem. An exhaustive explanation of the importance of cross-scale feedback in peatland can be found in Belyea and Baird (2006).

The data collected by Teh et al. (2010) has been statistically analyzed in order to capture some of the variability present in the area. These results are important since the experimental column previously described can only capture the heterogeneity at the laboratory scale while the field scale variability (i.e. the influence of different landforms on trace gases and soil moisture distribution) is characterized by the transect measurements shown in Figure 5.1. Comparing to the micro-scale (*i.e.* incubation jars and soil column), the field scale includes both the effects of soil heterogeneity as well as of vegetation which compete with bacteria in the natural system for nutrient access. Data available includes weekly measurements of trace gases (nitrous oxide, methane and carbon dioxide), soil temperature and soil moisture. Transect distribution corresponds to different landformaccording to the following:

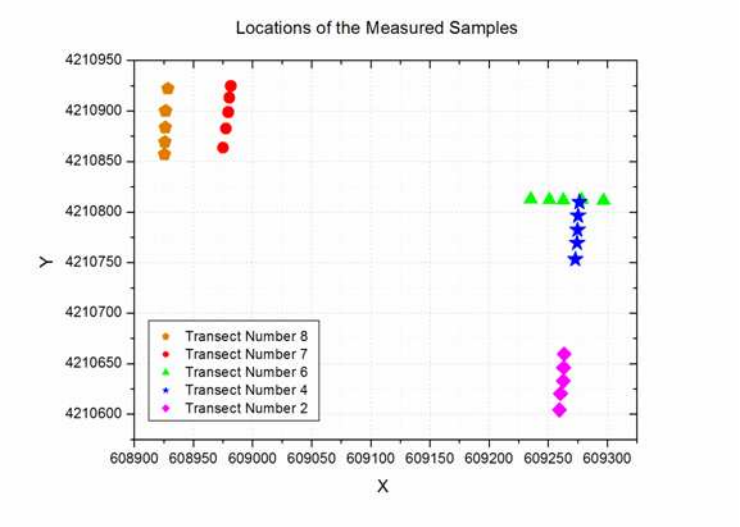

Figure 5.1: Location of the measured samples. Each symbol represents a transect where gas emissions where measured.

- Transect 2: Crown site
- Transect 4: Slope site
- Transect 6: Irrigation ditch site
- Transect 7 and 8: Hollow/hummuch site

The eddy covariance system was mounted on the tower on a 2.5 m boom oriented toward the West, the prevailing wind direction (for details of the system, see Runkle, 2009). Carbon dioxide has been measured in continuous manner. Figure 5.2(b) shows the measurements collected during year 2008. Data has been filtered in order to separate the daily measurements for photosynthesis (blue dots) and for respiration (black dots). Red dots, which correspond to the daily average of the respiration values, illustrate how the carbon oxide emissions are related to rainfalls events, as shown by the fluctuations of the data in the Julian days ranging from 300 to 350, which follow the shape of the rainfall events, see Figure 5.2(a). Also the wet period between days 300-420 shows higher respiration rate comparing to photosynthesis, given by the reduced light during the winter months. Finally Figure 2.13, Chapter 2 illustrate the fluxes of water vapor, carbon dioxide and methane measured with a multiple eddy covariance tower approach during years 2009, and show the potentially for N-rich irrigated peatland to significant impact in term of global warming (Teh et al., 2010).

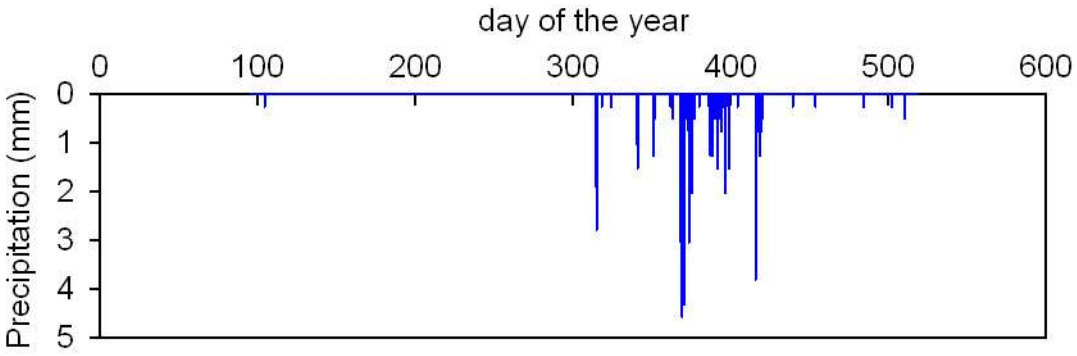

(a) Rainfall (mm)

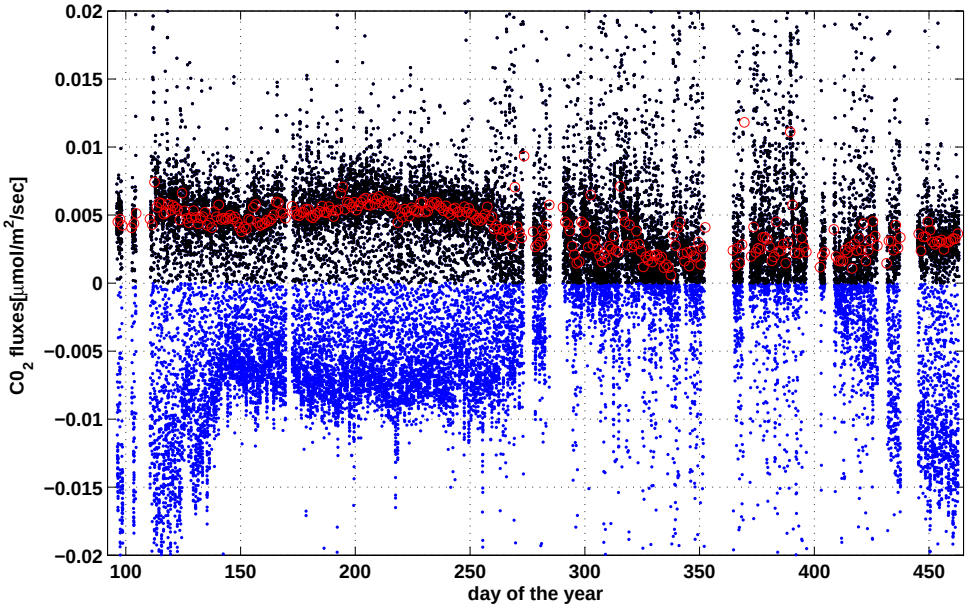

(b) CO_2 fluxes (μmole/m^2/d)

Figure 5.2: Precipitation recorded at the climate station in Antioch,California and CO_2 fluxes (μmole/m^2/d) measured in the pasture field Sherman island (California) with the eddy covariance tower.

In order to evaluate the role of water on trace gases emissions, measured values have been averaged annually and box-plots have been created. Coefficient of variation (CV), defined as ratio between the standard deviation and the mean has been also calculated in order to gain insights on the significance of spatial variability along the transect.

5.1.1 Rainfall Events in the Sherman Island.

From a climatic point of view, the Sherman island is characterized by dry summers and wet winters. The field area is characterized by a mean annual precipitation of 217 mm and a mean annual temperature of 9^{o}C. Figure 5.3 shows the monthly average of temperature and precipitation values recorded over twenty years at the meteorological station located in Anthioch, California (USA), in the vicinity of the area where gas samples have been collected. Temperature and precipitation clearly show opposite behavior: months ranging from May to September (dry season) are characterized by scarce rainfall events and high temperatures, while the months ranging from October to April (wet season) shows the opposite behavior. A closer inspection of the precipitation data indicate that the site is characterized by events of low duration and intensity.

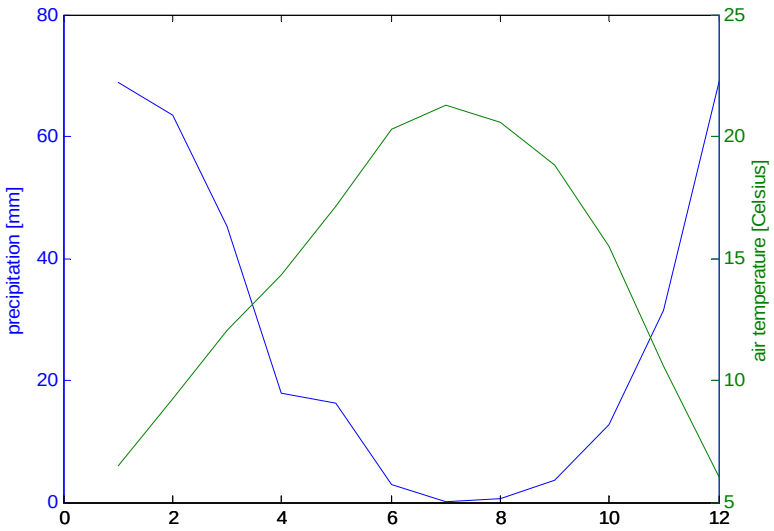

Figure 5.3: Monthly averaged precipitation and temperature value of data recorded at the climatic station in Antioch, California, USA between 1988 and 2008.

Table 5.1 reports duration, height, and inter-time of precipitation for events recorded during the years 2007 to 2008. It is possible to observe that most of the daily precipitation

are low.

Thresholds:		Ppt. (mm)	Duration (d)	Inter-time (d)	N° of events
1 mm	8 d	12.76	11.69	83.94	16
2 mm	4 d	10.56	7.00	69.94	19
2 mm	6 d	11.88	9.41	78.69	17
2 mm	8 d	13.53	12.4	89.93	15
2 mm	10 d	13.59	13.00	89.93	15
2 mm	16 d	20.52	29.20	134.89	10
2 mm	20 d	13.80	13.78	91.22	9
5 mm	20 d	13.98	14.14	92.43	6

Table 5.1: Threshold events for the precipitations recorded during year 2007-2008 at the meteorological station of Antioch, California, USA.

The dry and the wet seasons are thus characterized by different hydrological and climate conditions. This has an impact on the microbiological activity.

This is in agreement with the concomitant work of Parton and Shiemel (*personal communication*),which shows that the seasonal shifts in the nitrogen pool are due in part to temperature and in part to precipitation induced changes. In particular they hypothesize that the macro-scale dynamics of the N-cycling are the results of the processes happening at the micro-scale, and that the microbial landscape changes according to the changes in the hydrological connectivity (see Section 1.1.2 Chapter2), thus supporting the impact of water dynamic on microbiological activity. In the following subsection, simple statistical analysis was performed in order to better understand the link between soil moisture, temperature and gas emmissions.

5.2 Statistical Analysis: Scaling Micro-Site Fluxes to Ecosystem and Landscapes

Data collected shown both high methane (irrigation ditch) and N_2O emissions (transect 2). In particular N_2O emissions were comparable to the ones of agricultural field and tropical forest (peak of 200 $\mu gN/m^2/d$ has been recorded Teh et al. (2010)). In this section, statistics has been used to evaluate the influence of irrigation practices on spatial pattern of measurements.

5.2.1 Comparison Among Transects

The field site experienced rainfall events during the wet season(October-April) and was periodically flooded by the local farmer. Transect 2 was used as a *blanket*, since it has never been flooded, while transects 7 and 8, which were periodically flooded, provided some information on the influence of irrigation practices on the spatial variability defined by the measurements.

Figure 5.5 depicts the variability of trace gases and volumetric water content (VWC) among the transects. In this figure, we plotted the corresponding box-plots for each of the time series. The box-plot is a visually effective way to summarize graphically the distribution of the data (Kitanidis, 1997). The two horizontal sides of the box indicate the low (25%) and the upper (75%) quartiles. The line inside the box represents the median and the size of the box. The extension of the dashed line represents the *stretch* of the tail of the histograms.

It is possible to observe that there is significant variability among transects for all variables measured. In particular, transects 7 and 8, which are periodically flooded have a mean VWC of 0.5, while transect 2 has a mean VWC of 0.2. Transect 2 shows a high number of *outliers* for the N_2O emissions and a wider range of VWC values; the irrigation ditch (see transect 6), on the contrary, shows low N_2O emissions. In particular transect 2 has N_2O emissions one order of magnitude higher than transect 6 both as mean (3.59 nmol/m^2/s of transect 2 versus 0.37 nmol/m^2/s of the ditch) and peak values. This is in line with what observed in the column experiment, small N_2O emissions at high water content. It is interesting to observe that dry conditions observed in transects 2 and 4 lead to high carbon dioxide emissions, while the irrigation ditch shows extremely high fluxes of methane. Also, the mean value of CO_2 (0.048 μmole/m^2/d) was very close to the respiration data measured by the tower, indicating that both the eddy covariance tower and the distribution of the chambers were able to capture the average soil respiration of the field.

5.2.2 Comparison Between Wet and Dry Season

In order to measure the effect of water dynamics on trace gas emissions at the ecosystem scale, the data set has been split into dry and wet seasons, according to the distinction made in section 5.1.1. Figure 5.10 shows that wet and dry season affect trace gases, even though for methane, the emissions from the irrigation ditch were so high to mask all the variability due to changes in volumetric water content for transect 2, 4, 7 and 8. This is

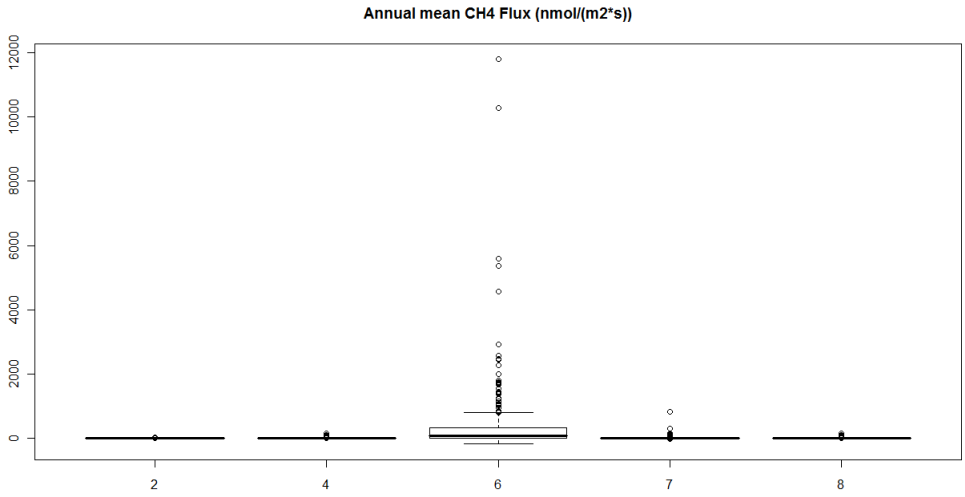

(a) CH_4

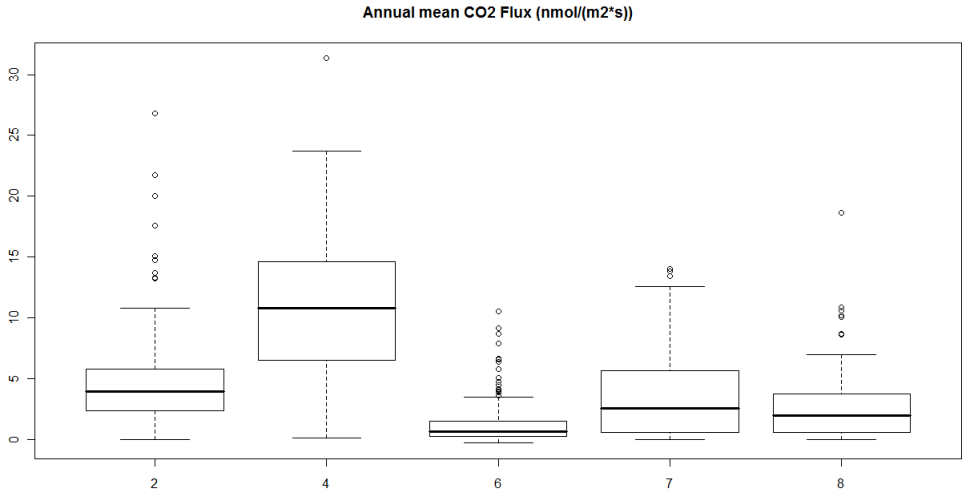

(b) CO_2

Figure 5.4: Trace gas measurements. Box-plots showing spatial variability of methane (CH_4 in nmol/m^2) and carbon dioxide (CO_2 in μmole/m^2s) fluxes among the transects as well as the presence of outliers.

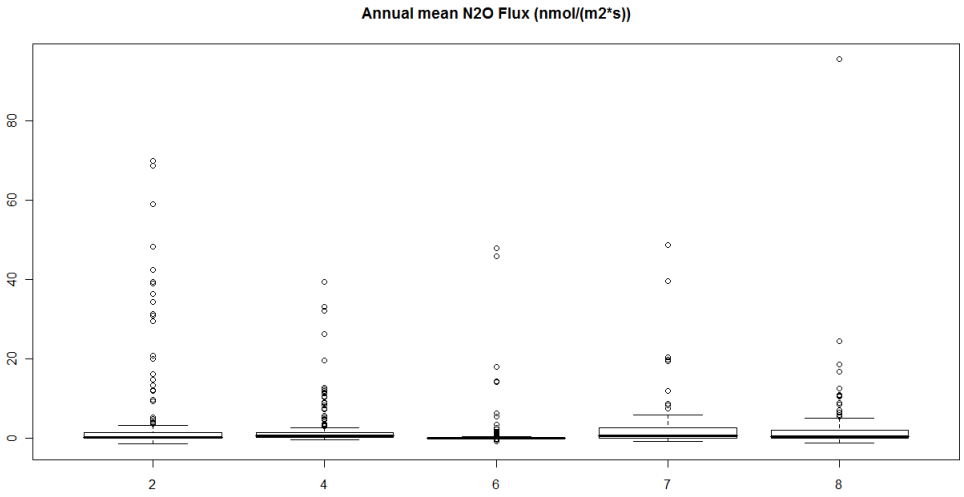

(a) N_2O

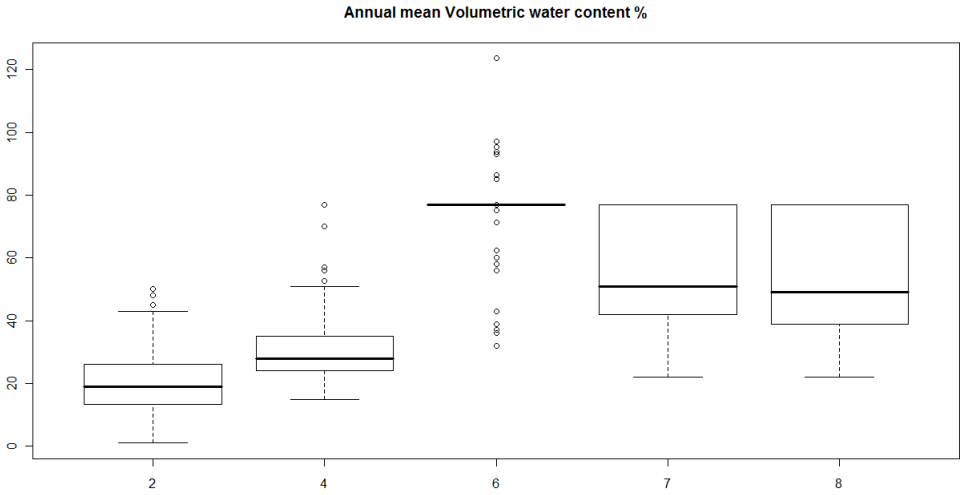

(b) VWC

Figure 5.5: Trace gas measurements. Box-plots showing spatial variability of nitrous oxide fluxes (N_2O in nmol/m^2s) and volumetric water content (VWC %) among the transects as well as the presence of outliers.

an important result, because it shows how the irrigation channel might be an important source of methane gases in a temperate peatland. Also, this is important locally, since 5% of the area (the ditch) produces 85% of the methane emissions.

Carbon oxide decreases as VWC increases; this behavior is clearly shown reported in transects 2 and 4 which have never been flooded (transect 4 was flooded only at the location of chamber 16 during monitoring weeks 41 and 42). Emissions decrease from 4.8 to 4 μmole/m^{2}s in transect 2 and from 14 to 6.8 μmole/m^{2}s in transect 4 as a response to a 15% increase in VWC. On the contrary, the irrigation ditch shown emissions of 1 μmole/m^{2}s for both the seasons, while transects 7 and 8 which experienced flooding events (11 times for transect 7 and 14 for transect 8 during both dry and wet seasons), show a much higher dispersion of the value around the mean when compared to other transects. CO_2 emissions for transect 7 were in the range of 3 μmole/m^{2}s for both seasons, despite the increase of VWC. This can be explained as a disturbance effect of the irrigation practice.

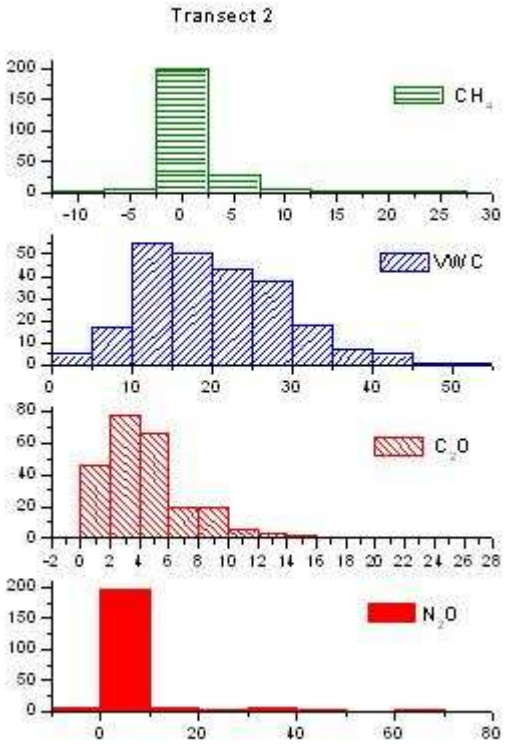

Figure 5.6: Hystogram for transect 2.

Figure 5.10 also illustrates how the wet season is responsible for outliers in the annual

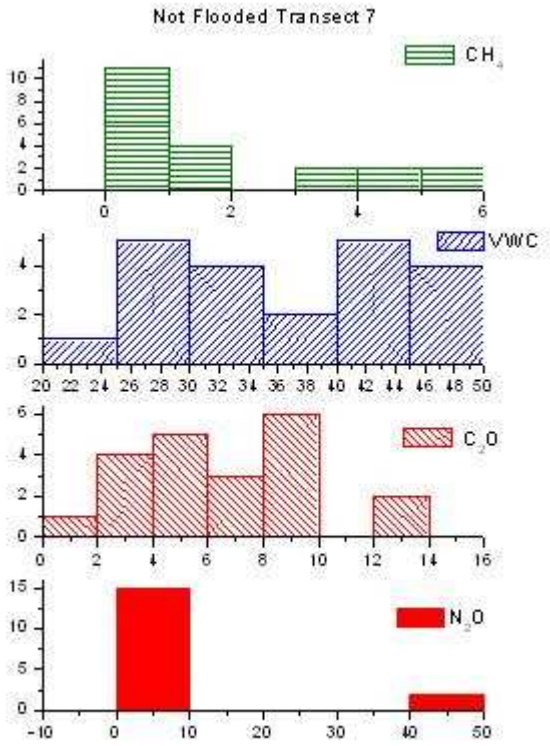

Figure 5.7: Histogram for transect 7 (non flooded).

mean of nitrous oxide fluxes and how this is associated to a lower variability of VWC values when compared to the dry season. Also in both seasons, the irrigation ditch shows low N_2O trace gas emissions, while transects 7 and 8 also shows that a more uniform distribution of the VWC values (see Figures 5.6, 5.7 and 5.8), results in a less uniform distribution of the N_2O fluxes. This seems to indicate that soil moisture drives variability of N_2O. A possible explanation for this is the fluid/air interface area, which is highly variable during the wet season in unsaturated conditions, than in a field subjected to permanent saturated conditions, where the majority of emissions are expected to be in form of N_2, while this physical consideration is not directly applicable to CO_2 and CH_4 emissions, whose dynamic is more complex and interconnected.

The dispersion of nitrous oxide emissions for dry season, when compared to the wet season is visible also through the comparison of the cumulative distribution function for transect 2, where the soil column has been collected (see Figure 5.11).

The spatial average along the transect varies from 21°C (in transect 2) to 14°C (in

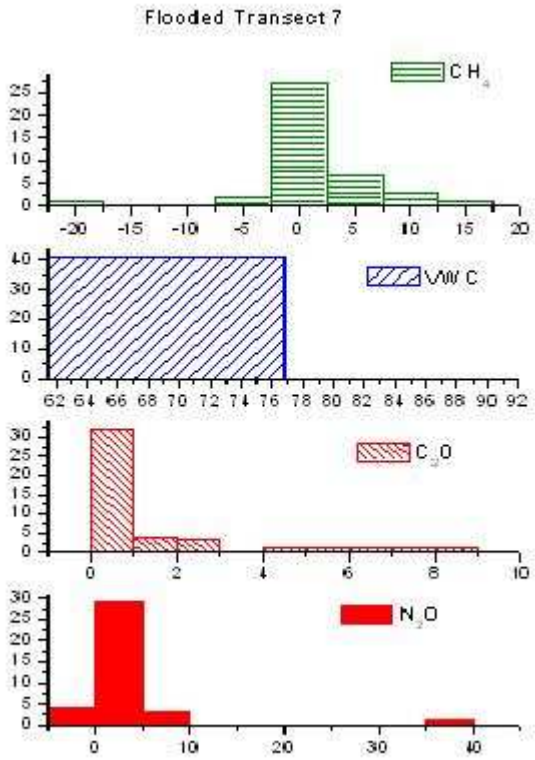

Figure 5.8: Histogram for transect 7 (flooded).

transect 8) in terms of annual average (data not shown).Figure 5.12 shows a different temperature trend during dry and wet season. The former is characterized by a stronger variability along the transect ranging from 27°C to 17°C, while the latter shows much smaller variations (range 17-13°C).

5.2.3 Influence of the Irrigation Ditch

The influence of the irrigation practice is also shown by the comparison of the flooded and non flooded weeks. Figure 5.13 shows a picture of the irrigation ditch.

Figures 5.14 and 5.15 show the effect of the temporary flooding event on the field scale. In particular, transect 7 shows that N_2O emissions have a higher dispersion in a flooded condition (when compared to the not flooded), where therefore the mean value is higher for the wet season. Also the flooding event tends to *average out* the effect of variability between dry and wet season, thus reducing the emissions of CO_2.

The irrigation ditch significantly alter the trace gases distribution measured in the

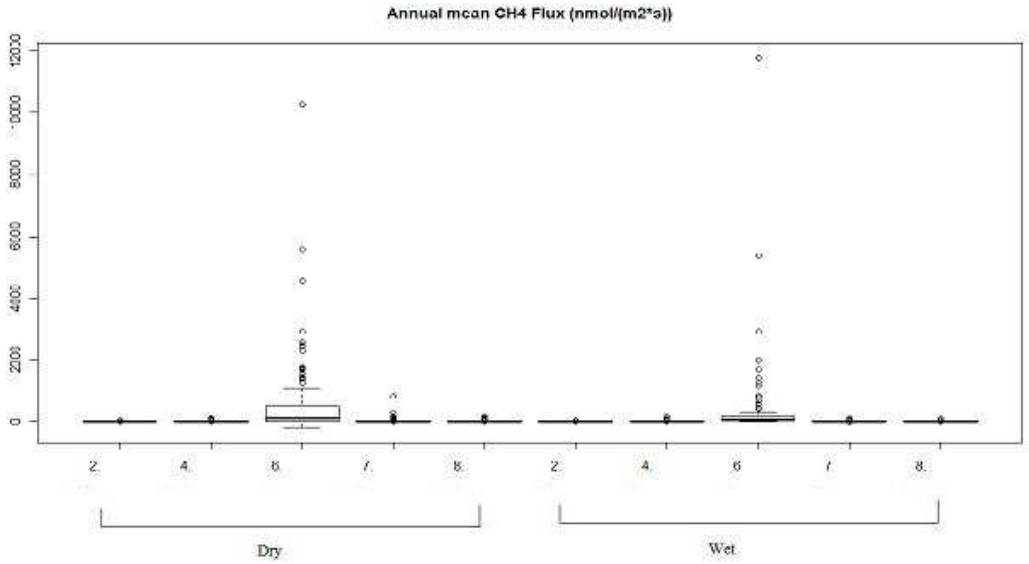

(a) CH_4

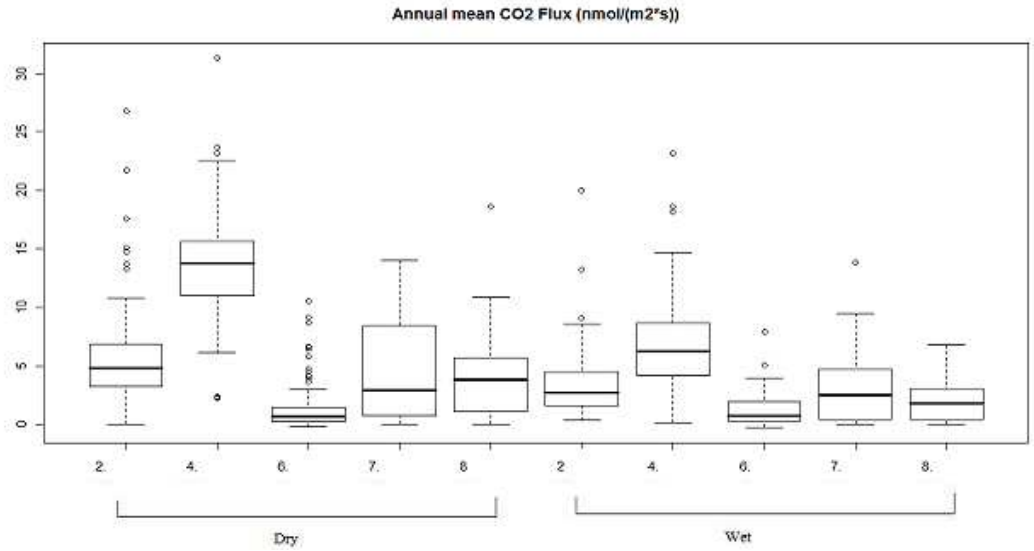

(b) CO_2

Figure 5.9: Box plots of trace gas fluxes (CH_4 in nmol/m^2 and CO_2 in μmole/m^2s) showing spatial variability of trace gases among the transects for the dry and the wet season.

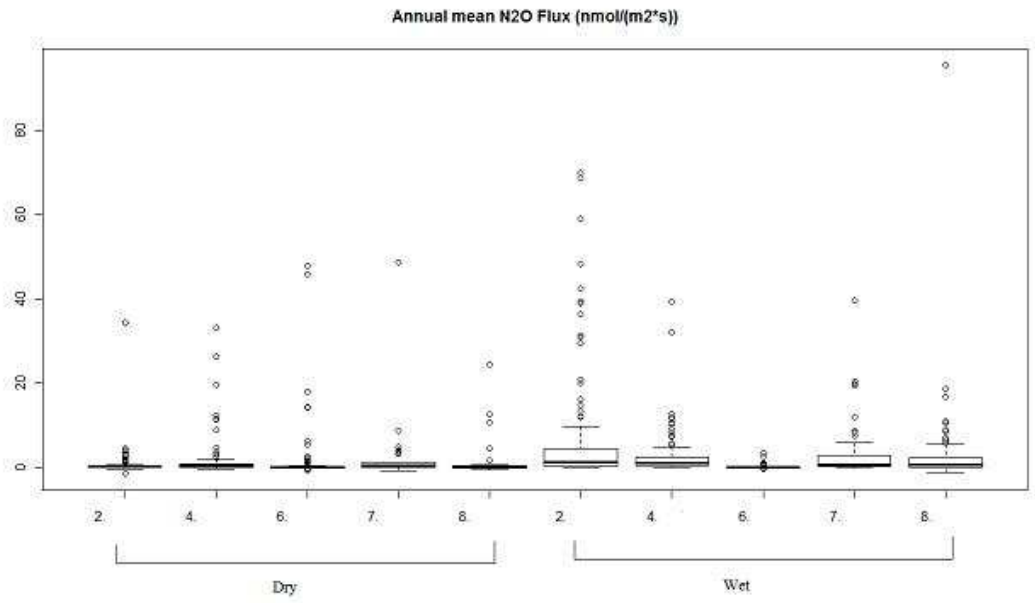

(a) N_2O

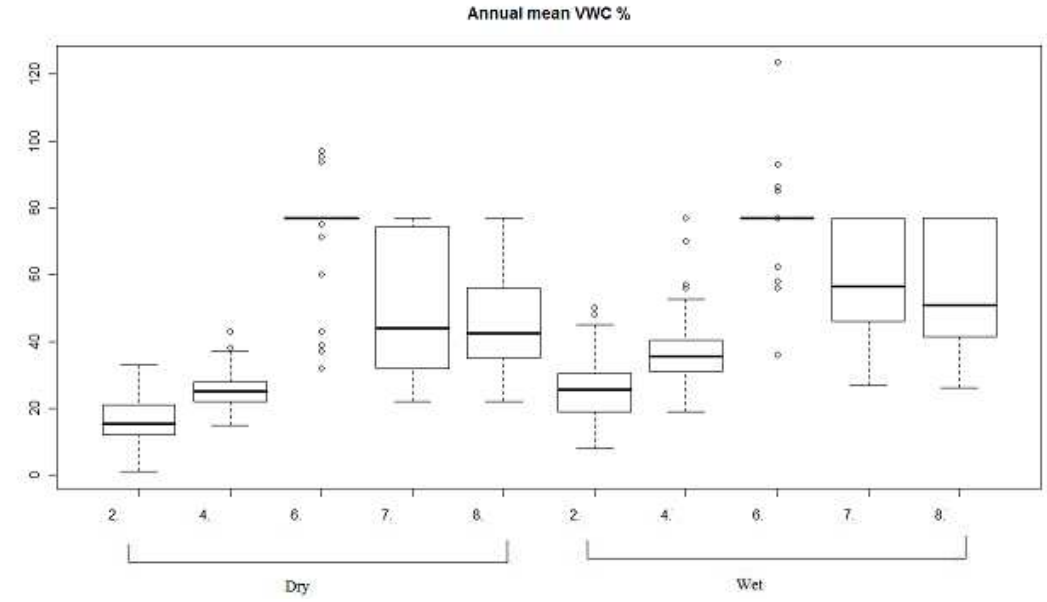

(b) VWC

Figure 5.10: Box plots of trace gas fluxes (N_2O in nmol/m^2s) and volumetric water content (VWC %), showing spatial variability of trace gases among the transects for the dry and the wet season.

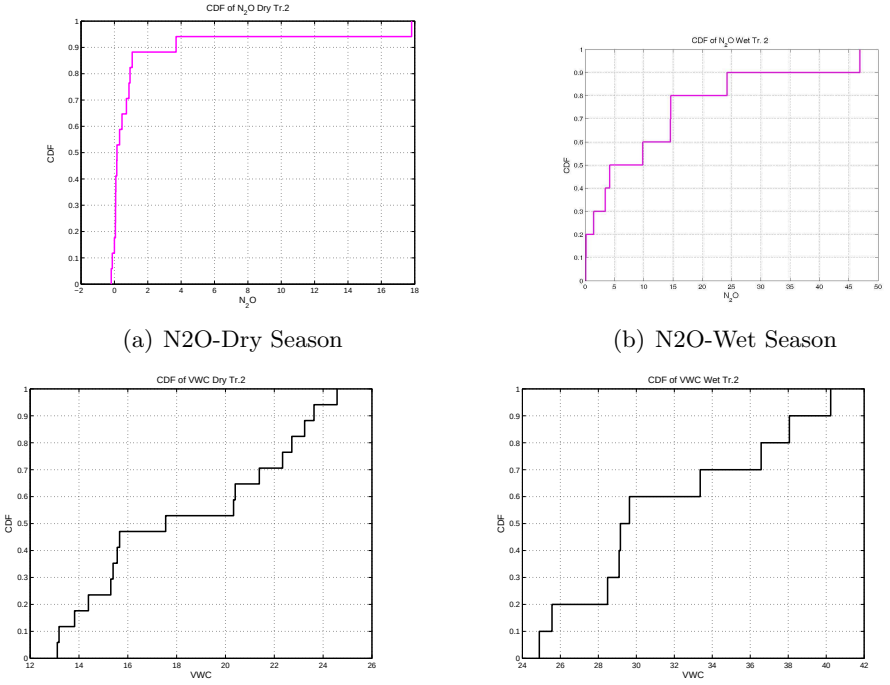

(a) N2O-Dry Season

(b) N2O-Wet Season

(c) VWC-Dry Season

(d) VWC-Wet Season

Figure 5.11: Empirical cumulative distribution function (cdf) for nitrous oxide emissions (N_2O) in nmol/m^2s and volumetric water content (VWC %) emissions during the dry and wet season.

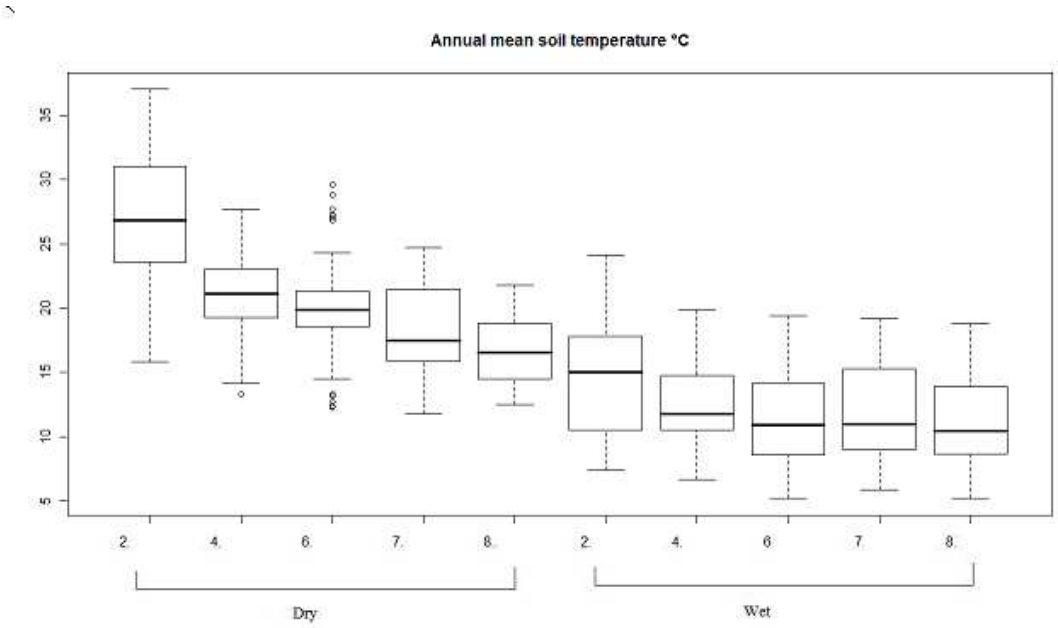

Figure 5.12: Soil temperature data (°C), showing the spatial variability among the transects for the dry and wet season.

soil as shown by the box-plot, lowering carbon dioxide emissions and significantly enhancing methane gas production. Neglecting the irrigation ditch lead to wrong evaluation of the spatial variability of the field areas. This is visible, for instance, by observing and comparing the variograms of Figure 5.16. The evident oscillation observed is due to the intrusive influence of the ditch. Also, histogram (plotted here in terms of a probability mass function)in figure 5.17 shows how the ditch emits methane trace gases fluxes which are of two orders of magnitude higher when compared to the ones measured along the other transects.

5.2.4 Comparison Along the Transects

In order to measure the impact of spatial variability along each transect, we calculated the coefficient of variation (CV), using the same approach described to quantify data variability along the experimental column (see Section 3, Chapter4). CV values has been computed for each chamber as reported in the tables 5.2,5.4 and 5.5. These values provide a measure of the variability in the time series at different spatial locations.

Assuming that precipitation is homogeneous along the area where the transects are

Figure 5.13: Picture of the irrigation ditch in the peat field of Joaquin, Sherman Island,Bay Delta Area, California, CA.

located (the length of the transect is about 30 meters), we can assume that the variability in values of VWC is somehow directly linked to the variability of hydraulic conductivity (K), which reflects soil heterogeneity. The role of changes in VWC on trace gases is a complex process to quantify since it does not only depend on the physical and chemical properties of the soil, but also on biological activity and hydraulic properties variation (which dictates how water flows in porous media). This is shown in expression (5.1), where f and g are non-linear transfer functions indicating that these relationship are complex to quantify.

$$K \longrightarrow f \longrightarrow \Theta \longrightarrow g \longrightarrow Gases\,(CO_2, CH_4, NO_2) \tag{5.1}$$

CV vales for VWC indicate that transect 2 presents high variability of hydraulic property along the transect. The CV varies from 0.58 from chamber 6 to 0.28 in chamber 10, with a decrease of 65% of the value. This indicates that chamber 6 experienced a more

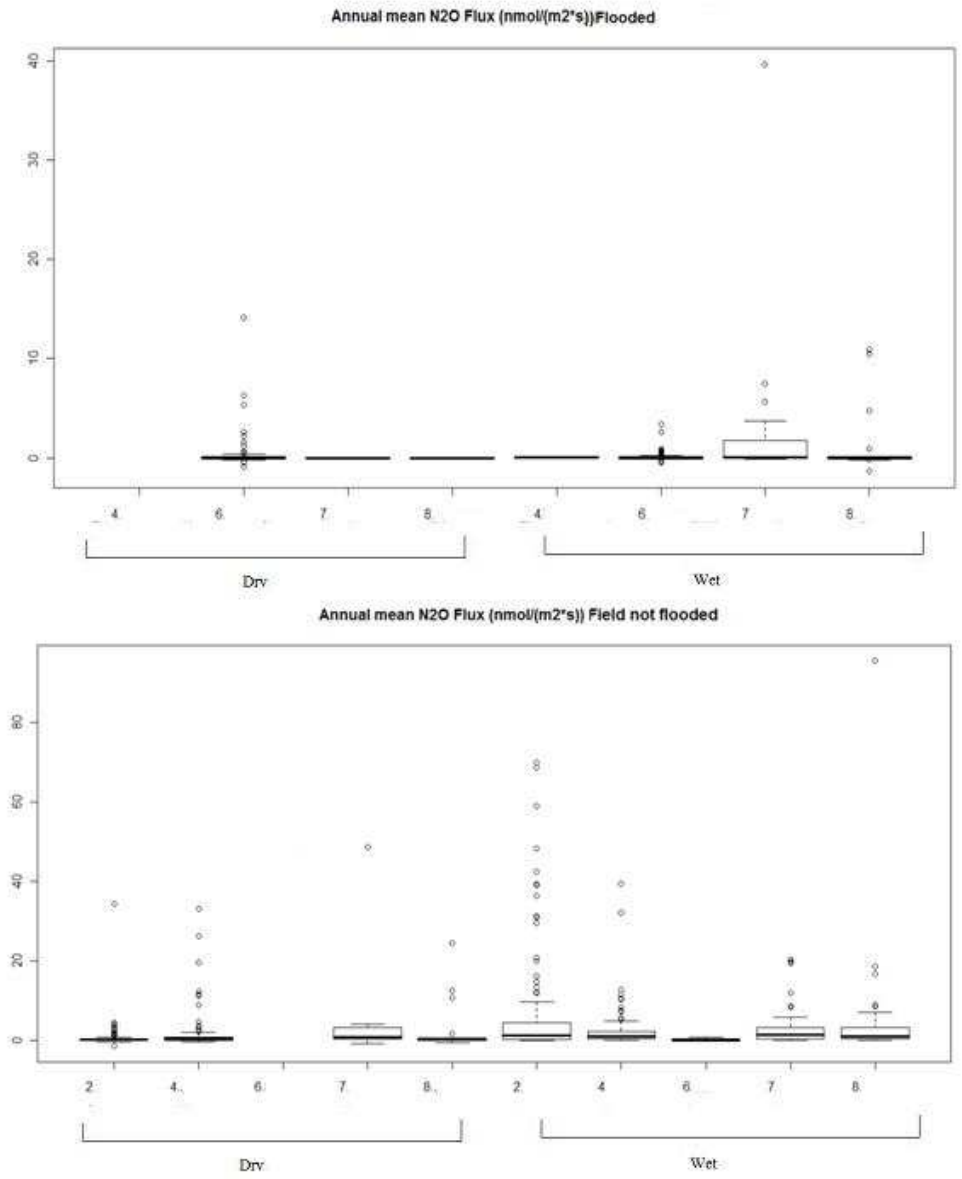

Figure 5.14: Nitrous oxide emissions (N_2O) in nmol/m^2/s for different field conditions: flooded and not flooded.

broad range of soil moisture values than chamber 10. The variability of N_2O is within the same range along the transect, while the maximum variation of CV for methane correspond to the maximum variation of CV for CO_2 and vice-versa. For instance, chamber 9 has a coefficient of variation for methane (CV_{CH_4}) of 8.3 which corresponds to the coefficient of variation for carbon dioxide (CV_{CO_2}) of 0.54. Also in chamber 10 CV_{CH_4} is

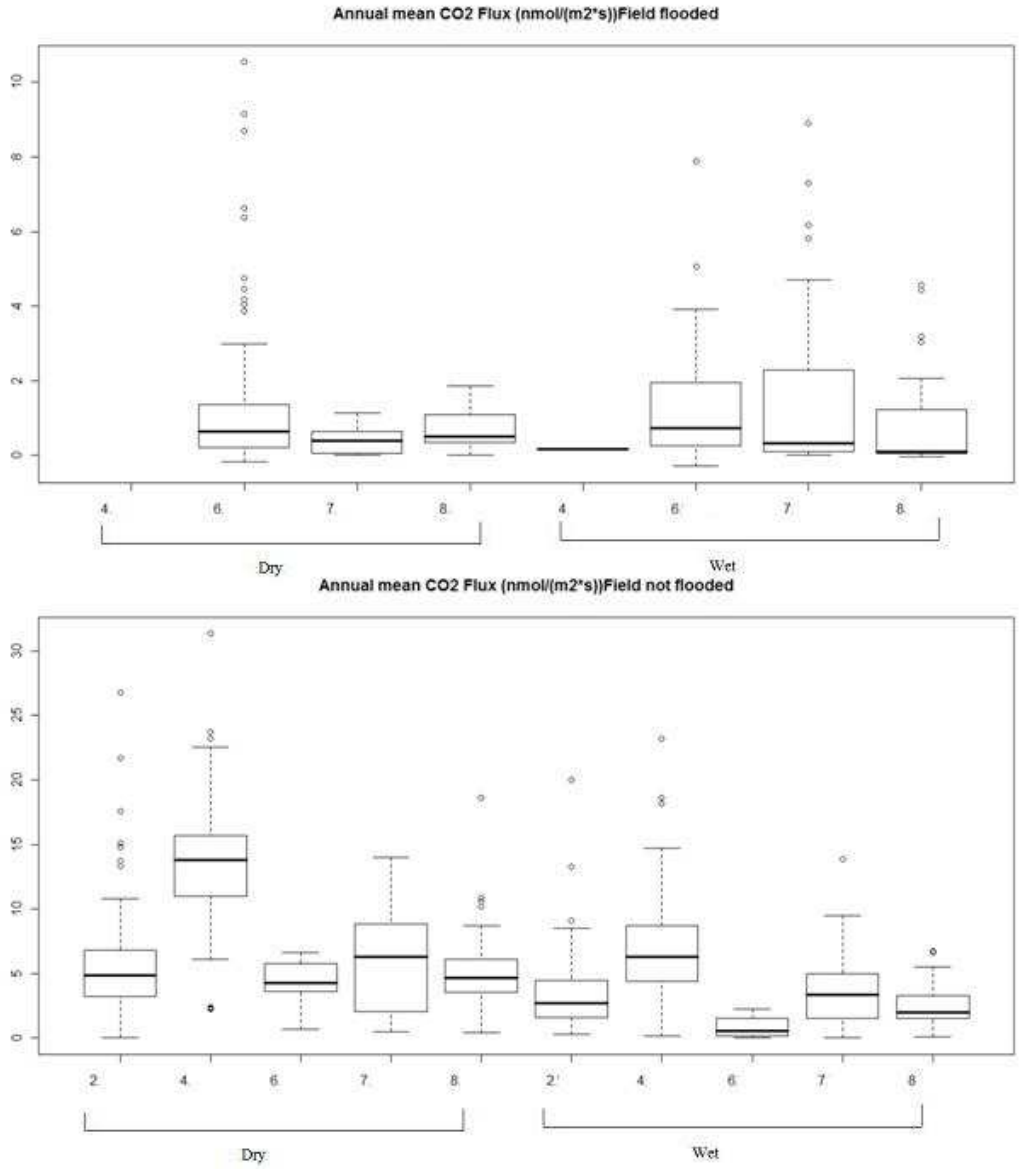

Figure 5.15: Carbon dioxide emissions (CO_2) in μmole/m^2/s for different field conditions: flooded and not flooded.

2.52, while CV_{CO_2}=0.81. This indicate that in this transect, a large temporal variability in methane fluxes can lead to a lower temporary variability in carbon dioxide or vice-versa. The CV for temperature (denoted by CV_T) is around 0.3 for all three transects. Only transects 7 and 8 show variability, especially chambers 35 ad 40. It is interesting to observe that the irrigation ditch show no variation of CV for VWC , CO_2 and CH_4, while

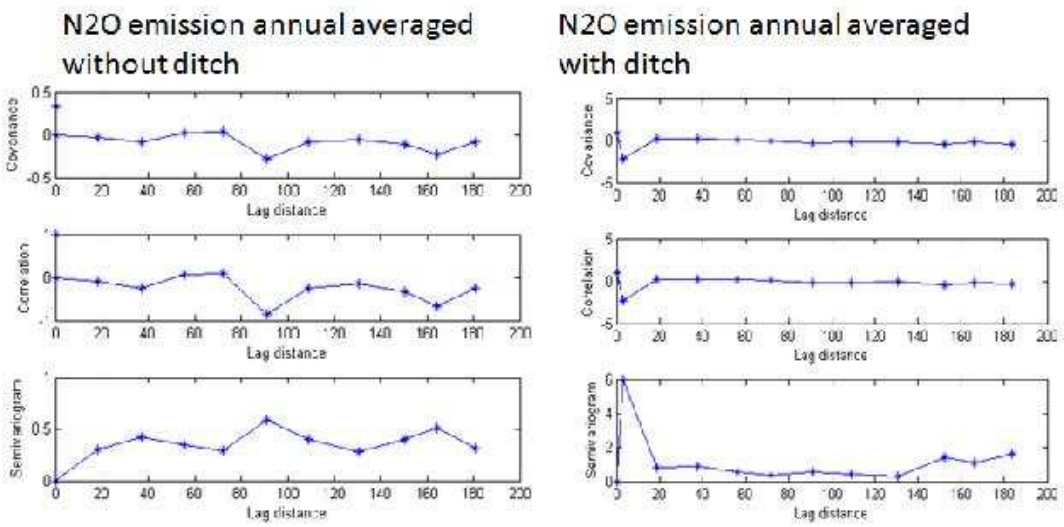

Figure 5.16: Covariances, correlations and variograms as a function of lag distances (m) of nitrous oxide emissions (N_2O) in nmol/m^2/s. Analysis done with (and without) the irrigation ditch.

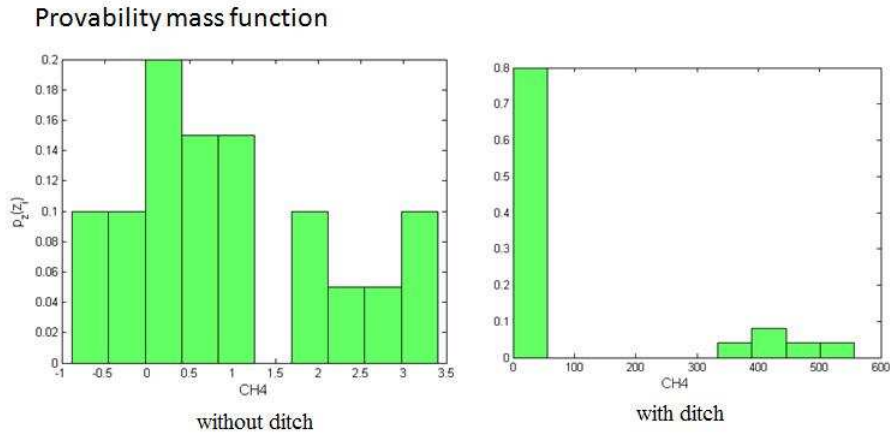

Figure 5.17: Probability Mass Function (PMF) for the annual average of methane fluxes (CH_4 in nmol/m^2/s) with and without the irrigation ditch.

coefficient of variation for nitrous oxide (CV_{N_2O}) varies 23% within the transect.

On the contrary to the irrigation ditch, transects 7 and 8 which are periodically saturated, present high variability along the transect for the CV of trace gases (see table5.2). A closer inspection in the data set revels that the variability of CV for methane and nitrous

oxide is linked to the flooding event (see tables 5.4 and 5.5). For example in transect 7 CV_{N_2O} is practically constant in non flooded condition, while it is ranging from 2.6 to 5.4 in flooded condition.

Finally by computing the ratio between coefficient of variation of soil moisture CV_Θ and of trace gases CV_{GHG_s} for the 5 transects, it is possible to note that for the transects 2 and 4 (never flooded) the fluctuation of soil moisture is stronger than that of trace gases. This effect decreases in periodically saturated transects (7 and 8) and considerably declines to less than 10% for the irrigation ditch. This indicates that the dynamic of trace gas emissions is correlated to the dynamic of soil moisture.

Transect 2							
Chamber #	**T**	**VWC**	**AFPS**	**WFPS**	**CH_4**	**CO_2**	**N_2O**
All	0.359995	0.443088	0.18041	0.445946	3.409717	0.764163	2.958295
6	0.377902	0.58002	0.166346	0.589444	3.986818	0.642143	2.857216
7	0.3595	0.446304	0.176749	0.461248	1.612496	0.652675	3.159218
8	0.367618	0.399374	0.147086	0.407091	3.997728	0.614225	2.703281
9	0.327276	0.343771	0.156999	0.346354	8.389267	0.549301	3.126959
10	0.330081	0.288678	0.188198	0.322062	2.527926	0.81327	2.513384
Transect 4							
Chamber #	**T**	**VWC**	**AFPS**	**WFPS**	**CH_4**	**CO_2**	**N_2O**
All	0.310167	0.345359	0.190039	0.340815	2.755037	0.467313	2.054177
16	0.292636	0.338914	0.313303	0.404259	2.457787	0.66467	1.830636
17	0.29813	0.21095	0.125029	0.235171	2.377822	0.363481	2.550278
18	0.303515	0.232953	0.167476	0.264323	4.576241	0.475938	3.164232
19	0.3134	0.33734	0.208486	0.352323	6.095973	0.486735	2.061833
20	0.310167	0.345359	0.190039	0.340815	2.755037	0.467313	2.054177
Transect 6							
Chamber #	**T**	**VWC**	**AFPS**	**WFPS**	**CH_4**	**CO_2**	**N_2O**
All	0.320822	0.098805	4.8304	0.092058	2.701183	1.331716	5.222563
26	0.323295	0.099629	4.78959	0.092812	2.680139	1.341209	5.187226
27	0.32257	0.099629	4.78959	0.092812	2.679162	1.351519	5.304867
28	0.321838	0.099629	4.78959	0.092812	2.710119	1.341531	5.35178
29	0.32129	0.088698	5.24975	0.079752	2.69002	1.270848	6.727168
30	0.325387	0.079895	5.817323	0.068416	2.599287	1.251385	5.957297
Transect 7							
Chamber #	**T**	**VWC**	**AFPS**	**WFPS**	**CH_4**	**CO_2**	**N_2O**
All	0.31731	0.315877	0.795028	0.328772	5.215013	0.973799	2.498806
26	0.105254	0.3269	0.852794	0.340939	2.4004249	0.937575	2.462115
27	0.166325	0.269034	0.698498	0.277291	1.779942	0.658898	1.420274
28	0.206904	0.214002	1.122204	0.221177	5.646117	1.24027	2.685556
29	0.156455	0.305275	0.855119	0.325162	3.008444	0.748193	1.401481
30	0.896022	0.612844	0.201008	0.597047	1.677321	0.523863	0.854489
Transect 8							
Chamber #	**T**	**VWC**	**AFPS**	**WFPS**	**CH_4**	**CO_2**	**N_2O**
All	0.313193	0.317243	0.735667	0.318794	4.507065	1.012686	3.43519
26	0.091438	0.292491	0.867696	0.301767	2.591245	1.065484	2.253452
27	0.181774	0.303246	0.792185	0.299788	4.322491	0.5092	2.50755
28	0.328339	0.265446	1.141585	0.266651	2.979128	1.287829	2.939439
29	0.17743	0.263316	0.430534	0.28267	3.121205	0.609227	1.27362
30	0.849314	0.613339	0.305615	0.605281	1.65497	0.470882	1.134355

Table 5.2: Coefficient of variation (CV=σ/μ) for volumetric water content (VWC), air soil filled porosity (AFPS), water filled soil porosity (WFSP), and trace gas emissions along the transects.

Transect #	CV_θ/CV_{CO_2}	CV_θ/CV_{CH_4}	CV_θ/CV_{N_2O}
Tr. 2	14.97781661	12.9948145	57.98344071
Tr. 4	16.81252395	12.53554852	73.90314415
Tr. 6	1.891887183	3.6578441768	7.419374702
Tr. 7	12.64111852	6.057069966	32.43758685
Tr.8	12.97969943	11.28767281	27.4514481

Table 5.3: Percent ratio of the coefficient of variation (CV=σ/μ) for soil moisture CV_Θ and coefficient of variation of trace gases CV_{GHG_s} for the 5 transects.

Transect 7 - non flooded							
Chamber #	**T**	**VWC**	**AFPS**	**WFPS**	**CH_4**	**CO_2**	**N_2O**
All	0.338247	0.472664	0.786086	0.459389	6.410132	1.059877	3.034743
31	0.339208	0.471868	0.789712	0.458417	6.39538	1.065456	3.024679
32	0.338864	0.471923	0.789713	0.458413	6.400848	1.065348	3.030357
33	0.338536	0.472339	0.789376	0.458846	6.402697	1.063406	3.032954
34	0.338345	0.472998	0.78852	0.459544	6.400921	1.063812	3.038158
35	0.350062	0.477414	0.782086	0.464594	6.320608	1.051197	2.99507
Transect 7 - flooded							
Chamber #	**T**	**VWC**	**AFPS**	**WFPS**	**CH_4**	**CO_2**	**N_2O**
All	0.34523	0.04981	11.48815	0.00111	4.622987	1.377145	5.423132
31	0.41543	0.20546	0	0.210588	112.929	1.63666	3.395718
32	0.391537	-	-	-	3.746611	1.742984	3.475967
33	0.419509	-	-	-	0.158504	1.679586	2.899412
34	0.365531	-	-	-	3.710554	1.709192	3.363091
35(*)	0.208884	-	-	-	-10.8475	2.481056	2.629676

Table 5.4: Coefficient of variation (CV=σ/μ) for transect 7, flooded and non flooded conditions.

Transect 8 - non flooded							
Chamber #	**T**	**VWC**	**AFPS**	**WFPS**	**CH_4**	**CO_2**	**N_2O**
All	0.314386	0.318111	0.738041	0.319639	4.523362	1.016349	3.454063
36	0.329347	0.327597	0.751613	0.329299	4.358699	1.02233	3.301439
37	0.31544	0.315684	0.754181	0.317636	4.501141	1.029131	3.518094
38	0.312885	0.317876	0.753168	0.320179	4.544567	1.017138	3.627486
39	0.310709	0.320166	0.751989	0.322564	4.544567	1.017826	3.854878
40	0.309597	0.32199	0.750598	0.324179	4.630079	1.017722	3.878444
Transect 8 - flooded							
Chamber #	**T**	**VWC**	**AFPS**	**WFPS**	**CH_4**	**CO_2**	**N_2O**
All	0.37233	0.026323	5.525785	0.00044	5.449143	1.474662	3.572625
36	0.395395	0.027727	5.239898	0.000464	4.910734	1.528342	3.572625
37	0.382692	0.027727	5.239898	0.000464	5.022275	1.536446	3.518561
38	0.369621	0.027727	5.239898	0.000464	5.203234	1.480663	3.472198
39	0.357272	0.027727	5.239898	0.000464	5.203234	1.449216	3.41628
40	0.319674	0.029845	4.858916	0.0005	25539.27	1.426468	3.069377

Table 5.5: Coefficient of variation (CV=σ/μ) for transect 8, flooded and non flooded conditions.

5.3 Comparison Between Measurements of Nitrous Oxides in the Soil Column and in the Field Site.

The soil used for the column experiment has been collected close to transect two. For that reason it is interesting to compare the response to changes in VWC for the soil collected in the transect and the one used in the column. Figure 5.18 reports the time series for N_2O versus VWC, which illustrate how water pulses are concomitant to nitrous oxide emissions. This is more evident in Figure 5.19, which shows the direct correlation among soil moisture and N_2O. The graph shows how to an increase of 0.3 in VWC, correspond an increase of N_2O emissions of one order of magnitude. This clearly show the potential for N_2O to be important as GHG in temperate pasture, having a GWP 310 times higher than CO_2 (ICPP, 2007).

The apparent disagreement with the column, where we found a negative correlation between rainfall and emissions (as shown previously in this dissertation), is related to the different time steps of the measurements in the laboratory and in the field.

Since the N_2O peak is related to the ancedent wet condition of the soil, it is interesting to observe that contrary to what observed in the field, the peak of N_2O emissions follows the peak of VWC with a delay that ranges from 3 days, for rainfall events, to 2 days for deposition, as described in Section3, Chapter4.

This indicate that the top layer of the peatland, which present a high saturated conductivity (Ks=2.610^{-6} m/s) drains and saturate much faster than the time required by bacteria to adapt to the new conditions, and is consistent to the observed difference between the time of drainage (which is in the order of 1 hour) and the time of the emission of the peak (which is in the order of days), found in the column.

Also it is interesting to know that oxygen and nitrous oxide emissions act on the same time scale, indicating that oxygen should be the key parameter to capture the pulse of N_2O emissions during rapid changes in water content (Figure 5.20). Obviously, if we average the column data on a weekly time sclae, we find the same correspondence between the VWC and the N_2O emissions, but this is because the average on VWC vanish out the variability on shorter scale.

The dependence on daily scale is therefore important to capture all the processes which are working on the daily scale, such as evapotranspiration, root and nutrient uptake. This implies that to model properly these processes, in soil where the time scale of the soil moisture (*i.e.* infiltration time) is shorter than the time scale of bacteria (*i.e.* oxygen consumption), the oxygen should be considered for modeling purpose, as described in the

following chapter.

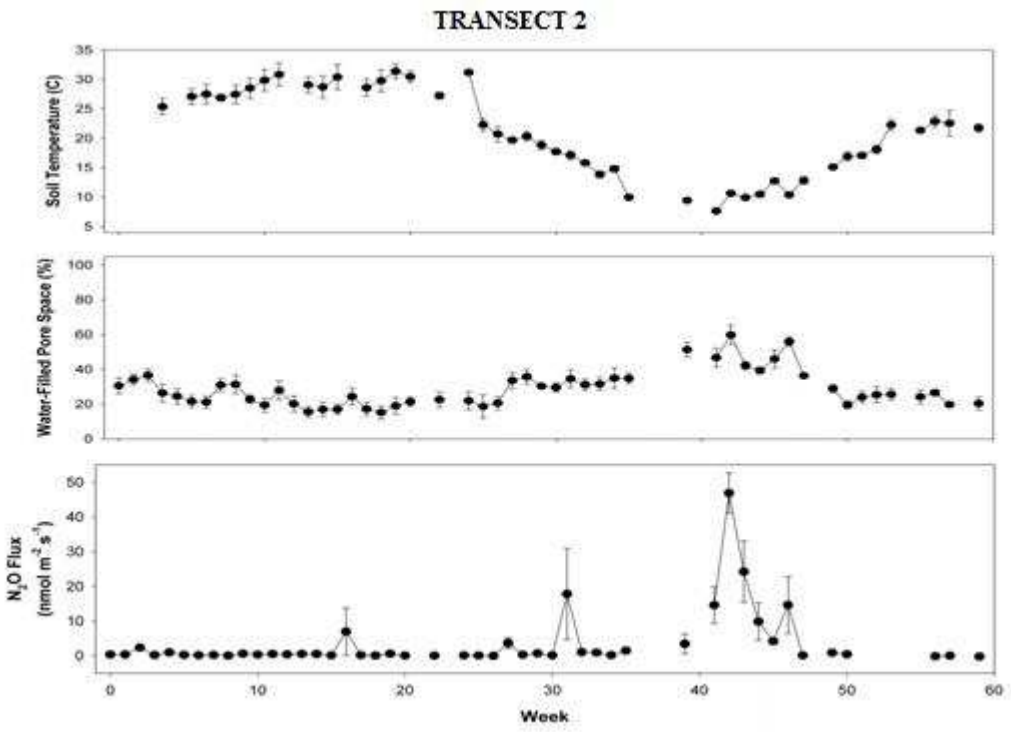

Figure 5.18: Time series of soil temperature (T), water filled pore space (WFPS) and nitrous oxide (N_2O) emissions for transect 2.

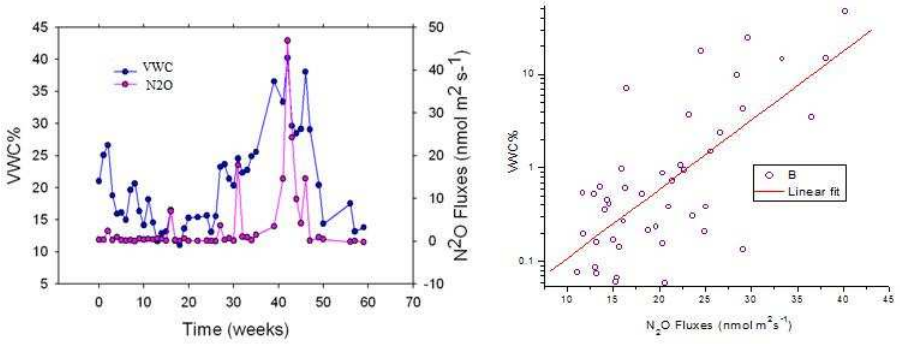

Figure 5.19: Time series of nitrous oxide emissions (N_2O) vs volumetric water content (VWC) (peaks comparison and data regression)for transect 2.

It is finally interesting to observe how in the field (where VWC has been measured

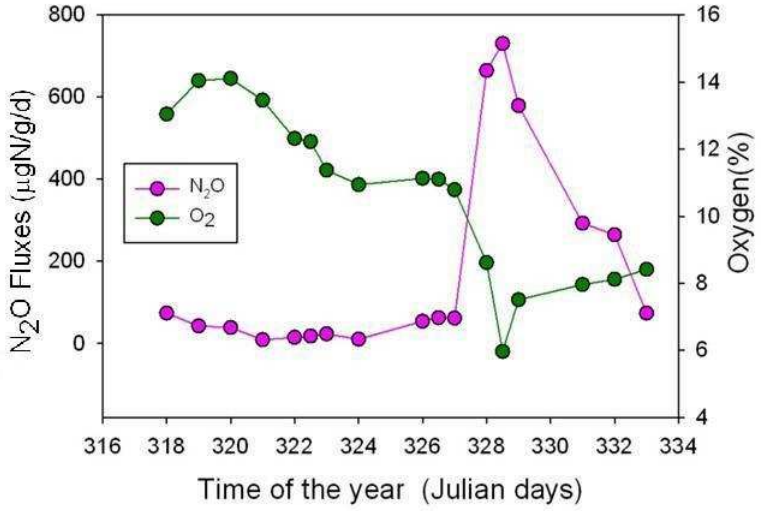

Figure 5.20: Time series of oxygen (O_2) vs nitrous oxide emissions (N_2O) in the soil column.

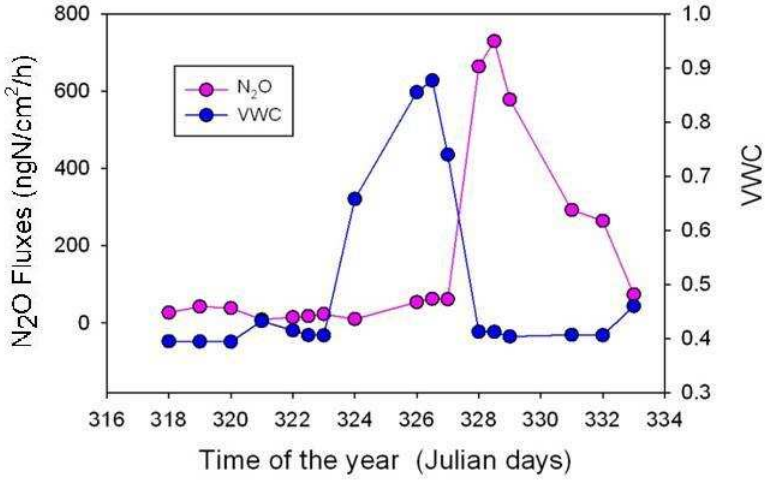

Figure 5.21: Time series of nitrous oxide emissions (N_2O) and volumetric water content (VWC) in the soil column.

on the weekly base), the relationship of VWC versus N_2O emissions is closer to the one predicted by Davidson et al. (2003) both for the field and transect 2.

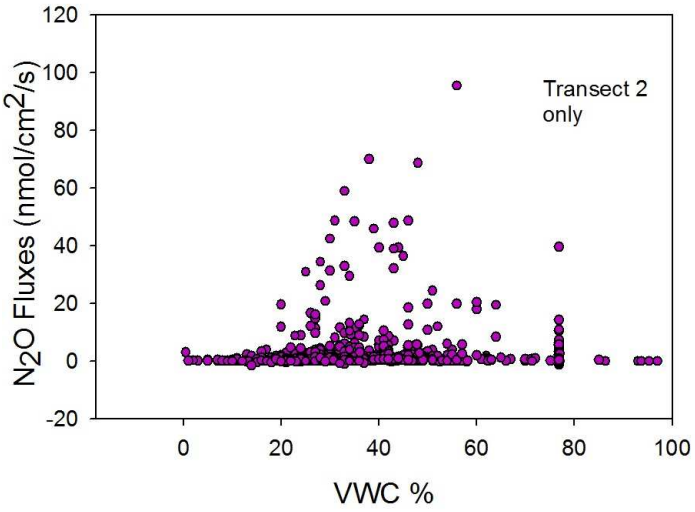

(a) N_2O vs VWC, transect2

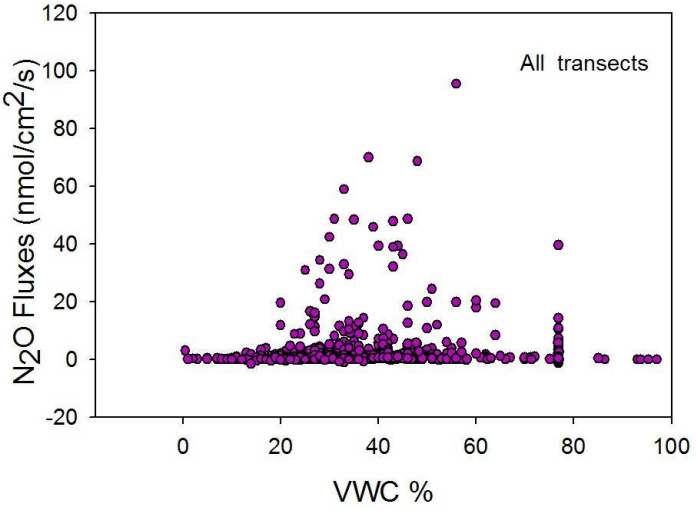

(b) N_2O vs VWC, field

Figure 5.22: Nitrous oxide emissions (N_2O) emissions versus volumetric water content (VWC) (transect 2 and field).

5.4 Chapter Summary

In this chapter, we showed the role of soil moisture, flooding event and irrigation ditch on trace emissions in Sherman island. Flooding extent and soil moisture strongly influenced the magnitude of N_2O fluxes, which responded strongly to increases in soil moisture, showing a 12-fold increase over 30-60% water-filled pore space. The sensitivity of N_2O fluxes to flooding and hydrological conditions suggests that alteration of existing water management practices in drained Delta peatlands have significant implications for regional GHG budgets. Likewise, re-flooding or controlled levee breaches are likely to greatly enhance GHGs fluxes, with potential deleterious effects for regional climate and atmospheric chemistry. Also, data show evidence of large GHG fluxes from managed and restored peatlands in the Sacramento-San Joaquin Delta of California, as reported in the analysis of Teh et al. (2010). Nitrous oxide fluxes measured were large (peaks of 200 μmole/m^2/d) when compared to emissions from heavily fertilized agricultural systems and tropical forests, which are considered the two largest N_2O sources globally (Skiba et al., 1999; Stehfest and Bouwman, 2006). The interactions between terrestrial biogeochemistry and the hydrological cycle are likely determinants of their role in global warming.

6 On Oxygen Dynamics and Nitrogen Cycle in Unsaturated Soils: A Modeling Perspective

6.1 Introduction

Crucially located on the earth surface at the interface between atmosphere and biosphere, soils are where important exchanges of water, organic matter, nutrients, and gases take place at time scales ranging between a few seconds to several centuries (Porporato et al., 2003).

Modeling the N-cycle in soils is important for many environmental issues; among those eutrophication, the destruction of the ozone layer in the stratosphere and the greenhouse effect in the troposphere (see Chapter 2). Given the chemical and radioactive properties of nitrous oxide gases (N_2O) in the atmosphere (Ramanathan, 1986; Davidson, 1991), understanding and predicting the mechanism of production in soils and and fate in the environment is crucial, since tropical forests and agricultural fields represent the main source of nitrous oxide emission in the atmosphere (IPCC, 2007; Galloway et al., 2008). Nevertheless modeling N_2O dynamics is extremely challenging, being N_2O emissions, the result of complex interaction between biotic and abiotc production, consumption and transport (Conrad, 1996; Smith et al., 2003) and thus, depending on soil chemical, physical and biological properties. Processes underlying the N-cycle are still under investigation (Francis et al., 2007). All the interaction between nitrogen and iron are only recently being discover in soils (Clement et al., 2005; Whendee et al., 2009) and their potential role is still unknown. Currently in models the ammonium pool is not directly linked to the production of nitrous oxides or molecular nitrogen (Boyer et al., 2006). Also, the dissimilatory reduction of nitrate to ammonium DRNA, which has been shown to be important in upland tropical soils and wetland (Silver et al., 2001), is neglected in soil

models with the except of few works (Kjellin et al., 2007).

In addition, even for well known processes, such as decomposition or nitrification, the modeling difficulties are linked to the choice of the most appropriate physical and biological parameters to be include in the model. N-cycle involves indeed spatial scale spanning from aggregate to regional and temporal scale ranging from diurnal to decadal, which require to incorporate different factor according to the spatial-temporal scale chosen. On short time scale, the most important factors to consider in the model are precipitation, soil temperature and the eventual use of fertilizer, while on the mid term soil texture, substrate and pH should be included. In addition, most of the processes involving the N-cycle are highly dynamics and require high quality measurements to be quantify (Werner et al., 2007). This challenge raises in the unsaturated zone, where process are highly non-linear and infiltration process may alter soil structure and consequently nutrient redistributing, soil re-aeration and trace gases emissions. Basically N-cycling involves (Edwards,2nd NitroEurope Summer School):

- Sources and sinks for Nitrogen;
- Storage and release;
- Transformations (chemical and physical);
- Movement/transport through system components;
- Environmental impacts of N cycling.

Understanding processes is fundamental since transformation often changes (Edwards,2nd NitroEurope Summer School):

- Reactivity (e.g. nitrification lead to more reactive forms);
- Mobility (e.g. form cation less mobile to anion more mobile);
- Bio-availability (e.g. ammonium is energetically proffered);
- Toxicity (e.g. ammonium is highly toxic).

A review of the main biogeochemical models used in ecosystem and global change studies can be found in (Parton et al., 1996), along with comparative analyses of their performances. Most of these models were developed for long-term studies (Parton et al., 1996; Jenkinson et al., 1990), in particular, of the nitrogen (N) and carbon (C) cycles. Manzoni and Porporato (2009) review more than 250 mineralization mathematical models which

span spatial scales from few mm to thousands of km and temporal scales from hours to centuries, underlying the importance of the scale-dependence in the mathematical formulations, in order to avoid inconsistencies between theoretical formulations and model application. Also Heinen (2006) analyzed more than 50 models for denitrification.

A large quantity of the existing models have emphasized on long-term analysis, neglecting the smaller scales of variability of soil moisture, temperature, nitrogen content or plant uptake. However, a fraction of soil moisture and nitrate variance is at scales of a few days or weeks (Dodorico et al., 2003). Given the highly non-linear properties of the carbon and nitrogen dynamics, the common use of average monthly climatic conditions neglects the effects of high-frequency fluctuations, leading to estimates of SOM stocks and fluxes different from what is found with analysis at higher resolution (e.g., Moorhead et al.; Bolker et al., 1998). These results indicates the need for an accurate study of the soil nutrient cycle at shorter time scales (e.g., Porporato et al., 2003). Studies in the literature (e.g., Aber and Driscoll, 1997; Gusman and Marino, 1999; Birkinshaw and Ewen, 2000; Butterbach-Bahl et al., 2000) have investigated the effect of climate and hydrologic conditions on nutrient and carbon budgets. Moorhead et al. highlights how models that with capacity to operate at high resolutions are needed to provide an adequate representation of the coupling between soil moisture and nutrient dynamics. To this end, a daily version of the CENTURY model (Parton and Rasmussen, 1994), named DAYCENT (Parton et al., 1998) was developed. In this model, soil moisture dynamics are calculated dividing the soil into a number of layers and performing a soil water balance for each of them. The fluxes are modeled through a simplified and discretized version of Richards' equation. The objective of this chapter is include the oxygen dynamics in a simplified decomposition-nitro-denitro model, which account for effect of water dynamics on nitrous oxide emissions. To the knowledge of the authors, this approach has not been done before.

6.1.1 Oxygen and Soil

The role of oxygen (O_2) dynamics in soils has been investigated in the past both from the experimental and the modeling perspective (Simunek et al., 1999). Three main mechanisms are responsible for the recharge of oxygen into soils:

1. Oxygen dissolved into rain;
2. Oxygen diffusion into soil air (given the gradient create by biological activity);
3. Movement of the bulk.

Advection of the gaseous phase into and out of the soil (e.g., under atmospheric pressure changes or effects of temperature) carries the oxygen species with it. Inside the unsaturated zone, where both an aqueous phase (primarily water, but also dissolved matter, dissolved air, etc.) and a gaseous phase (air and water vapor) coexist, if we assume that the system is continuously at equilibrium, the relationship between water vapor content and pressures in the water and in the air) capillary pressure, in the form of Kelvin's law (Bear J., *personal communication*). The equation of advection dispersion for oxygen is the following:

$$\frac{\partial(C_a\theta_a + C_w\theta_w)}{\partial t} = -\frac{\partial}{\partial z}(q_a C_a + q_w C_w - \theta_a D_a \frac{\partial C_a}{\partial z} - \theta_w D_w \frac{\partial C_w}{\partial z}) + P, \tag{6.1}$$

where C_a, C_w are the concentration in the gas and liquid phase, D_a, D_w are the soil matrix diffusion in the gas phase and dispersion in the liquid phase, θ_a, θ_w are the volumetric air and water content. $q_a C_a$ describe the O_2 flux caused by diffusion in the gas phase, is the O_2 flux caused by dispersion in the dissolved phase, is the flux caused by convection in the gas phase, is the flux caused by convection in the liquid phase. P is a source/sink term. This approach is followed by complex model, such us HYDRUS (Simunek et al., 1999) and TOUGHREACT-N (Riley et al., 2008).

The effects of oxygen dynamics on the N-cycle has been study in the past by different authors: Allison et al. (1960); Goreau et al. (1980); Cho (1982); Silver et al. (1999) and Venterea and USDA (2007). However, to the best of our knowledge there are no experiments, where oxygen dynamics was coupled to water dynamics under controlled condition as described in Chapter 4. Usually, models do not explicitly consider oxygen. Most models uses a function of volumetric water content (Ridolfi et al., 2003a; Heinen, 2006), assuming that low water content correspond to high soil oxygen levels, while high value of soil moisture (e.g. saturation close to saturation) correspond to low oxygen condition. The implicit assumption is that oxygen diffusion so that it equilibrates rapidly with water. However, for a fixed range of volumetric water content, the level of oxygen may vary in time, since reareation process is highly dependent on the type od soil, on water dynamics and on possible phenomena of ebullient and entrapment which can inhibit escape of trace gases from the soil to the surface or oxygen diffusion from the surface to the soil (Heincke and Kaupenjohann, 1999; Smith et al., 2003). In addition, rainfall may cause clogging of the surface, which may significantly alter the exchange between surface and atmosphere (Zejun et al., 2002). These mechanisms may delay the re-oxygenation on consequent result in a higher oxygen consumption, which can no be capture by model which account only for

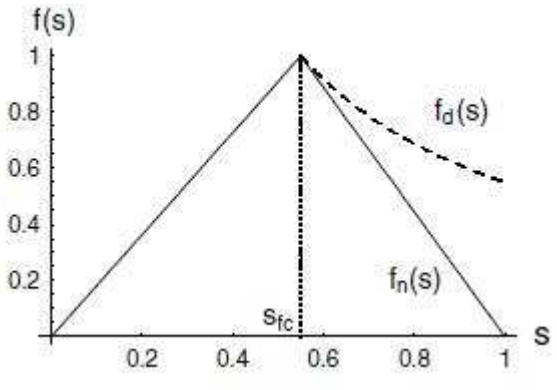

Figure 6.1: Fundamental dependence of decomposition and nitrification on the relative soil moisture used in Porporato (2003).

water limitation. Experiment described in Chapter 4, for instance, shown, that changes in oxygen and water may act on different time scales.

This, and the reducing effect of reareation trough the soil profile, given by changing in soil compactation and surface clogging, may result in delay of reareation and trace gas emissions. In addition the changes in bacteria community driven by water addition may cause changes in the hydraulic properties (e.g., Soares et al., 1991).

In the present work, we do not consider explicitly oxygen transport, since we are using a "bucket" approach, as explained in the following section. However, we account for microbiological oxygen consumption and the reareation. The first term include the consumption of oxygen during decomposition and nitrification, while the second term is model trough a function of volumetric water content, porosity and a coefficient of reareaction as described in later in this chapter, allowing us to reproduce indirectly the effect of ebullient, entrapment and clogging effects given by water addition, and also to consider different type of soil (for instance clay has a reareaction rate minor than sand). The oxygen dynamics has been applied successfully to N-cycle in the Activated Sludge Model (ASM) (Henze, 2000) and more recently in wetland system (Langergraber and Simunek, 2005). However, sludge model describe saturated condition. Here we propose a model in which the limitation of water for value greater than the field capacity ($s \leq s_{fc}$) is given by the expression used by Porporato et al. (2003), while we consider that for values greater than field capacity ($s > s_{fc}$) the limitation is given by the oxygen dynamics, see Figures (6.1,6.2).

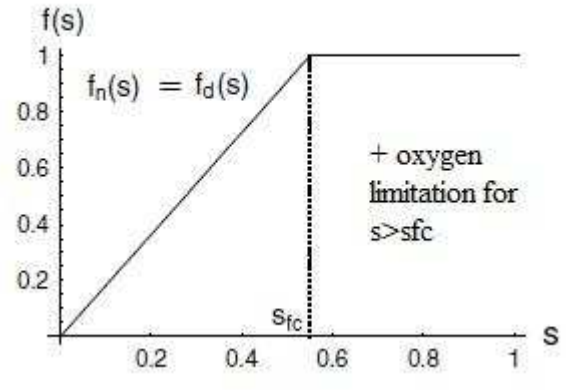

Figure 6.2: Fundamental dependence of decomposition and nitrification on the relative soil moisture when oxygen dynamics is included. Water is a limiting function only for soil moisture value lower than field capacity ($s \leq s_{fc}$). The limitation for ($s > s_{fc}$) is given by oxygen level.

Oxygen dynamics is implemented following the approach used in the activate sludge models (ASM1,SM2 ad ASM3 , Henze 2000). According to the soil literature (Sylvia et al., 1998), see Chapter 1 we know that :

- Oxygen is required by hypertrophy decomposition of organic matter and nitrification
- Oxygen is limiting nitrate ammonificiation (DNRA), denitrification, nitrous oxide emissions from denitrification
- Oxygen favours nitrous oxides production from nitrification for intermediate values of oxygen (Venterea and USDA, 2007)

Therefore we consider:

- A oxygen Monod function for the processes which are enhanced by oxygen: $\frac{O_2}{K_{O2}+O_2}$
- An inhibition function for processes limited by oxygen: $\frac{K_{Io2}}{O_2+K_{Io2}}$

In the above expression O_2 is the dissolved oxygen concentration in (mg/l) and K_{O2}, K_{Io2} are the oxygen semi-saturation constant for Monod and inhibition functions (see Figure 6.3 and 6.4).

We therefore consider that oxygen acts as a non-linear factor, even though we consider for now that reareaction is a linear function of soil moisture, as accepted in most of the

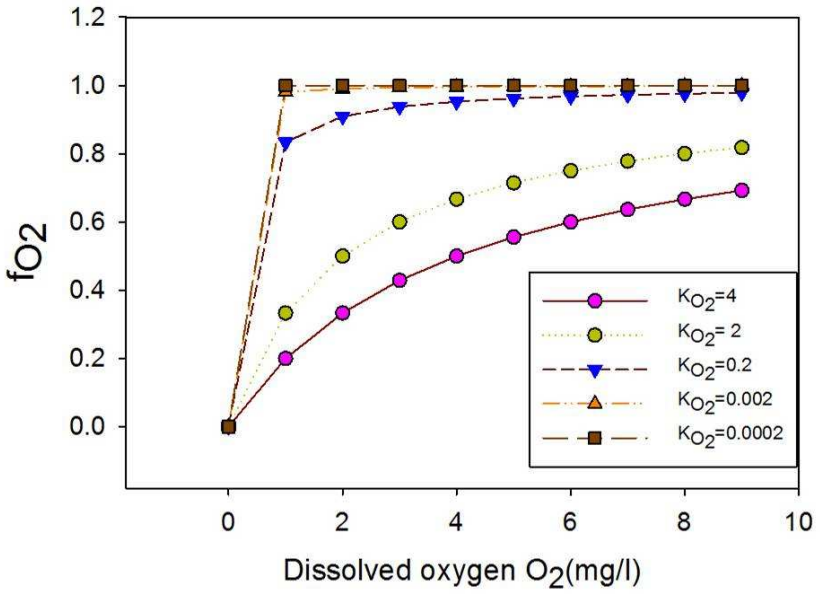

Figure 6.3: Fundamental dependence of decomposition and nitrification on dissolved oxygen level (mg/l).

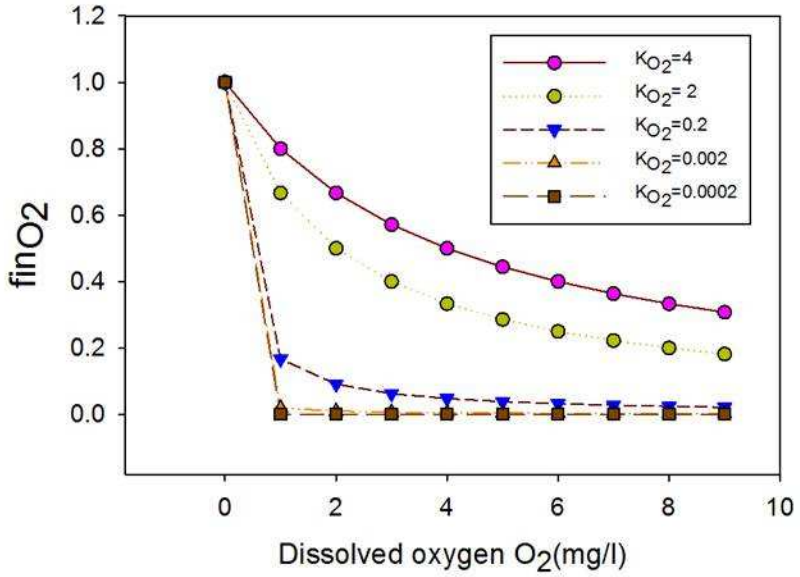

Figure 6.4: Fundamental dependence of nitrate ammonificiation and denitrification on dissolved oxygen level (mg/l).

current model (Gilmour, 1984; Simunek et al., 1999). In reality the relationship is not-linear (Amer and Bartholomew, 1951).

In addition, differently from sludge model, we consider that the C:N ratio of the organic pool may non match the one required by bacteria leading to immobilization of mineralization (Barak et al., 1990). Sludge model consider instead that bacteria assimilate the exact ratio of carbon and nitrogen which match their demand and mineralized the excess, as described in the following sections, but this approach is usually not used for soil mdels (e.g., Manzoni and Porporato, 2009).

6.2 Modeling Oxygen and Soil Moisture Effects on Decomposition and Nitrification

Porporato et al. (2003) uses only one soil layer in a "bucket" model calculating the soil water content. The suitability of single-layer models to study soil moisture dynamics in the root zone has been assessed by Guswa et al. (2002) who compared the performances of the one-layer bucket model with the results of numerical simulations of Richards equations for the unsaturated root-zone dynamics. Soil moisture dynamics is modeled here as in Porporato et al. (2003) through a stochastic soil water. The model of Porporato et al. (2003) is a process-based model which couple carbon (C) and nitrogen (N) at the daily time scale to model soil moisture and soil C–N variations in savanna ecosystems. The original model was developed for water-limited systems by Porporato et al. (2003), then the model was applied by Porporato et al. (2007), Manzoni et. al. (2008) and Wang et al.(2009). A prior application of this model to a South African savanna ecosystem can be found in Dodorico (2003).

The C and N cycles are modeled using three soil organic matter pools (*i.e.*, litter, humus and microbial biomass, indicated by subscripts l, h and b, respectively), and two pools describing mineral N (i.e., ammonium and nitrate, indicated by N^+ and N^-, respectively; see Figure 6.5). Since the C/N ratios of humus and microbial biomass can be assumed constant, the system is described by six mass balance equations (seven with the oxygen dynamic), where the state variables are expressed in terms of grams per cubic meter. The equations describing the system are the following:

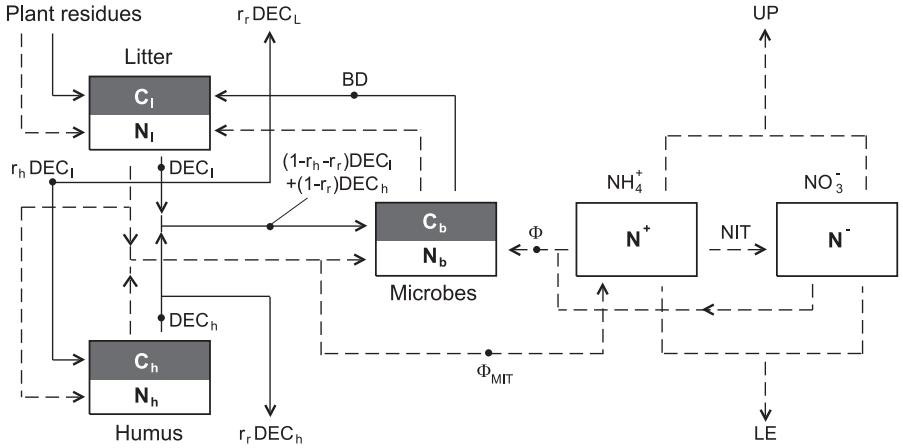

Figure 6.5: Schematic representation of compartments and fluxes of the coupled C–N model (Porporato et al. 2003; Manzoni and Porporato 2007). White compartments and dashed lines represent N pools and fluxes; shaded compartments and continuous lines refer to the corresponding C pools and fluxes. The combination of the fluxes (defined to keep CNb constant) and MIT (the fraction of decomposed N transferred to ammonium) define gross mineralization and immobilization, as described by Porporato et al. (2003), Manzoni and Porporato (2007) and Manzoni et al. (2008).

$$\frac{dC_h}{dt} = -DEC_h + r_h \cdot DEC_l \tag{6.2}$$

$$\frac{dC_l}{dt} = ADD - DEC_l + BD \tag{6.3}$$

$$\frac{dC_b}{dt} = -BD + (1 - r_h - r_r) \cdot DEC_l + (1 - r_r) * DEC_h ... \tag{6.4}$$

$$\frac{dN_l}{dt} = \frac{ADD}{(\frac{C}{N})_{ADD}} - \frac{DEC_l}{(\frac{C}{N})_l} + \frac{BD}{(\frac{C}{N})_B}$$

$$\frac{dN^+}{dt} = MIT_{gross} - IMM_{gross} - NIT - LE^+ - UP^+ \tag{6.5}$$

$$\frac{dN^-}{dt} = NIT - IMM_{gross} - LE^+ - UP^+ \tag{6.6}$$

The term ADD is the external organic matter input into the system. The model assume that only external C and N inputs are through vegetation litter and that the rates are constant. The term BD describe the rate at which C returns to the litter pool due to microbial biomass death. DEC_l represents the litter decomposition rate and DEC_h is the humus decomposition rate. The decomposition fluxes drive both soil respiration

and microbial growth and non linearly depend on soil moisture, microbial activity being inhibited both at low water potential and in conditions close to saturation (see Figure6.1) as described in the previous section. Nitrogen decomposition fluxes are equal to the C fluxes divided by the C/N ratio of the source pool. However, only a fraction of the decomposed N from litter and humus is directly assimilated by the microbes (Fig. 6.5), while the remaining is mineralized to ammonium according to the parallel mineralization scheme (Manzoni and Porporato, 2007). Net mineralization is defined as the difference between gross mineralization (MINgross) and immobilization (IMM+ gross, IMM- gross), *i.e.*, it refers to the transformation of organic N into NH_4^+. Details on the definition of the gross N fluxes are reported in Porporato et al. 2003 ad Manzoni and Porporato 2007. The dynamics of ammonium and nitrate (N+ and N-) were described by the balance of mineralization, immobilization, nitrification (NIT), leaching (LE+, LE-) and root uptake (UP+, UP-), which in turn strongly depend on soil moisture (see eqs 6.36 and 6.59). Wet and dry deposition as well as N fixation are important only in the long-term balance and are neglected in this modeling framework. Denitrification, which may take place when soil moisture is high, is also neglected in Porporato et al. 2003, since it is assumed that the losses due to plant uptake and evaporation are much higher than the losses due to denitrification in arid system. The oxygen dynamics in the model was inserted in a simplified version of this model, where we did not consider plant uptake and leaching and we considered only the decomposition of the litter pool. In this condition the oxygen is consumed by bacteria during decomposition and nitrification. Here we assume that nitrifier bacteria are not limiting, thus we can use only one pool of bacteria. Under these conditions the equations 6.8,6.7 describe the rate, while the oxygen dynamics is describe trough equation 6.9, where K_{rear} is the reareation constant in day^{-1}, n is the soil porosity, s is the soil moisture, O_{2sat} is the saturated oxygen concentration (which is 9.1 mg/l for standard condition), and the coefficient which multiply the rate account for the conversion of gC and gN to g of O_2. Finally, the factor $(1/sn)$ account for the conversion of g/m^3 to mg/l

$$DEC_l = k_1 \cdot C_b \cdot C_R \cdot N^- \cdot \frac{K_{o2}}{O_2 + K_{o2}} \cdot f_{den} \cdot \varphi \tag{6.7}$$

$$NIT = k_n \cdot N^+ \cdot \frac{O_2}{K_{O2} + O_2} \cdot f_{nit} \tag{6.8}$$

$$\frac{dO_2}{dt} = K_{rear} \cdot (n - s) \cdot (O_{2sat} - O_2) - (\frac{1}{s \cdot n}) \cdot \left(\frac{32}{12}\right) \cdot r_a \cdot DEC_R - (\frac{1}{s\,n}) \cdot 1.42 \cdot r_{NIT} \cdot NIT \tag{6.9}$$

6.2.1 Results

The modified model has been run using the same parameter of Porporato (2003). We simulated different reaereation condition, assuming porosity equal to 0.5 and $K_{O2} = 0.2$. Also we simulate different values of soil moisture: less than field capacity (not reported here), above field capacity (s=0.3) and saturated condition (s=0.5). Finally we test the sensibility of the system to different oxygen semi-saturation values. To solve the system of ordinary differential equations, the built-in function NDSolve in Mathematica 6 software was used. The advantage of this routine is that its algorithm adapts its step size so that the estimated error in the solution is just within the user-specified tolerances.

Results show that soils with low reaereation constant (e.g. $K_{rear} < 2.4$) are more sensible to oxygen dynamics than soil with high reareaction value (e.g. K_{rear}=240), see Figure (6.6). This indicates, for instance, the different behavior of silty soil versus sandy soil and how the reaereaction effects modify the N-cycle. In particular, we found that well aerated soil lead to higher decomposition rates as well as higher nitrification rates (see Figures 6.7-6.11). This result is already established but we found it through the inclusion of oxygen dynamics. Model which consider oxygen limitation through a function of soil moisture (see Figure 6.1) need to incorporate the soil texture effects to reproduce the same effect. Our model thus reduces the numbers of parameter needed and is able to reproduce different field conditions. Also, accounting only for water dynamics, in general lead to a behavior which is intermediate to the ones of well aerated and poor aerated soil. (The values of K_{rear} has been chosen in agreement with Langergraber and Simunek (2005). The figure reports the oxygen dynamics for different reareation values. It is interesting to note that only for K_{rear}= 2.4 the physical reareation is comparable with the biotic oxygen consumption, while for poor aerated soil bacteria consumption is predominant, as shown in the following figures.

We also performed a sensibility analysis for the oxygen semi-saturation constant (K_{O2}), and we observed that this parameter considerably affects the N-cycle dynamics. In particular, only for very low value of K_{O2}, our model overlaps with the one given by Porporato (2003). This is valid for soil moisture values below and above the field capacity, but is not valid for saturated condition6.13, where, being reareation inhibited, the oxygen level consumed relatively fast 6.14, even if K_{O2} is low. It general therefore (*i.e.* higher value of K_{O2}), not accounting for oxygen dynamics lead to different n-dynamics. This is ad example visible in figures 6.11, where Manzoni models is indicated with blue line. In this case the oxygen dynamics il less sensible to changes of the semi-saturation value than for k_{rear} (see Figure 6.12).

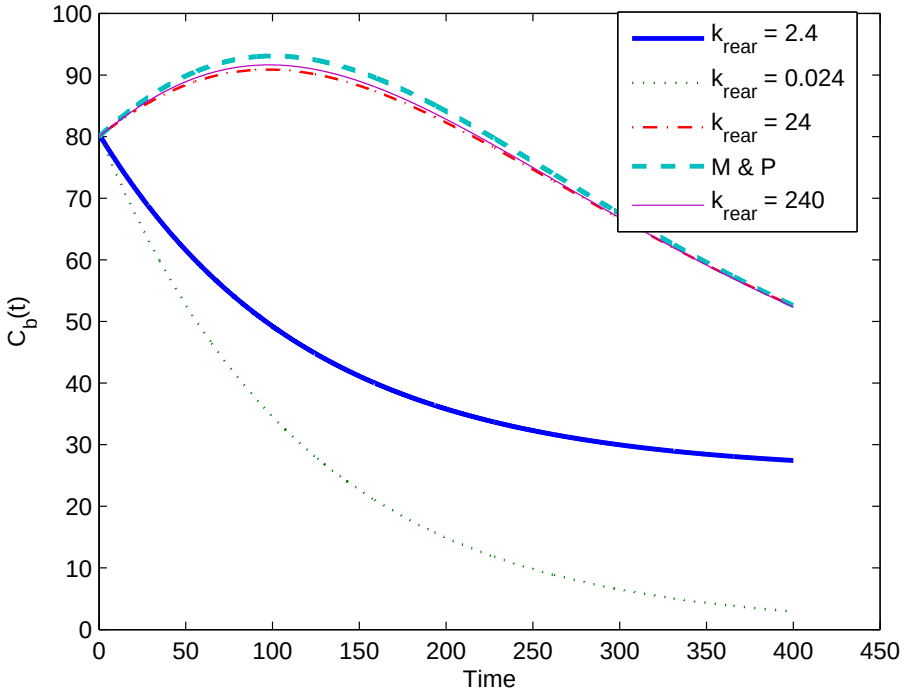

Figure 6.6: Comparison of bacteria dynamics (C_b) for different value of reareation constant (K_{rear} [d^{-1}]). Dotted blue line indicate the model of Porporato and Manzoni (2003). Time is in day and C_b in gC/m^3.

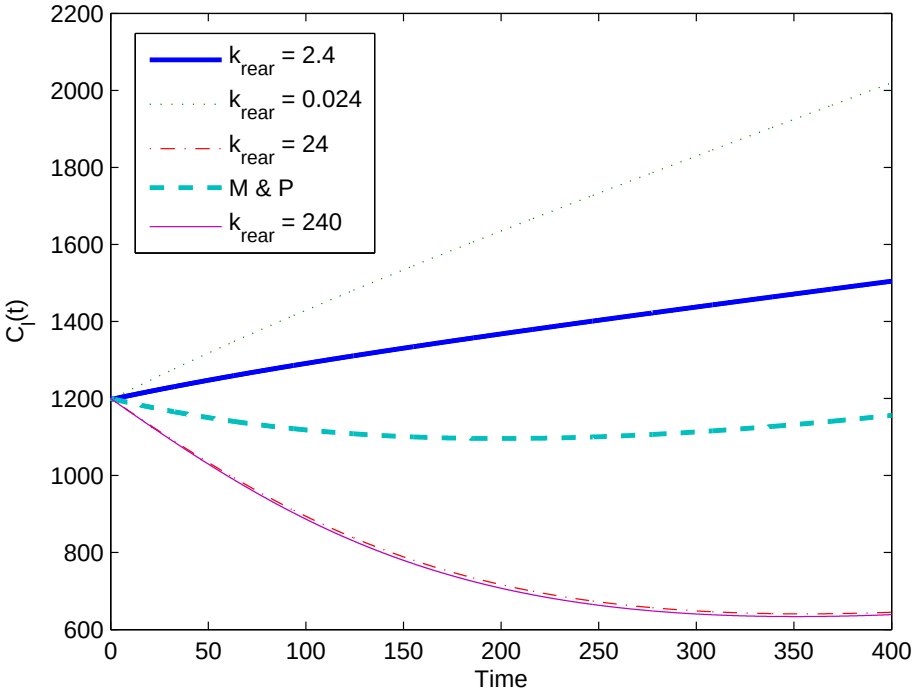

Figure 6.7: Comparison of litter pool (C_l) for different value of reareation constant (K_{rear} [d^{-1}]). Dotted blue line indicate the model of Porporato and Manzoni (2003). Time is in day and C_l in gC/m^3.

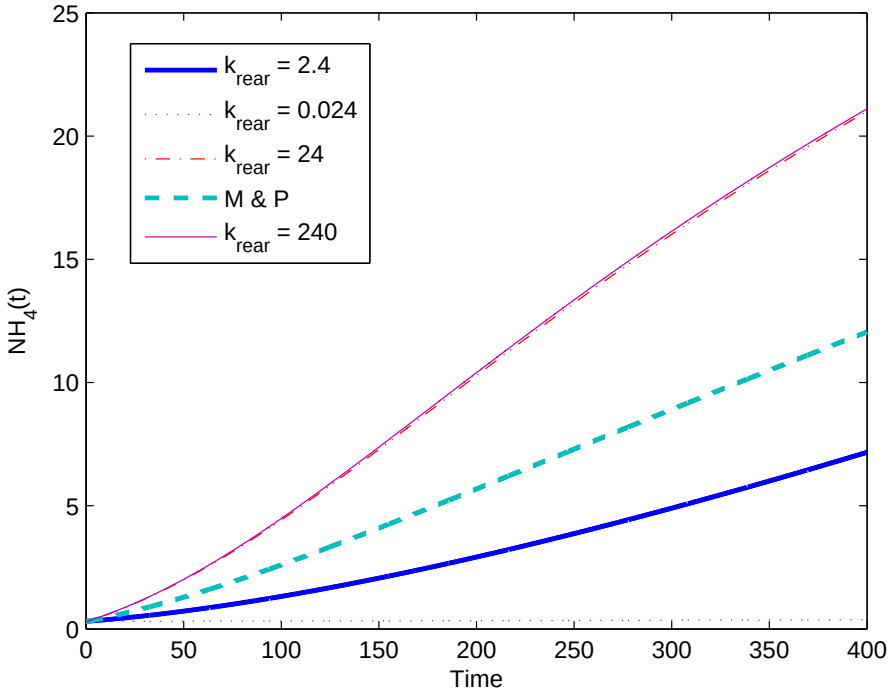

Figure 6.8: Comparison of ammonium pool (NH_4^+) for different value of reareation constant (K_{rear} [d^{-1}]). Dotted blue line indicate the model of Porporato and Manzoni (2003). Time is in day and NH_4^+ in gN/m^3.

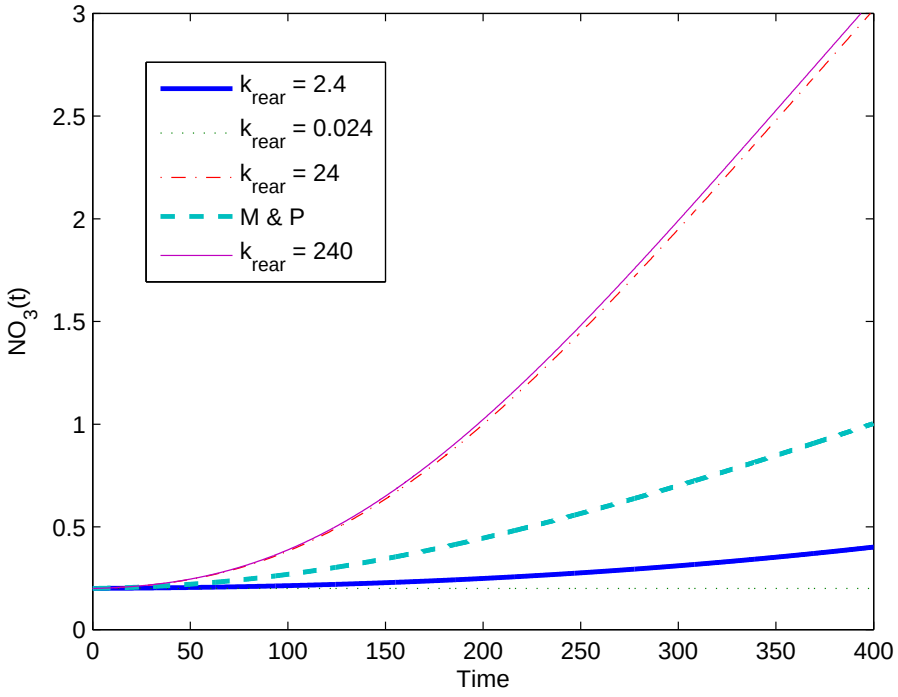

Figure 6.9: Comparison of nitrate pool (NO_3^-) for different value of reareation constant (K_{rear} [d^{-1}]). Dotted blue line indicate the model of Porporato and Manzoni (2003). Time is in day and C_b in gC/m^3.

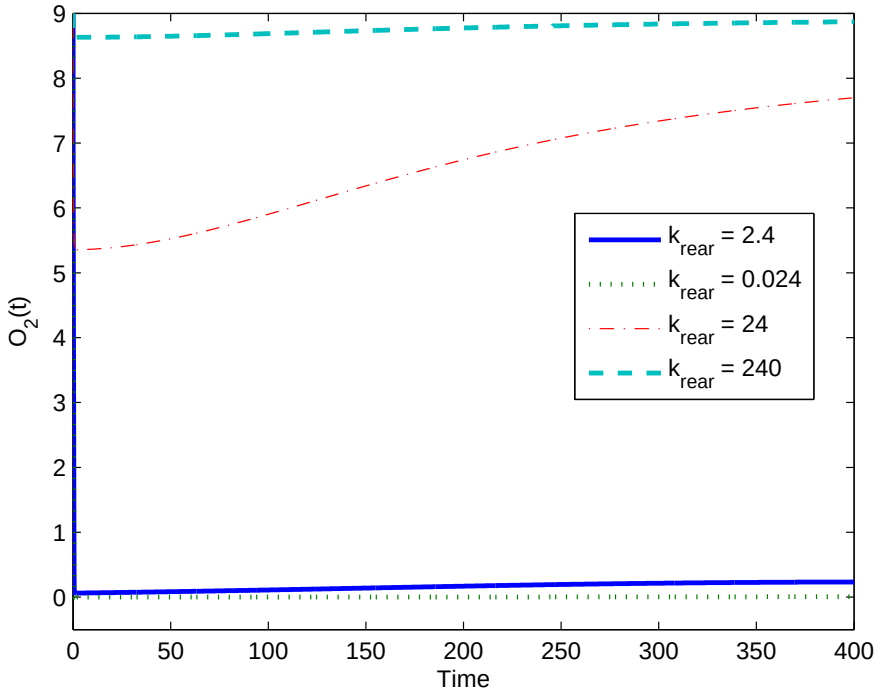

Figure 6.10: Oxygen dynamics (O_2) for different value of reareation constant (K_{rear} [d^{-1}]). Dotted blue line indicate the model of Porporato and Manzoni (2003). Time is in day and O_2 in mg/l.

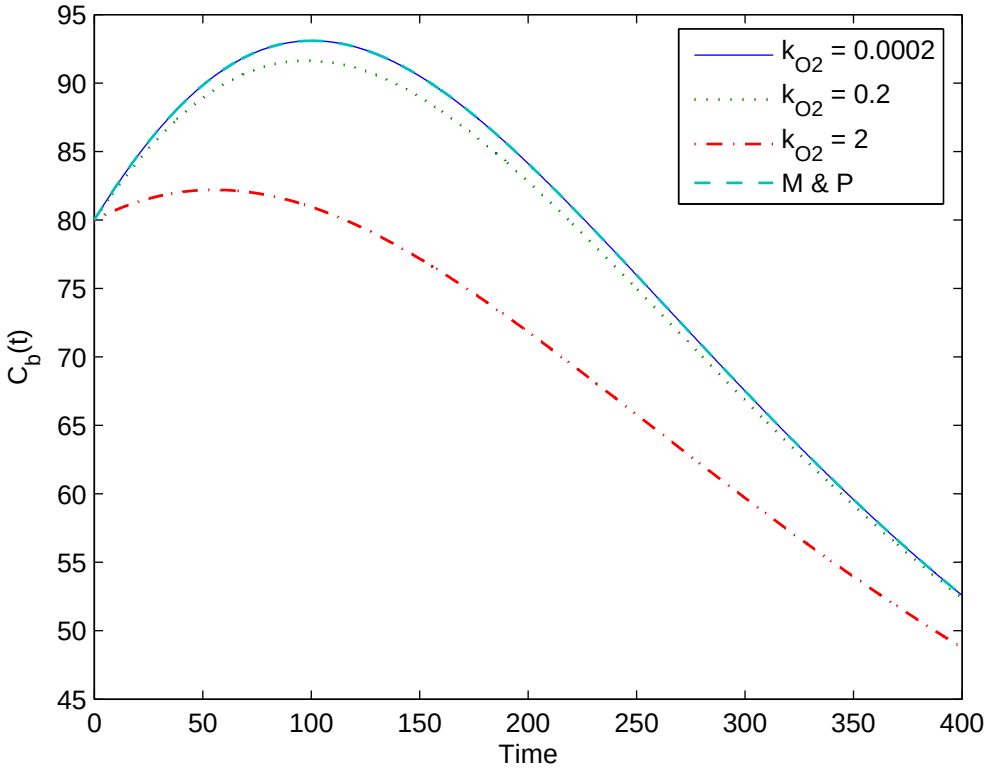

Figure 6.11: Comparison of bacteria dynamics(C_b) for different value of constant ($K_{O2}[d^{-1}]$), for soil moisture s=0.3 and reareation K_{rear} =240. Dotted blue line indicate the model of Porporato and Manzoni (2003). Time is in day and C_b in gC/m^3.

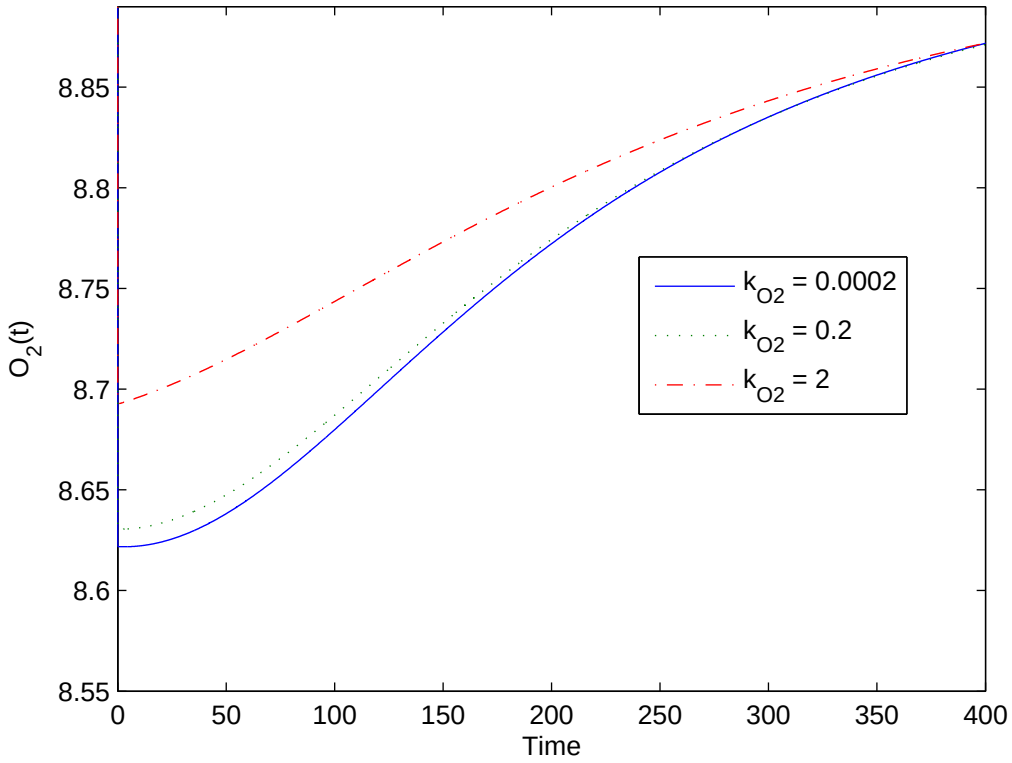

Figure 6.12: Oxygen dynamics (O_2) for different value of semi-saturation constant ($K_{O2}[d^{-1}]$), for soil moisture s=0.3 and reareation K_{rear} =240. Dotted blue line indicate the model of Porporato and Manzoni (2003). Time is in day and O_2 in mg/l.

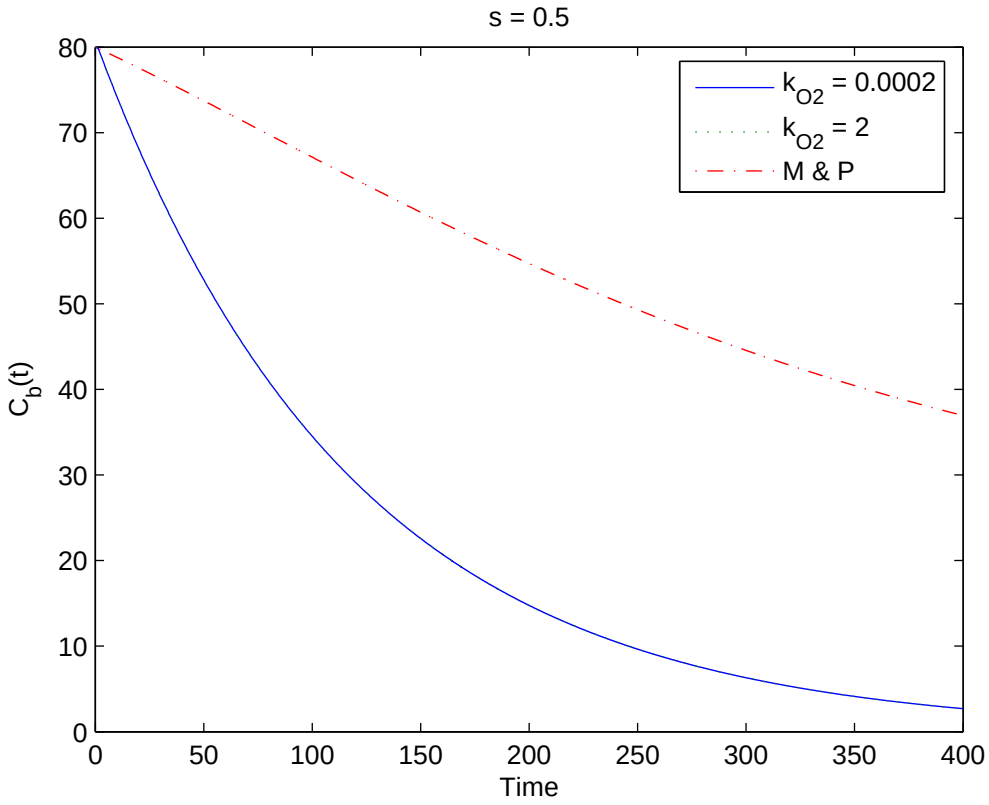

Figure 6.13: Comparison of bacteria dynamics(C_b) for different value of semi-saturation constant ($K_{O2}[d^{-1}]$), for soil moisture s=0.5 (saturated condition) and reareation K_{rear} =240. Dotted blue line in). Time is in day and $C_b$in gC/m^3.

Finally it is interesting to observe that in saturated condition, *i.e.* when oxygen reareation is inhibited, it takes few days to the oxygen to be consumed. This is important, because underline the experimental evidence of Chapter4, that bacteria oxygen consumption acts on a slower time scale than soil moisture dynamics (see Figures **??**, **??**,as swown in ours experiments (see Chapter4).

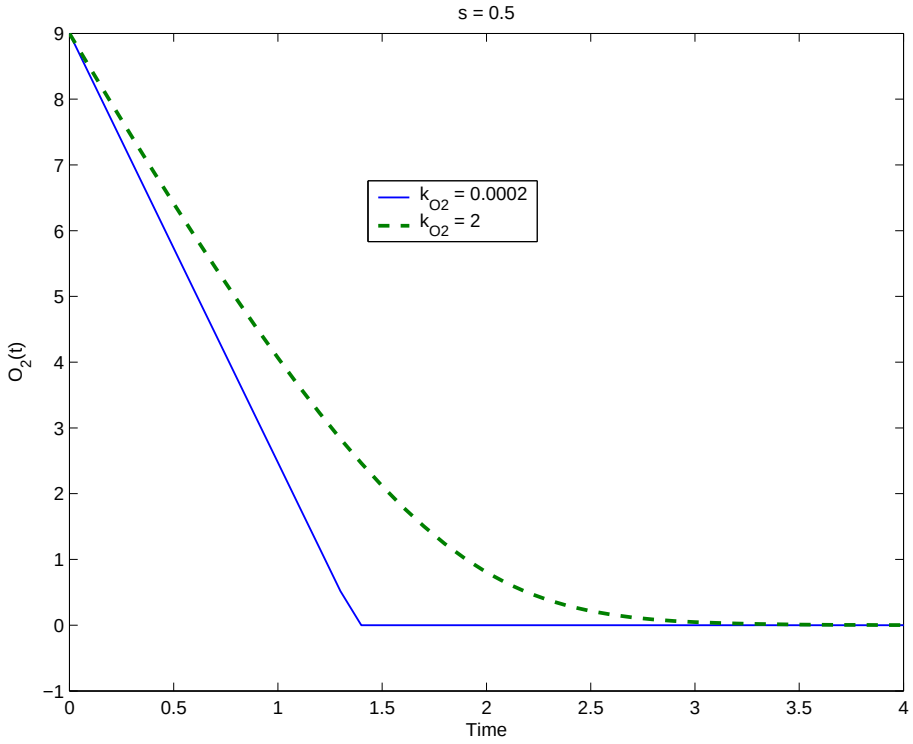

Figure 6.14: Oxygen dynamics (O_2) for different value of semi-saturation constant ($K_{O2}[d^{-1}]$), for soil moisture s=0.3 and reareation K_{rear} =240. Dotted blue line indicate the model of Porporato and Manzoni (2003). Time is in day and O_2in mg/l.

6.3 Modeling Oxygen and Soil Moisture Effects on Denitrification

Denitrification (see Chapter 1) is an extremely challenging process to model (e.g. Groffman et al., 2009) given the difficulties to incorporate "hot moments" and "hot spots". Higher soil water contents are associated with lower soil aeration and low oxygen availability, leading to enhanced emissions of N_2O with maximum emission rates at s $\approx$0.6 (e.g Davidson 1991). When soils are close to saturation, N_2 is the main by product of denitrification. Also in this case, due to the strong nonlinearities of the emission-soil moisture dependence any analysis based on average monthly or seasonal conditions (e.g., Potter et al., 1996) would miss part of the effect of the high-frequency fluctuations of soil moisture (Parton et al., 1998). It is apparent that short-term temporal variation in the emission of N_2O is too large to be explained by simple functions of soil water content, temperature, or N and C substrates (Robertson and Gross, 1994; Flessa et al., 1995). The accurate simulation of water transfer form soil hydraulic function is a key requirement for the modeling of N_2O emissions from denitrification (Frolking et al., 1998). In that sense Grant et al. (2006) developed a model which account for the electron preference coupled to heat transport, water , oxygen , the energetics of NOx oxidation reaction and the microbial activity. The model has been set to test hourly and daily N_2O flues a lab and field scale. Other mechanistic models exists (e.g. NLOSS,TOUGHREACT-N) which account for N_2O emissions as described for example by Li et al. (1992); Venterea and Rolston (2000); Bateman and Baggs (2005); Kremen et al. (2005)and Maggi(2008).

Here we present a stochastic modeling framework which couples oxygen and soil water dynamics with the aim of quantifying the importance of biochemical reaction and oxygen consumption on trace gases emission at short time scale. The model accounts for N_2O production from nitrification and denitrification, as well as the competition for nitrate by denitrification and dissimilatory reduction of nitrate to ammonium (DNRA). Preliminary results indicate that neglecting oxygen dynamics may significantly alter the rate of trace gas emission, while considering rainfall variability and its feedbacks on soil moisture fluctuations is fundamental to predict the subsequent peaks in trace gas emissions (results not shown ere). The target is to develop a physical based mechanistic model which is able to describe the nitrogen cycle at the microbiological scale in soil by using the biological oxygen dynamics used for waste water treatment plants and estimate fluxes of a field.

We present first the description of a nitrification model based on the decomposition model of Porporato et al. (2003) which consider the rates as the product of the maximum

rate value (given by the rate constant per the bacteria pool kCb) multiplied by Monod functions of the different variables. We then propose a simplified version of the model, where only oxygen concentration is express trough Monod and report the main results for the short term analysis on the simplified model.

6.3.1 Complete Non-Linear Short-Term Model

The C and N cycles are modeled using three soil organic matter pools (*i.e.*, litter, humus and microbial biomass, indicated by subscripts l, h and b, respectively), and four N pools describing mineral N (*i.e.*, ammonium, nitrate, nitrous oxide and dinitrogen) . The model also account for oxygen dynamics, nitrate ammonification (DNRA), carbon dioxide production and nitrous oxide emissions from nitrification and denitrificiation (see Figure 6.15). In addition:

- Organic nitogen pool includes also N_l and Nh (nitrogen into soil) and N_b which is related to the carbon pool through the ratio $\left(\frac{C}{N}\right)$ assumed constant for bacteria and humus, and variable in time for soluble carbon;
- Oxygen variation with time is given by the input from diffusion minus the consumption by reaction, while the evolution of carbon dioxide is given by the production by reaction minus the "losses" by diffusion. We assume that oxygen dynamics account for oxygen limitation when soil moisture is bigger than field capacity, while the limitation related to diffusion of substrates at soil moisture lower than field capacity is given by the functions f_{dec} and f_{nit}.
- The limitation in denitrification is already given by the oxygen dynamics, so $f_{den} = 1$. $f_{dec} = f_{nit}$ and represent the correction factor for both decomposition and nitrification, according to the following expression: $f_{dec} = \frac{s}{s_{\text{fc}}} < s \leq s_{fc}$ and 1 otherwise.

The reactions include decomposition (DEC), nitrification (NIT), aerobic production of nitrous oxides (N_2O_{nit}), two terms which account for denitrifcation of nitrate to nitrous oxide (DEN_1) and denitrification to dinitrogen (DEN_2). In our model, substrates are expressed as Michaelis Mentem factors *i.e.* $\frac{Ci}{Ki+Ci}$ where C is the substrate and Ki is the semi-saturation constant. The inhibition coefficient is expressed as follows: $\frac{Ii}{Ii+Ki}$ where I is the inhibit factor and Ki is the semi-saturation constant. Here, the expressions for the above mentioned rates, which in general are given by multiplying the maximum rate μ_{max} by the substrate and the inhibition factors:

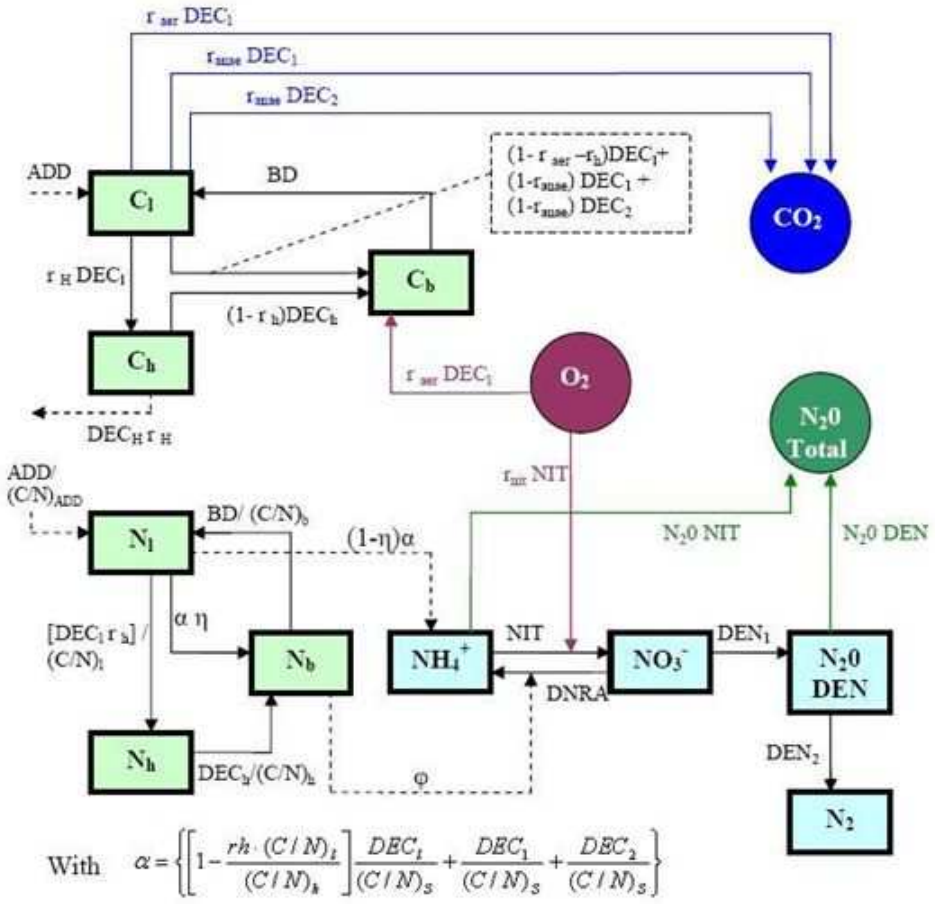

Figure 6.15: Model Schema. The model includes the following processes: decomposition, nitrification, denitrification, DNRA, carbon dioxide production, nitrous oxide and dinitrogen dynamics.

$$DEC_h = k_h \cdot C_b \cdot \frac{C_h}{K_{ch} + C_h} \cdot \frac{O_2}{K_{o2} + O_2} \cdot f_{dec} \cdot \varphi \tag{6.10}$$

$$DEC_l = k_1 \cdot C_b \cdot \frac{C_l}{K_{cl} + C_l} \cdot \frac{K_{o2}}{K_{o2} + O_2} \cdot \frac{NO_3^-}{NO_3^- + K_{NO3}} \cdot f_{dec} \cdot \varphi \tag{6.11}$$

$$DEC_2 = k_2 \cdot C_b \cdot \frac{C_l}{K_{cl} + C_l} \cdot \frac{K_{o2}}{K_{o2} + O_2} \cdot \frac{N_2O}{N_2O + K_{N_2O}} \cdot f_{dec} \cdot \varphi \tag{6.12}$$

$$DEC_l = k_l \cdot C_b \cdot \frac{C_l}{K_{cl} + C_l} \cdot \frac{O_2}{K_{o2} + O_2} \cdot f_{dec} \cdot \varphi \tag{6.13}$$

$$BD = k_b \cdot C_b \tag{6.14}$$

$$NIT = k_n \cdot \frac{NH_4^+}{NH_4^+ + K_{NH4}} \cdot \frac{O_2}{K_{O2} + O_2} \cdot f_{nit} \tag{6.15}$$

$$N_2O_{nit} = k_{nit} \cdot NH_4^+ \cdot \frac{K_{o2nit}}{O_2 + K_{o2nit}} \cdot \frac{O_2}{O_2 + K_{o2}} \tag{6.16}$$

$$DEN_1 = k_{d1} \cdot C_b \cdot \frac{C_l}{Cl + Kcs} \cdot \frac{NO_3^-}{NO_3^- + K_{NO3}} \cdot \frac{K_{o2}}{O_2 + K_{o2}} \cdot f_{den} \tag{6.17}$$

$$DEN_2 = k_{d2} \cdot C_b \cdot \frac{C_l}{Cl + Kcl} \cdot \frac{N_2O}{N_2O + K_{N_2O}} \cdot \frac{K_{o2}}{O_2 + K_{o2}} \cdot f_{den} \tag{6.18}$$

$$DNRA = k_{DNRA} \cdot \frac{NO_3^-}{NO_3^- + K_{NO}} \cdot \frac{K_{o2}}{O_2 + K_{o2}} \cdot \frac{C_l}{K_{cl} + C_l} \tag{6.19}$$

In this case k_i,with i=h,l,b,d1, d2, NIT are expressed in d^{-1},while k_{DNRA} and k_n are expressed in gN/m^3d. Only few work report values of Ks for soils, therefore the value used in the sludge system can be convert, by the following relationship:

$$Ks_{ssoil} = (\frac{Ks_{sludge}}{2.29}) \cdot \frac{s \cdot n}{1000} \tag{6.20}$$

This expression converts the mg of COD (chemical oxygen demand) to mg of carbon considering the ration between the molecular weight of oxygen and carbon ($\frac{32}{14} = 2.29$) and the l of soil water into Kg. This conversion increase the complexity of the system since the Ks_{ssoil} are not constant in time and also vary according to the soil moisture content of the soil and its physical characteristic (n).

$$Ks_{ssoil} = f(s(t)) \tag{6.21}$$

Also the values used for sludge are not directly applicable to soils, being the rates in general different.

In the following we report the values for ϕ and φ (see eqs. 6.29 and 6.30) which accounts, respectively, for the fluxes of nitrogen among compartment and the reduction of decomposition processes when the nitrogen is not sufficient to meet the bacteria needs. A detailed explanation of the physical meaning of this terms and also on the mathematical used to derive the expression is reported in Porporato et al.(2003). These are the expressions:

$$\begin{aligned}\phi &= DEC_l \cdot (\eta_l \cdot (1/(\frac{C}{N})_l - r_h/(\frac{C}{N})_h) - (1 - ra - rh)/(\frac{C}{N})_b)... \\ &\quad ... + DEC_h \cdot (\eta_h \cdot (1/(\frac{C}{N})_h - (1 - rh)/(\frac{C}{N})_b)... \\ &\quad + + DEC_1 \cdot (\eta_l \cdot (1/(\frac{C}{N})_l - (1 - ran)/(\frac{C}{N})_b) \\ &\quad ... + DEC_2 \cdot (\eta_l \cdot (1/(\frac{C}{N})_l - (1 - ran)/(\frac{C}{N})_b).\end{aligned} \tag{6.22}$$

$$\begin{aligned}\phi_{pot} &= k_l \cdot C_b \cdot \frac{C_l}{K_{cl} + C_l} \cdot \frac{O_2}{K_{o2} + O_2} \cdot fdec \cdot (\eta l \cdot (1/(\frac{C}{N})_l - r_h \cdot (\frac{C}{N})_h)... \\ &\quad ... - (1 - ra - rh)/(\frac{C}{N})_b) + \ k_h \cdot C_b \cdot \frac{C_h}{K_{ch} + C_h} \cdot K_{o2}... \\ &\quad .... + O_2 \cdot fdec \cdot (\eta_h \cdot (1/(\frac{C}{N})_h - (1 - rh)/(\frac{C}{N})_b) + \\ &\quad ....k_1 \cdot C_b \cdot \frac{C_l}{K_{cl} + C_l} \cdot \frac{NO_3}{K_{NO_3} + NO_3} \cdot fdec \cdot (\eta_l \cdot (1/(\frac{C}{N})_l)... \\ &\quad .... - fdec(1 - ran)/(\frac{C}{N})_b) + k_2 \cdot C_b \cdot \frac{C_l}{K_{cl} + C_l} \cdot \frac{N_2O}{K_{N_2O} + N_2O}... \\ &\quad ...fdec \cdot (\eta_l \cdot (1/(\frac{C}{N})_l - (1 - ran)/(\frac{C}{N})_b)\end{aligned} \tag{6.23}$$

$$IMM_{max} = -(k_i NH_4^+ \cdot NH_4^+ + k_i NO_3^- \cdot NO_3^-) \cdot f_d \cdot C_b \tag{6.24}$$

$$\begin{aligned}\varphi &= 1 \cdot (\text{if } \phi_{pot} > IMM_{maxt} \,\text{then}\, 1, \,\text{else}\, 0)... \\ &\quad ... + IMM_{max}/\phi_{pot}\end{aligned} \tag{6.25}$$

$$
\begin{aligned}
grossMIN &= k_l \cdot C_b \cdot \frac{C_l}{K_{cl}+C_l} \cdot \frac{O_2}{K_{o2}+O_2} \cdot fdec \cdot (1-\eta) \cdot (1/(\frac{C}{N})_l \times ... \\
&\quad ...k_1 \cdot C_b \cdot \frac{C_l}{K_{cl}+C_l} \cdot \frac{NO_3}{K_{NO_3}+NO_3} \cdot \frac{K_{o2}}{O_2+K_{o2}} \cdot fdec \cdot (1-\eta_l) \cdot (1/(\frac{C}{N})_l ... \\
&\quad ... + k_2 \cdot C_b \cdot \frac{C_l}{K_{cl}+C_l} \cdot \frac{N_2O}{K_{N_2O}+N_2O} \cdot \frac{K_{o2}}{O_2+K_{o2}} \cdot fdec \cdot (1-\eta_l) \cdot (1/(\frac{C}{N})_l ... \\
&\quad ... - r_h \cdot (\frac{C}{N})_h) \cdot \varphi + kh \cdot C_b \cdot \frac{C_h}{K_{ch}+C_h} \cdot \frac{O_2}{K_{o2}+O_2} \times ... \\
&\quad ... \times fdec \cdot (1-\eta_h) \cdot (1/(\frac{C}{N})_h) \cdot \varphi + \phi
\end{aligned} \tag{6.26}
$$

$$
\begin{aligned}
grossIMM_{NH_4} &= -\left[kiNH_4^+ \cdot NH_4^+ / (kiNH_4^+ \cdot NH_4^+ + kiNO_3^- \cdot NO_3^-)\right] \times ... \\
&\quad ... \times \varphi \cdot \phi_{pot}
\end{aligned} \tag{6.27}
$$

$$
\begin{aligned}
grossIMM_{NO_3} &= -\left[kiNO_3^- \cdot NO_3^- / (kiNH_4^+ \cdot NH_4^+ + kiNO_3^- \cdot NO_3^-)\right] \times ... \\
&\quad ... \times \varphi \cdot \phi_{pot}
\end{aligned} \tag{6.28}
$$

Notice that ϕ and ϕ_{pot} defined as follows:

$$\phi = \text{if } \phi > 0, \text{then } 1, \text{ else } 0 \tag{6.29}$$

$$\phi_{pot} = \text{if } \phi_{pot} > IMM_{max} \text{ then } 0, \text{ else } 1 \tag{6.30}$$

Oxygen is limiting both decomposition (it is not affecting hydrolysis, but this process is not considered at the moment) and nitrification, while favoring denitrification. Concerning the production of nitrous oxide from nitrification, here we assume that it is a function of soil moisture and ammonium, according model of Parton 1983 and Li 1992. In reality the nitrous oxide emissions in aerobic conditions are produced by : nitrification, nitrifier denitrification, chemo-denitrification, heterotrophic nitrification and aerobic denitrification. Among those the nitrification, nitrifier denitrification, chemo-denitrification are not a function of organic carbon (C_s). In particular nitrification and nitrifier denitrification depend on carbon dioxide CO_2.

The scheme illustrating the model is presented in Fig.1. The lumped model is given by the resolution of the following system of equations:

$$\frac{dC_h}{dt} = -DEC_h + r_h \cdot DEC_l \tag{6.31}$$

$$\frac{dC_l}{dt} = ADD - DEC_l + BD - DEC_1 - DEC_2 \tag{6.32}$$

$$\frac{dC_b}{dt} = -BD + (1 - r_a - r_h) \cdot DEC_l + (1 - r_h)DEC_h ... \tag{6.33}$$

$$... + (1 - r_{an})DEC_1 + (1 - r_{an})DEC_2 \tag{6.34}$$

$$\frac{dN_l}{dt} = \frac{ADD}{(\frac{C}{N})_{ADD}} - \frac{DEC_l}{(\frac{C}{N})_l} + \frac{BD}{(\frac{C}{N})_B} - \frac{DEC_1}{(\frac{C}{N})_l} - \frac{DEC_2}{(\frac{C}{N})_l} \tag{6.35}$$

$$\frac{dNH_4^+}{dt} = (1 - \eta) \cdot \frac{DEC}{(\frac{C}{N})_l} + (1 - \eta) \cdot \frac{DEC1}{(\frac{C}{N})_l} + (1 - \eta) \cdot \frac{DEC2}{(\frac{C}{N})_l} ... \tag{6.36}$$

$$... - N_2O_{nit} - NIT + DNRA = groosMIN - grossIMM_{NH_4} ...$$

$$... - N_2O_{nit} - NIT + DNRA$$

$$\frac{dNO_3^-}{dt} = NIT - DEN_1 - grossIMM_{NO_3} - DNRA \tag{6.37}$$

$$\frac{dN_2O_{den}}{dt} = (\tfrac{1}{s \cdot n}) \cdot \quad DEN_1 - (\frac{1}{sn})DEN_2 - K_{rear}(N_2O_{den} - N_2O_{atm})(\frac{n - s}{sn}) \tag{6.38}$$

$$\frac{dN_2O_{nit}}{dt} = (\tfrac{1}{s \cdot n}) \cdot \quad N_2O_{nit} - (\frac{1}{s \cdot n}) - K_{rear} \cdot (N_2O_{nit} - N_2O_{atm}) \cdot (\frac{n - s}{s \cdot n}) \tag{6.39}$$

$$\frac{dN_2}{dt} = (\frac{1}{s \cdot n}) \cdot DEN_2 - K_{rear} \cdot (N_2 - N_{2atm}) \cdot (\frac{n - s}{s \cdot n}) \tag{6.40}$$

$$\frac{dO_2}{dt} = K_{rear} \cdot (n - s) \cdot (O_{2sat} - O_2) \cdot -(\frac{1}{s \cdot n}) \cdot \left(\frac{32}{12}\right) \cdot r_a \cdot DEC_l ...$$

$$... - (\frac{1}{s \cdot n}) \cdot (1.42) \cdot r_{NIT} \cdot NIT \tag{6.41}$$

$$\frac{dCO_2}{dt} = (\frac{1}{s \cdot n}) \cdot \frac{44}{12} \cdot [r_a \cdot DEC + r_{an} \cdot DEC_1 + r_{an} \cdot DEC_2] \tag{6.42}$$

This model captures the oscillation of the biomass better than linear model, as shown in Manzoni (2007). Nevertheless, it includes semi-saturation values, substantially increase the number of parameter to used in the model. In addition there is a large variation of this coefficient among different authors Leffelaar and Wessel (1988); Riley and Matson (2000); Kremen et al. (2005); Grant et al. (2006); Maggi et al. (2008) which may difficult

to choose realistic values, since preliminary run indicate that the model is highly sensible to the semi-saturation values (data not shown here). For that reason we prefer to focus on a simplified version at a short time scale, considering that the expression, $\frac{C}{C+K_s}$, can be simplified as follows:

- If specie C in the soil is low comparing to K_s, *i.e.* $Ks \ll C$ then $C/(C+K_s) \approx C/K_s$ so that k_i can be redefined as $k_{i^*} = ki/K_s$.
- If specie C in the soil is high comparing to K_s, *i.e.* $Ks \gg C$ then $C/(C+K_s) \approx 1$ so that k_i does not change $k_{i^*} = ki$.

6.3.2 Simplified Short-Term Model

In this subsection, we ere interested in accounting for short time changes. For that reason we consider that there are two pools of soil carbon, one pool which include the fractions of carbon which are slowly biodegradable (C_S) and one pool which include carbon rapidly decomposed (C_R). The other are equal to the long-term model. Figure report a scheme of the model. Here we determine the nitrification rates and the production of carbon dioxide as function of the carbon pool DEC1 and DEC2, which account for the C required by heterotrophic bacteria during denitrification. The conversion is explain in the following section.

$$
\begin{aligned}
DEC_s &= k_h \cdot C_b \cdot C_h \cdot \frac{O_2}{K_{o2} + O_2} \cdot f_{dec} \cdot \varphi && (6.43)\\
DEC_R &= k_R \cdot C_b \cdot C_R \cdot \frac{O_2}{K_{o2} + O_2} \cdot f_{dec} \cdot \varphi && (6.44)\\
DEC_1 &= k_1 \cdot C_b \cdot C_R \cdot NO_3^- \cdot \frac{K_{o2}}{O_2 + K_{o2}} \cdot f_{den} \cdot \varphi && (6.45)\\
DEC_2 &= k_2 \cdot C_b \cdot C_R \cdot N_2O \cdot \frac{K_{o2}}{O_2 + K_{o2}} \cdot f_{den} \cdot \varphi && (6.46)\\
BD &= k_b \cdot C_b && (6.47)\\
NIT &= k_n \cdot NH_4^+ \cdot \frac{O_2}{K_{O2} + O_2} \cdot f_{nit} && (6.48)\\
N_2O_{-nit} &= k_{nit} \cdot NH_4^+ \cdot \frac{K_{o2nit}}{O_2 + K_{o2nit}} \cdot \frac{O_2}{O_2 + K_{o2}} && (6.49)\\
DEN_1 &= r_{an} \cdot 1.17 \cdot DEC_1 && (6.50)\\
DEN_2 &= r_{an} \cdot 4.67 \cdot DEC_2 && (6.51)\\
DNRA &= k_{DNRA} \cdot NO_3^- \cdot \frac{K_{o2}}{O_2 + K_{o2}} \cdot C_R && (6.52)
\end{aligned}
$$

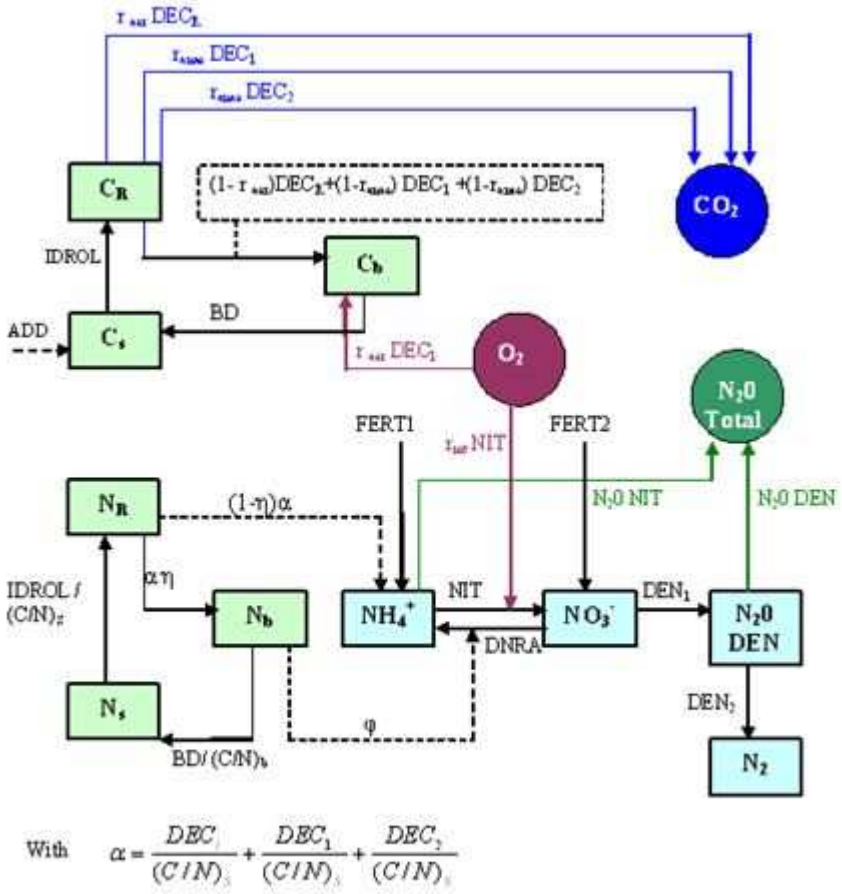

Figure 6.16: Model scheme for short-term analysis.

Using a model for shorter time scale, in which $DEC_h = 0$, we have a pool of carbon readably C_R and a pool of carbon slowly biodegradable C_s. Here, C_s is converted to C_R through the processes of hydrolysis, defined as:

$$IDROL = k_{idrol} \cdot C_b \cdot C_l \tag{6.53}$$

Also fertilizer might be added to the system throughout ADD (as solid organic fertilizer), as nitrate base fertilizer ($FERT$) or ammonium based fertilizer as $FERT_1$. In this case the system of equations become:

$$\begin{aligned}
\frac{dC_S}{dt} &= -IDROL + ADD + BD && (6.54)\\
\frac{dC_R}{dt} &= -DEC_R + IDROL - DEC_1 - DEC_2 && (6.55)\\
\frac{dC_b}{dt} &= -BD + (1 - r_a) \cdot DEC_R + (1 - r_{an}) \cdot DEC_1 ... && (6.56)\\
&\quad ... + (1 - r_{an}) \cdot DEC_2
\end{aligned}$$

$$\begin{aligned}
\frac{dN_l}{dt} &= \frac{DEC_R}{(\frac{C}{N})_R} + \frac{DEC_1}{(\frac{C}{N})_R} + \frac{DEC_2}{(\frac{C}{N})_R} && (6.57)\\
\frac{dNH_4^+}{dt} &= (1 - \eta) \cdot \frac{DEC}{(\frac{C}{N})_R} - (1 - \eta) \cdot \frac{DEC1}{(\frac{C}{N})_R} - (1 - \eta) \cdot \frac{DEC2}{(\frac{C}{N})_R}\\
&\quad -N_2O_{nit} - NIT + DNRA + FERT_1\\
&\quad ... = grossMIN - grossIMM_{NH_4} ...\\
&\quad ... - N_2O_{nit} - NIT + DNRA + FERT_1 && (6.58)
\end{aligned}$$

$$\begin{aligned}
\frac{dNO_3^-}{dt} &= NIT - DEN_1 - grossIMM_{NO_3} - DNRA + FERT && (6.59)\\
\frac{dN_2O_{den}}{dt} &= (\tfrac{1}{s \cdot n}) \cdot \; DEN_1 - (\frac{1}{s \cdot n}) \cdot DEN_2 - && (6.60)\\
&\quad K_{rear} \cdot (N_2O_{den} - N_2O_{atm}) \cdot (\frac{n - s}{s \cdot n})\\
\frac{dN_2O_{nit}}{dt} &= (\tfrac{1}{s \cdot n}) \cdot \; N_2O_{nit} - (\frac{1}{s \cdot n}) - K_{rear} \cdot (N_2O_{nit} - N_2O_{atm}) \cdot (\frac{n - s}{s \cdot n}) && (6.61)
\end{aligned}$$

$$\frac{dN_2}{dt} = (\frac{1}{s\cdot n})\cdot DEN_2 - K_{rear}\cdot(N_2 - N_{2atm})\cdot(\frac{n-s}{s\cdot n}) \quad (6.62)$$

$$\frac{dO_2}{dt} = K_{rear}\cdot(n-s)\cdot(O_{2sat}-O_2) - (\frac{1}{s\cdot n})\cdot\left(\frac{32}{12}\right)\cdot r_a\cdot DEC_l... \\ ... - (\frac{1}{s\cdot n})\cdot(1.42)\cdot r_{NIT}\cdot NIT \quad (6.63)$$

$$\frac{dCO_2}{dt} = (\frac{1}{s\cdot n})\cdot\frac{44}{12}\cdot[r_a\cdot DEC + r_{an}\cdot DEC_1 + r_{an}\cdot DEC_2] \quad (6.64)$$

In this case the expression for ϕ needs to be re-derived by posing $\frac{dC_b}{dt} = \frac{dN_b}{dt}\cdot(\frac{C}{N})_b$, *i.e.* the constancy of the bacteria ratio C:N.The expression leads to:

$$\phi = DEC_R\cdot(\eta_R\cdot(1/(\frac{C}{N})_R) - (1-rr)/(\frac{C}{N})_b) + DEC_1\cdot(\eta_R\cdot(1/(\frac{C}{N})_R... \\ -(1-ra)/(\frac{C}{N})_b) + DEC_2\cdot(\eta_R\cdot(1/(\frac{C}{N})_R - (1-ra)/(\frac{C}{N})_b). \quad (6.65)$$

$$\phi_{pot} = k_R\cdot C_b\cdot\frac{O_2}{K_{o2}+O_2}fdec\cdot(\eta_R\cdot(1/(\frac{C}{N})_R)... \\ ... - (1-rr)/(\frac{C}{N})_b) + k_1\cdot C_b\cdot C_R\cdot\frac{NO_3}{K_{NO_3}+NO_3}... \\ ...\cdot fdec\cdot(\eta_R\cdot(1/(\frac{C}{N})_R) - (1-r1)/(\frac{C}{N})_b) + k_2\cdot C_b\cdot C_R\cdot\frac{N_2O}{K_{N_2O}+N_2O}... \\ ...\cdot fdec\cdot(\eta_R\cdot(1/(\frac{C}{N})_R) - (1-r2)/(\frac{C}{N})_b) \quad (6.66)$$

$$IMM_{max} = -(k_iNH_4^+\cdot NH_4^+ + k_iNO_3^-\cdot NO_3^-)\cdot f_d\cdot C_b \quad (6.67)$$

(6.68)

$$\varphi = 1\cdot(\text{if } \phi_{pot} > IMM_{maxt} \text{ then } 1, \text{ else } 0)... \\ ... + IMM_{max}/\phi_{pot}\cdot(\text{if } \phi_{pot} > IMM_{max} \text{ then } 0, \text{ else } 1) \quad (6.69)$$

(6.70)

$$
\begin{aligned}
grossMIN &= k_l \cdot C_b \cdot C_R \cdot \frac{O_2}{K_{o2} + O_2} \cdot fdec \cdot (1 - \eta_R) \cdot (1/(\frac{C}{N})_R)... \\
&\quad ....k_1 \cdot C_b \cdot C_R \cdot \frac{NO_3}{K_{NO_3} + NO_3} \cdot fdec \cdot (1 - \eta_R) \cdot (1/(\frac{C}{N})_R)..... \\
&\quad .... + k_2 \cdot C_b \cdot C_R \cdot \frac{N_2O}{K_{N_2O} + N_2O} \cdot fdec \cdot (1 - \eta_R) \cdot (1/(\frac{C}{N})_R)... \\
&\quad ... + \phi \,(\text{if } \phi > 0, \text{then } 1, \text{ else } 0)
\end{aligned} \tag{6.71}
$$

$$
\begin{aligned}
grossIMM_{NH_4} &= -(kiNH_4^+ \cdot NH_4^+ / (kiNH_4^+ \cdot NH_4^+ + kiNO_3^- \cdot NO_3^-))... \\
&\quad ... \cdot \varphi \cdot \phi_{pot} \cdot (\text{if } \phi_{pot} < 0 \,\text{then } 1, \text{ else } 0)
\end{aligned} \tag{6.72}
$$

$$
\begin{aligned}
grossIMM_{NO_3} &= -(kiNO_3^- \cdot NO_3^- / (kiNH_4^+ \cdot NH_4^+ + kiNO_3^- \cdot NO_3^-))... \\
&\quad ... \cdot \varphi \cdot \phi_{pot} \,(\text{if } \phi_{pot} < 0 \,\text{then } 1, \text{ else } 0)
\end{aligned} \tag{6.73}
$$

6.3.3 Determining Oxygen Consumption, Conversion of Carbon Fluxes in Nitrogen Fluxes and the Production of CO_2

Oxygen Consumption during Nitrification

In order to determine the oxygen consumption, we need to determine how much oxygen is required by bacteria during decomposition and how much is used during nitrification. The former factor is linked to the production of carbon dioxide, so to the coefficient rr=0.6, which account for this consumption. For nitrification, we know that the conversion of ammonium/ ammonia to nitrite is in reality a two step equation which required $6\,e^-$, while the second step required $2\,e^-$, see eqs **??**.

$$
NH_4^+ + 1.5O_2 \longrightarrow NO_2^- + H_2O + 2H^+ \tag{6.74}
$$

$$
NO_2^- + H_2O \longmapsto NO_3^- + 2H^+ + 2e^- \tag{6.75}
$$

In addition chemical oxygen demand (COD)test for sludge system showed that Ekama et al. (1984) :

$$1g\,COD \equiv 1g\,O_2 \equiv \frac{1}{8}\,electron\,equivalent \tag{6.76}$$

This imply that $8e^-$ are used during the nitrification process which correspond to 64g of oxygen. Nevertheless only the quantity (1-r) is respired, since the r-fraction is used by bacteria to growth. So the gO_2 consumed by gN are given by : $\frac{64\cdot(1-r)}{14} = 1.83$ (14 is the molecular weigh of N in NH_4, used to convert gN-NH_4 to gN).

Carbon used During Denitrification

To calculate the consumption of nitrogen and the production of carbon dioxide from denitrification, we need to use the following:

$$2NO_3^- + 4H^+ + 4e^- \longrightarrow 2NO_2^- + 2H_2O \tag{6.77}$$
$$2NO_2^- + +4H^+ + 2e^- \longrightarrow 2NO + 2H_2O \tag{6.78}$$
$$2NO + 2H^+ + 2e^- \longrightarrow N_2O + H_2O \tag{6.79}$$
$$N_2O + 2H^+ + 2e^- \longrightarrow N_2 + H_2O \tag{6.80}$$

According to equation 6.76, we know that:

- For equation 6.77 the conversion of $2mol\,NO_3^- - N \longrightarrow 2mol\,NO_2^- - N$ required $4e^- \equiv 32g\,COD$
- For equations 6.78,6.79 the conversion of $2mol\,NO_2^- - N \longrightarrow 1mol\,N_2O$-N required $4e^- \equiv 32g\,COD$
- For equation6.80 the conversion of $1mol\,N_2O - N \longrightarrow 1mol\,N_2 - N$ required $2e^- \equiv 16g\,COD$

This is equivalent to the following:

- For equation 6.77 the conversion of $28g\,NO_3^- - N \longrightarrow 28g\,NO_2^- - N$ implies $\frac{32g\,COD}{28gNO_3-N^-reduced\,to\,NO_2^--N} = 1.14\frac{g\,COD}{gNO_3^--Nreduced\,to\,N-NO_2^-}$
- For equations 6.78,6.79 the conversion of $28g\,NO_2 - N^- \longrightarrow 28g\,N_2O - N$ implies: $\frac{32g\,COD}{28gN-NO_3^-\,reduced\,to\,N-NO_2^-} = 1.14\frac{g\,COD}{gN-NO_3^-\,reduced\,to\,N-NO_2^-}$
- For equation6.80 the conversion of $28g\,N - N_2O \longrightarrow 28g\,N - N_2$ implies $\frac{16g\,COD}{28gN_2O-Nreduced\,to\,N_2-N} = 0.58\frac{g\,COD}{gN_2O-Nreduced\,to\,N_2-N}$

In our model we consider eqs. 6.77, 6.78 and 6.79 as one single step in which nitrate are converted to nitrous oxide, while the second step of denitrification account for the conversion of nitrous oxide to dinitrogen (6.80). So we have a total total consumption of:

- $2.28 gN - N_2O reduced\, to\, N_2 - N$ for the first step of denitrification DEN_1, which is given by the sum of carbon needed in eqs. 6.77, 6.78 and 6.79.
- $0.58 \frac{g\, COD}{gN_2O - N reduced\, to\, N_2 - N}$ for the second step of denitrification DEN_2 which considers the carbon needed in 6.80.

In order to convert the COD in term of C we need to divide by 32/14=2.27,*i.e.* by the ratio of oxygen and carbon weights.

From the literature, we know experimentally that, the coefficient for carbon consumption in denitrification are lower than the one in nitrification. In particular, the value for aerobic processes is r_a=0.67, while for anaerobic processes we assume r_{an}=0.53.

Thus rates of denitrification (eqs. 6.17-6.18) are linked to the decomposition rates (eqs. 6.11,6.12) through the following relationship:

$$DEN_1 = \frac{2.27}{2.28} \cdot r_{an} \cdot DEC_1 = r_{an} \cdot 1.17 \cdot DEC_1 \quad (6.81)$$

$$DEN_2 = \frac{2.27}{0.58} \cdot r_{an} \cdot DEC_2 = r_{an} \cdot 4.67 \cdot DEC_2 \quad (6.82)$$

The production of CO_2 from the two step of denitrification is simply given by:

$$CO_2^{(1)} = r_{an} \cdot \frac{44}{12} \cdot DEC_1 \quad (6.83)$$

$$CO_2^{(2)} = r_{an} \cdot \frac{44}{12} \cdot DEC_2 \quad (6.84)$$

Going back to equations in the model, we obtain eq.6.64:
$\frac{dCO_2}{dt} = \frac{44\cdot}{12}(\frac{1}{s\cdot n}) \cdot r_a \cdot DEC_R + (\frac{1}{s\cdot n}) \cdot r_{an} \cdot \frac{44}{12} \cdot DEC1..... + r_{an} \cdot \frac{44}{12} \cdot (\frac{1}{s\cdot n}) \cdot DEC_2$ with r_a=0.6 and r_{an}=0.53

which can also be written in terms of denitrification rates as:
$\frac{dCO_2}{dt} = \frac{44}{12} \cdot (\frac{1}{s\cdot n}) \cdot r_a \cdot DEC_R + (\frac{1}{s\cdot n}) \cdot \frac{1.}{1.17} \cdot \frac{44}{12} \cdot r_{an} \cdot DEN_1 ..... + (\frac{1}{s\cdot n}) \cdot \frac{1.}{4.67} \cdot \frac{44}{12} \cdot r_{an} \cdot DEN_2$

Alternatively, the same relationships can be found considering that during the first step of denitrification two mole of nitrate are needed to produce two mole of CO_2, so that 28g of NO_3-N lead to 24 g of CO_2-C, whose ratio is 1.17, *i.e.* the same value found trough the COD approach. For the second denitrification step one mole of N_2O is needed

to produce one mole of CO_2 leading to the ratio (28/6) which is equal to 4.57, where 28 is the g of N in N_2O and 6 is the g of C in half mole of CO_2.

6.3.4 Results and Discussions

In order to test the response of the model, we compare the model for two different fixed values of soil moisture s=0.3 and saturated condition (*i.e.* s=0.5) and for two different curves of soil moisture in time (s[t]). The first curve is a step function, reproducing a rapid de-saturation process, as the one observed in the column (see Chapter 4), while the second curve account for soils which drain much slower, as the ones with an appreciable clay content (see Figure 6.17).

As expected,in saturated condition, nitrification is inhibited, while nitrate consumption and nitrous oxide production in enhanced (see Figure 6.18).

Results including water dynamics, show that both the bacteria pool (C_b) and the litter pool (C_r) are sensible to the shape of the soil moisture curve in time. In particular a more gentle variation of soil moisture in time, lead to lower decomposition rates, as shown in Figure 6.19, where is visible how litter is decomposed less quick than when the soil drain rapidly. In this case, decomposition of litter is enhanced by the presence of oxygen. Models which do not account for oxygen dynamics might overestimate the decomposition rate.

Also, nitrification is delayed when there is a sharp variation of soil moisture, since it takes time for the oxygen to reareate the soil. This is not capture by the models which do no account for oxygen. Nitrate dynamics and nitrous oxide emissions also vary for different s[t]curves (see Figure 6.23).

In particular, for rapid variation of soil moisture we found that emission are higher for low water content and then decrease (as shown in the soil column), while for slower drainage process, the peak of emission is emitted for higher volumetric water content. It is interesting to observe than both the behaviors are non capture by the theoretical model of Davidson. These behaviors are highly dependent on reareation values. For slow variation in soil moisture and low reareation value indeed, the oxygen consumption is faster and anoxic condition become predominant, thus leading to a a peak of N_2O emission for s=0.6, as described by Davidson. The value is therefore low, comparing to the case when soils are more reareated, since the lack of oxygen inhibits the carbon decomposition, and nitrification, thus indirecting limiting the substrate for denitrification, see figure 6.22.

Non accounting for oxygen dynamics seems to underestimate N_2O emission during sharp variation of VWC and overestimate for less rapid drainage curve.

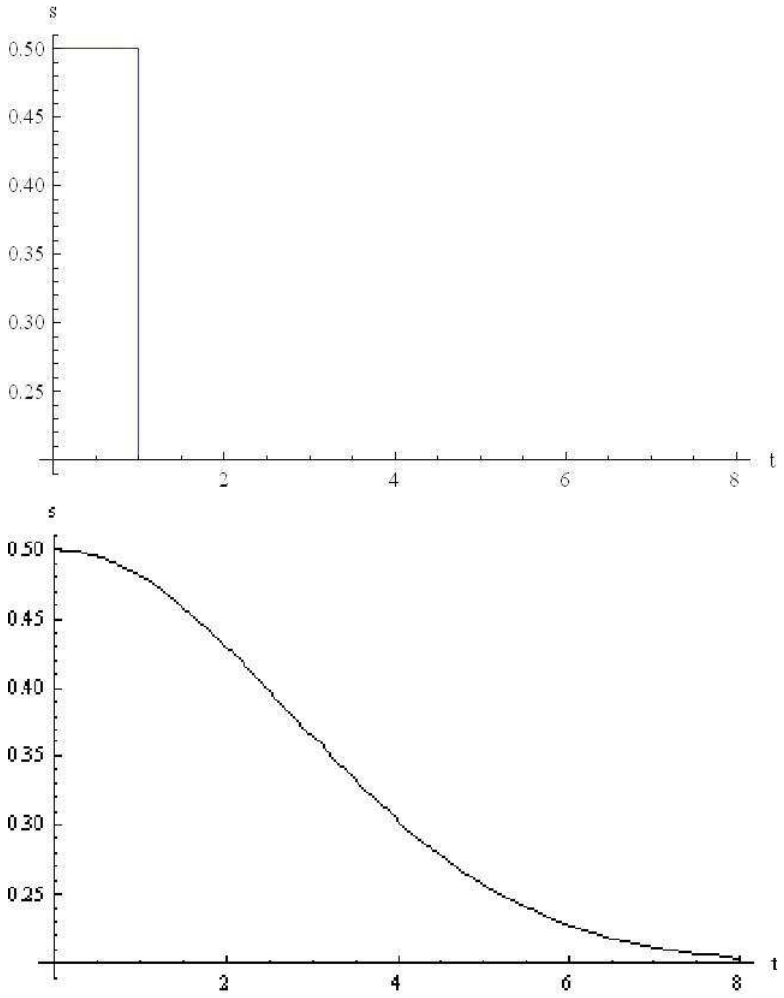

Figure 6.17: Sharp variation of soil moisture (s) vs time (t). The first behavior is based on the soil column experiment, while the second account for a mild variation of soil moisture in time. Time is in day.

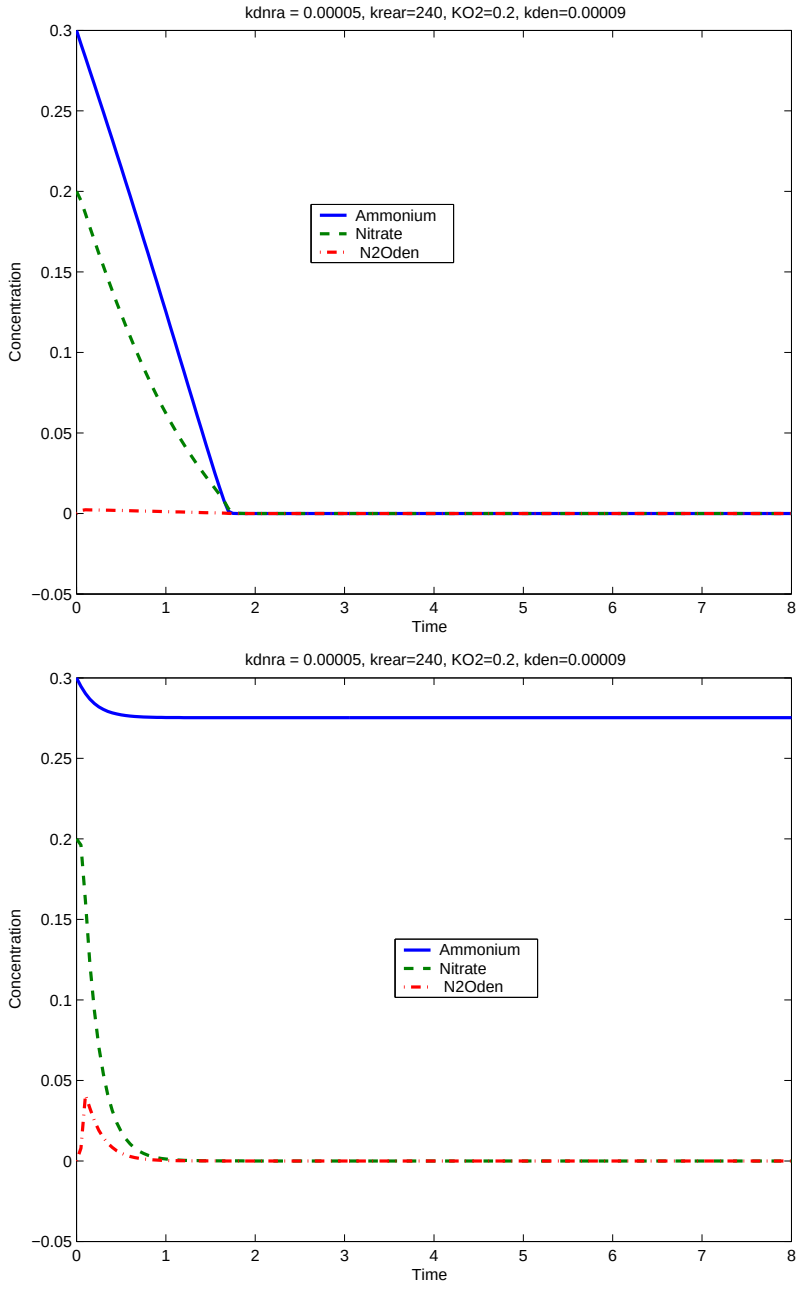

Figure 6.18: Comparison on ammonium (NH_4^+), nitrate (NO_3^-) and nitrous oxide concentrations (N_2O) for unsaturated (s=0.3) and saturated (s=0.5) conditions. The first graph refers to unsaturated condition, while the second describe nutrient dynamics when the soil is saturated. Concentration are in gC/m^3 for and mg/l for N_2O. Time is in day.

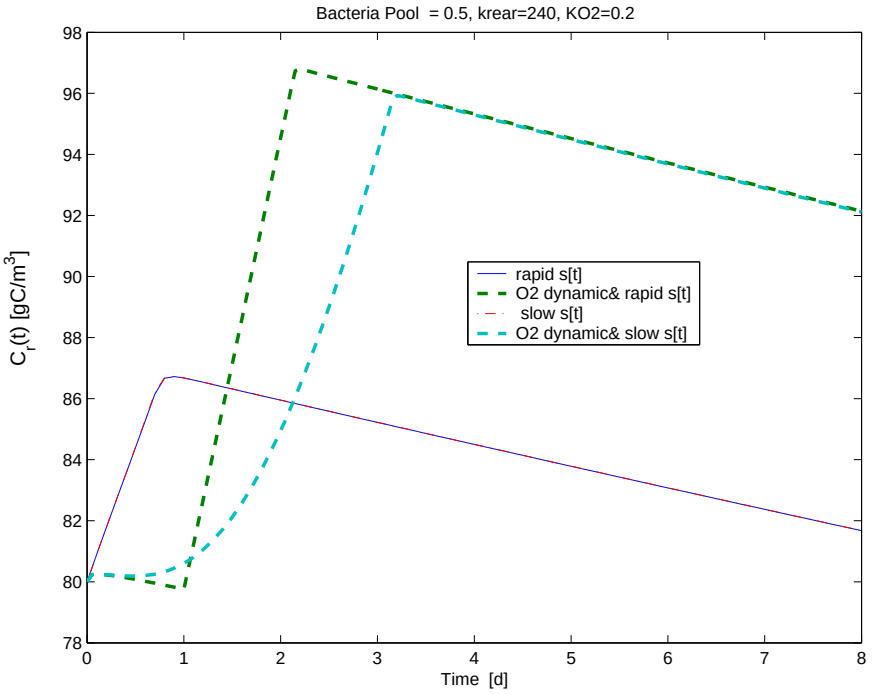

Figure 6.19: Comparison of bacteria dynamics (C_b) for different saturation curves (K_{O2} [d^{-1}]) for the model short-time scale denitrification model with and without including the oxygen dynamics the oxygen dynamics and time is in day and C_b in gC/m^3.

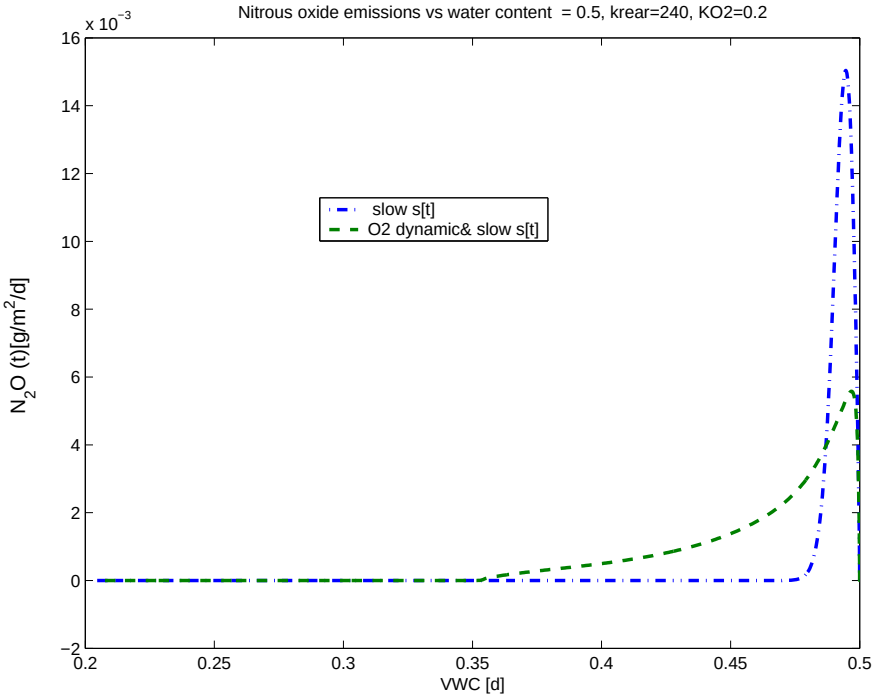

Figure 6.20: Comparison of nitrous oxides emissions (N_2O) for slow de-saturation curves. for the model short-time scale denitrification model with and without including the oxygen dynamics the oxygen dynamic and. Time is in day and the fluxes are in $gN/m^2/d$.

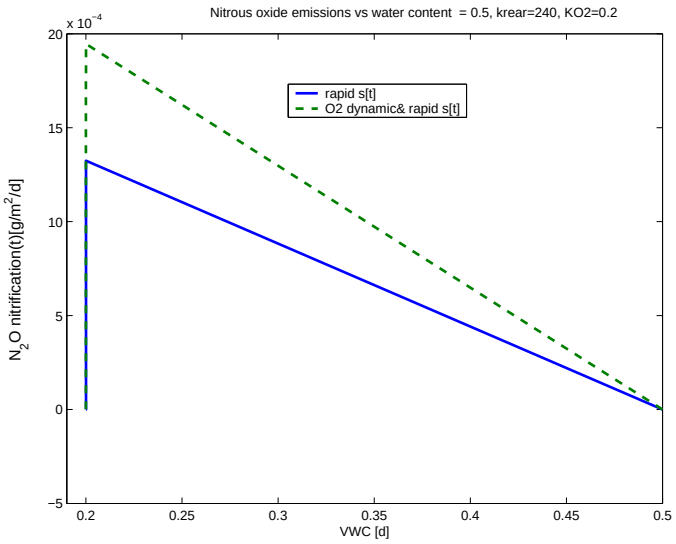

Figure 6.21: Comparison of nitrous oxides emissions (N_2O) for rapid de-saturation curves. for the model short-time scale denitrification model with and without including the oxygen dynamic the oxygen dynamics and. Time is in day and the fluxes are in $gN/m^2/d$.

Nitrate pool changes are given by different factors: denitrification, leaching and plant uptake.In these simulations we did not include leaching and plant uptake, in order to better understand the role of N losses trough trace gas emissions. These pathways can be easily added, following the approach of Porporato (2003).

However, an other important pathway which is often neglected is nitrate ammonification. This pathway, may be important in wetlands and upland soil with fluctuationg condition and avaiability of carbon and nitrate as tropical forests (Tiedje, 1988; Silver et al., 2001).

DNRA also can compete with denitrification process. Here we report different curves for different value of kinetic constant of DNRA (k_{dnra}). Results indicate that when the rate of DNRA is significant comparing to the ones of denitrification, this reduce the production of nitrous oxide emissions, though the conversion of nitrate to ammonium. This process thus retains nitrogen into soil. Therefore, increasing in ammonium pool, may enhance production of nitrous oxide from nitrification, if the carbon availability and the oxygen level are not too low.

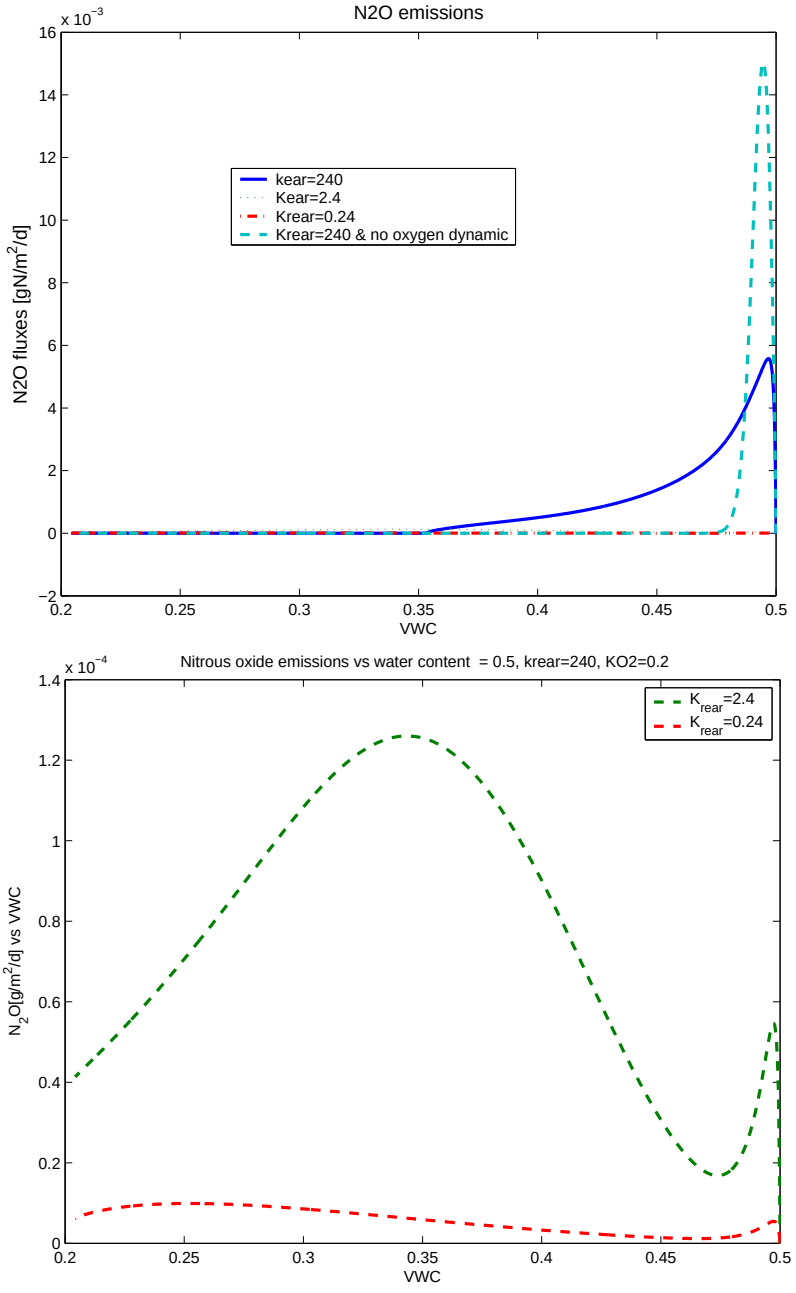

Figure 6.22: Comparison of nitrous oxides emissions (N_2O) for slow de-saturation curves at different reareation values for the model short-time scale denitrification model with and without including the oxygen dynamics the oxygen dynamics .Time is in day and the fluxes are in $gN/m^2/d$. Plot (b) is a zoom of (a) for lower K_{rear}.

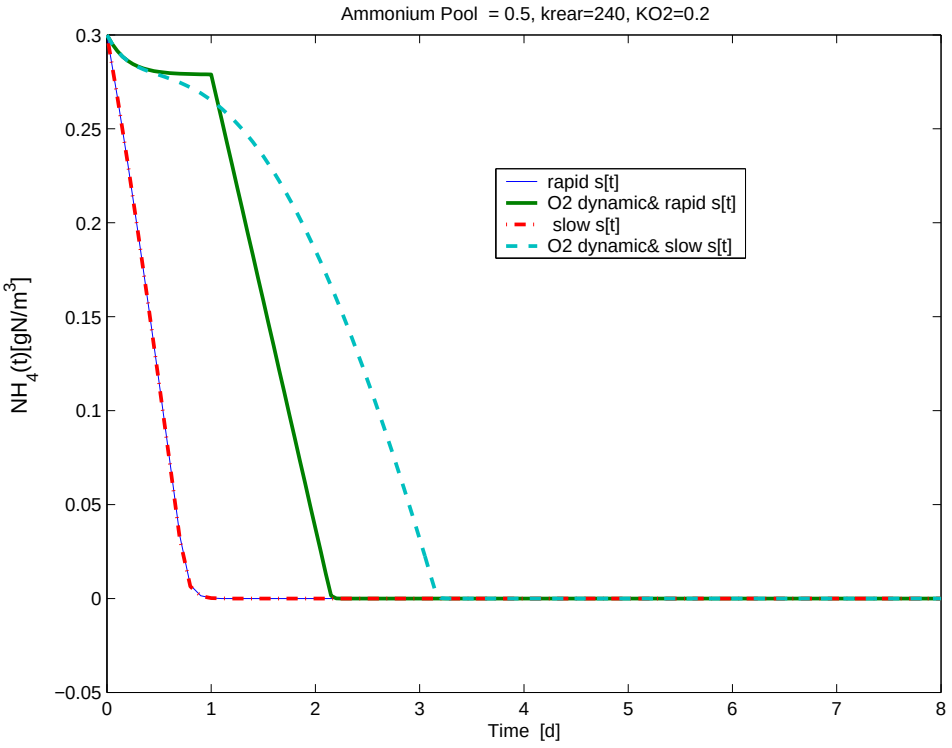

Figure 6.23: Comparison of ammonium dynamics (NH_4^+) for different saturation curves (K_{O2} [d^{-1}]) for the model short-time scale denitrification model with and without including the oxygen dynamics the oxygen dynamics and time is in day and NH_4^+) in gN/m^3.

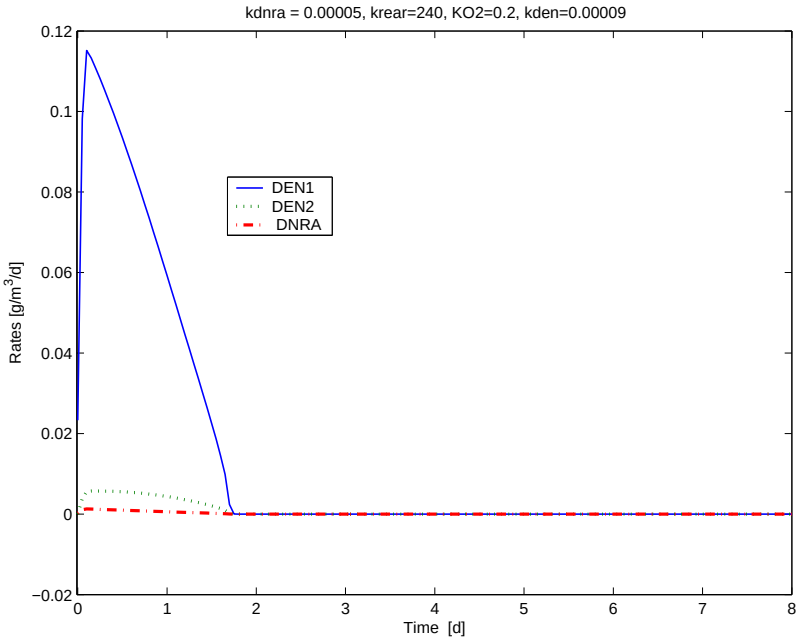

Figure 6.24: Comparison of denitrification rates (DEN1, DEN2) and nitrate ammonification rate (DNRA) for k_{dnra}=0.00005. DEN1 account for the conversion of nitrate (NO3) to nitrous oxide (N_2O), while DEN2 accounts for the conversion of N_2O to dinitrogen (N_2). Simulation has been done considering soil moisture s=0.3, porosity n=0.5, k_{dEN}=0.00009, semisaturation constant K_{O2}=0.2 and reareation K_{rear}=240. Time is in day and the fluxes are in $gN/m^3/d$.

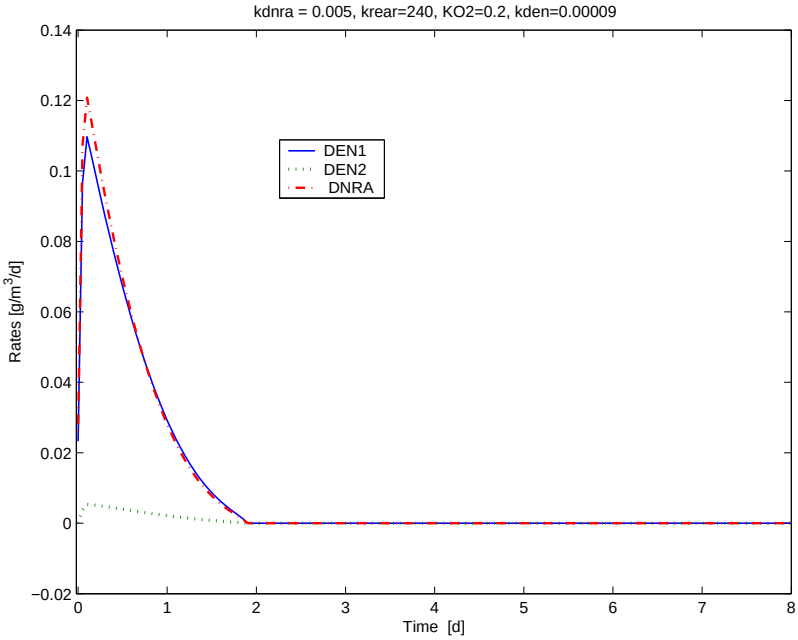

Figure 6.25: Comparison of denitrification rates (DEN1, DEN2) and nitrate ammonification rate (DNRA) for k_{dnra}=0.005. DEN1 account for the conversion of nitrate (NO3) to nitrous oxide (N_2O), while DEN2 accounts for the conversion of N_2O to dinitrogen (N_2). Simulation has been done considering soil moisture s=0.3, porosity n=0.5, k_{dEN}=0.00009, semisaturation constant K_{O2}=0.2 and reareation K_{rear}=240. Time is in day and the fluxes are in gN/m^3/d.

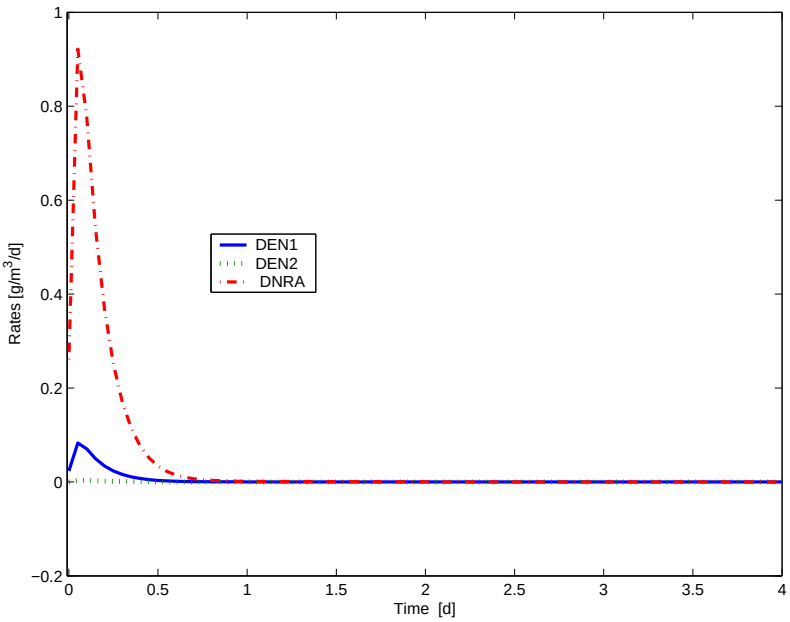

Figure 6.26: Comparison of denitrification rates (DEN1, DEN2) and nitrate ammonification rate (DNRA) for k_{dnra}=0.05. DEN1 account for the conversion of nitrate (NO3) to nitrous oxide (N_2O), while DEN2 accounts for the conversion of N_2O to dinitrogen (N_2). Simulation has been done considering soil moisture s=0.3, porosity n=0.5, k_{dEN}=0.00009, semisaturation constant K_{O2}=0.2 and reareation K_{rear}=240. Time is in day and the fluxes are in gN/m^3/d.

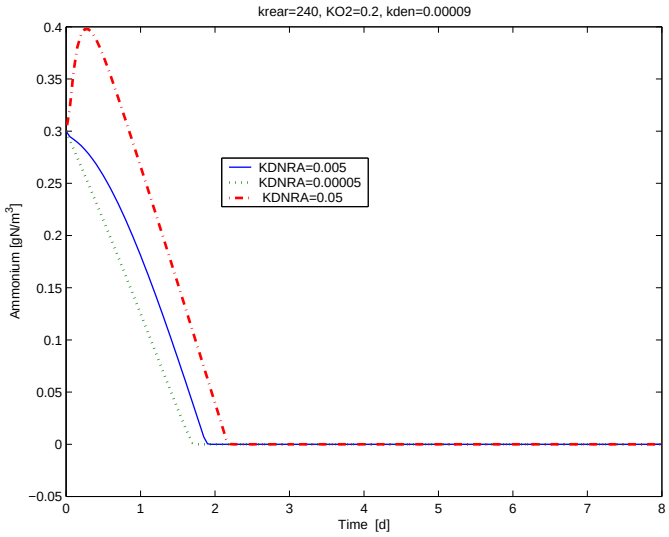

Figure 6.27: Comparison of ammonium (NH_4^+) evolution in time for different values of k_{dnra}. Simulation has been done considering soil moisture s=0.3, porosity n=0.5, k_{dEN}=0.00009, semisaturation constant K_{O2}=0.2 and reareation K_{rear}=240. Time is in day and the concentrations are in gN/m^3.

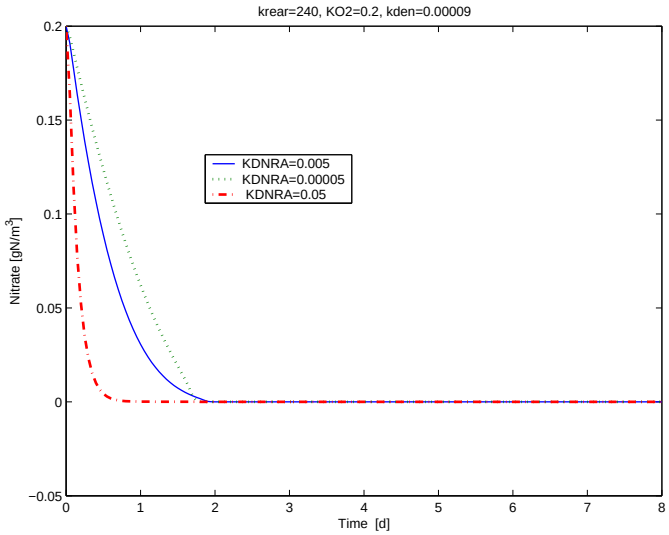

Figure 6.28: Comparison of nitrate (NO_3^-) evolution in time for different values of k_{dnra}. Simulation has been done considering soil moisture s=0.3, porosity n=0.5, k_{dEN}=0.00009, semisaturation constant K_{O2}=0.2 and reareation K_{rear}=240. Time is in day and the concentrations are in gN/m^3.

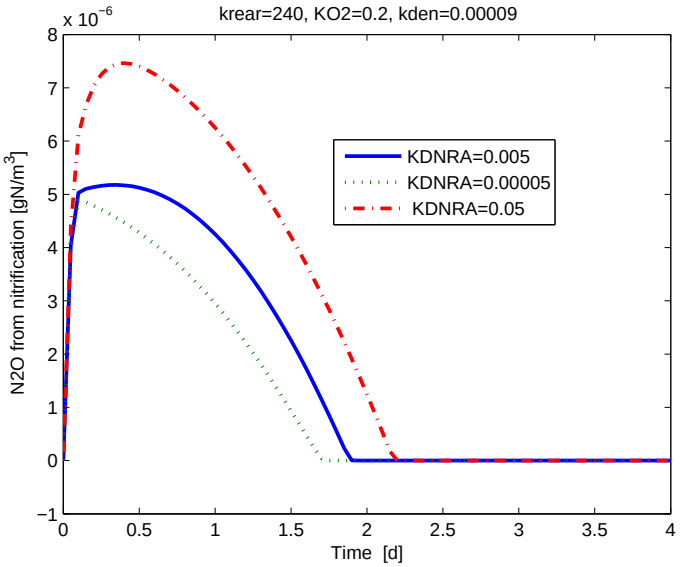

Figure 6.29: Evolution of nitrous oxides (N_2O) produced during nitrification for different values of k_{dnra} Simulation has been done considering soil moisture s=0.3, porosity n=0.5, k_{dEN}=0.00009, semisaturation constant K_{O2}=0.2 and reareation K_{rear}=240. Time is in day and the concentrations are in mg/l.

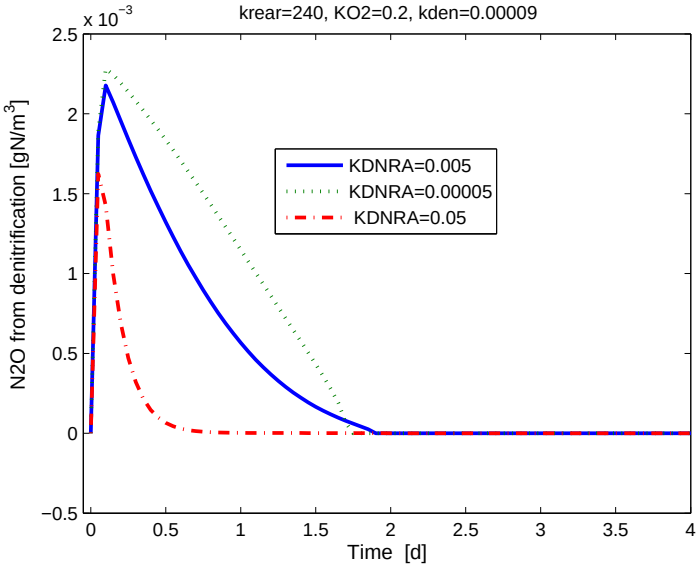

Figure 6.30: Evolution of nitrous oxides (N_2O) produced during denitrification for different values of k_{dnra}. Simulation has been done considering soil moisture s=0.3, porosity n=0.5, (k_{dEN}=0.00009, semisaturation constant K_{O2}=0.2 and reareation K_{rear}=240. Time is in day and the concentrations are in mg/l.

6.4 Chapter Summary

A model which consider oxygen dynamic has been implemented. The model include decomposition, nitrification, denitrification, production of carbon dioxide and dinitrogen emissions.

The model accounts for N_2O production from nitrification and denitrification, as well as the competition for nitrate by denitrification and dissimilatory reduction of nitrate to ammonium (DNRA). Preliminary results indicate that neglecting oxygen dynamic may significative alter rates and the compares of trace gases peaks. In particular from our simulation, the following consideration ca be drawn:

From the previous discussion we can conclude that:

- Soil with high value of reareaction enhance aerobic processes towards anaerobic, even though this effect vary according to different value of soil moisture;
- For low K_{rear} aerobic processes may stop because oxygen is depleted. Thus is soil with low reareaction and high soil moisture non account for oxygen dynamics might overestimate C and N fluxes;
- Neglecting DNRA in soils, which have carbon and nitrate availability and low oxygen conditions, may lead to an oversextimation of the fluxes.

However, there are still further extensions of the model proposed here. For instance, some future directions can be the inclusion of:

- A stochastic variation of soil moisture, and determine the oxygen consumption during the plant uptake;
- Soil heterogeneity ;
- Two distinct groups of bacteria (heterotrophy and autotroph).

To simulate the rainfall regime during the wet growing season, rainfall inputs are modeled at the daily time scale as a compound Poisson process of storm arrival rate λ, and exponentially distributed depth event with mean α (Laio et al., 2001). Soil moisture dynamics are thus modeled through a stochastic soil water balance following Laio et al. (2001):

$$nZ_r \frac{ds}{dt} = I(s,t) - E(s) - T(s) - L(s) \tag{6.85}$$

where s is the relative volumetric water content, n is the soil porosity, Zr is active soil depth, $I(t,s)$ is the rate of rainfall infiltration, $ET(s)$ is the rate of evapotranspiration,

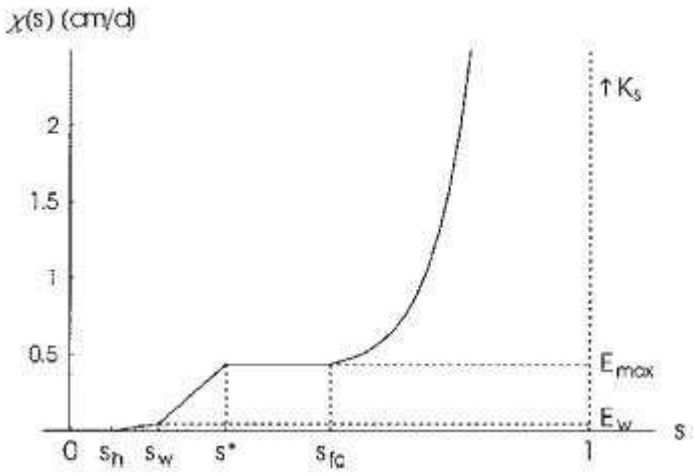

Figure 6.31: Behavior of soil water losses (evapotranspiration and leakage), $\chi(s)$, as a function of the relative soil moisture for typical climate, soil, and vegetation characteristics in semiarid ecosystems (E_{max}, E_w and T_{max}) Porporato et al. (2003).

and $L(s)$ the rate of leakage through the bottom of the soil layer. The same soil depth, Zr , was used for the water, C and N budgets. Equation 6.85, thanks to the random infiltration $I(t, s)$, describes a stochastic soil water balance, which can be solved in terms of soil moisture probability density function (pdf), $p(s)$ according to Figure 6.31 .

This relationship has been explored by Ridolfi 2003 with static model, but so far has not been explored by dynamics model.

7 Summary and Conclusions

The present work demonstrates the complex role of water dynamics in trace gas emissions and N-cycling. Both physical and biological processes are at play, and likely interact, as shown in the soil column experiment, trough for example: (i) changes in soil oxygen (O_2) concentrations with compaction; (ii) the effects of water movement as a conduit for increased O_2 concentrations, and (iii) the possibility of gas displacement of with water additions. Trace gases emissions, dissolved nitrate and ammonium changed considerably along the soil column profile as a response of the microbial community to the high variability in redox, soil moisture, and concentrations of oxygen along the soil column.

The following conclusions can be drawn from the research results:

1. Microbiological activity is buffered against short-term changes in soil moisture and water filled pore space;

2. The relationship between N_2O emissions and soil water content(VWC) under dynamic conditions (shown in the soil column) significantly differ from those determined under static conditions (incubation/jars) indicating that when the time scale of soil water is faster than that of bacteria activity, the theoretical relationship between emissions and soil water content described by Davidson (1991) is a too rough approximation of the real dynamics;

3. The interaction between N-cycle and iron may lead to production of nitrous oxide emissions (feammox);

4. Periodic flooding/saturation has a stronger impact than soil water dynamics induced by rainfall variabilities;

5. Water, oxygen and soil heterogeneity are the key controlling factors in understanding nitrous oxide (N_2O) emissions and explaining the different delay in peak emissions following rainfall pulses(3 days) and flooding event (2 days) cousing deposition of nutrients;

6. Water table fluctuations in temperate peatland of the Bay Delta area lead to nitrous oxide emissions comparable to those typical of tropical forests and agricultural fields. This indicate the potential for these types of peatland to significant contribute to global warming.

Jars (incubation) and column experiments shown that, small-scale variability in soil water content (or soil physical properties) can lead to fundamental differences in N-cycling and associated greenhouse gas dynamics. This level is likely to be the most difficult to model. At larger spatial scales, *i.e.* at the field scale, landscape position can provide a reasonable proxy for soil physical characteristics and help identify the relative role of "hot spots or hot moments" with regard to greenhouse gas fluxes. In addition oxygen concentration is much better correlated to nitrous oxide emissions than soil water content, when this (VWC) varies rapidly in time.

Therefore, the soil column experiments are a valuable tool to describe the interplay between the nitrogen cycle and the different ways in which water may vary (e.g rainfall, saturation and deposition) under controlled conditions and should be used as means to inform future field experiments and modeling efforts.

In addition to the experimental component of this dissertation, a model is proposed to better understand the interaction between physical and biological processes. Based on experimental evidence, given on the column and incubation results, a mathematical model based on the work of Porporato and co-workers (Porporato et al., 2003; Manzoni and Porporato, 2007; Wang et al., 2009) has been developed. The model consisted of a system of ordinary differential equations to account for the dynamics, decomposition, nitrification, denitrification, nitrate ammonification, carbon dioxide production and nitrous oxide dynamics. The model proposed proved useful since if gives insight of the main biogeochemical processes without having to rely on more complex models (involving flow and transport through partial differential equations). Preliminary results indicate that not taking into account limiting oxygen condition, might lead to an overestimation of the nitrogen and carbon fluxes in soils close to saturated condition and where reareation is low. Also higher values of reareation enhance aerobic processes towards anaerobic processes, but this effect vary for different values of soil moisture.

In addition, although not a perfect representation of reality, the models seems to mimic the behavior observed in the column.

As a conclusion, the current work represents a step towards linking physical and chemical processes underlying the impact of redox dynamics on gas emissions.

References

J. Aber and C. Driscoll. Effects of land use, climate variation, and N deposition on N cycling and C storage in northern hardwood forests. *Global Biogeochemical Cycles*, 11 (4):639–648, 1997.

F. Allison, J. Carter, and L. Sterling. The effect of partial pressure of oxygen on denitrification in soil. *Soil Science Society of America Journal*, 24(4):283, 1960.

K. Allton, J. Harris, R. Rickson, and K. Ritz. The effect of microbial communities on soil hydrological processes: A microcosm study utilising simulated rainfall. *Geoderma*, 142 (1-2):11–17, 2007.

F. Amer and W. Bartholomew. Influence of oxygen concentration in soil air on nitrification. *Soil Science*, 71(3):215, 1951.

E. Baggs. A review of stable isotope techniques for N2O source partitioning in soils: recent progress, remaining challenges and future considerations. *Rapid Communications in Mass Spectrometry*, 22(11):1664, 2008.

P. Barak, J. Molina, A. Hadas, and C. Clapp. Mineralization of amino acids and evidence of direct assimilation of organic nitrogen. *Soil Science Society of America Journal*, 54 (3):769, 1990.

E. Bateman and E. Baggs. Contributions of nitrification and denitrification to N 2 O emissions from soils at different water-filled pore space. *Biology and Fertility of Soils*, 41(6):379–388, 2005.

L. Belyea and A. Baird. Beyond 8460;the limits to peat bog growth: Cross-scale feedback in peatland development. *Ecological Monographs*, 76(3):299–322, 2006.

S. Birkinshaw and J. Ewen. Modelling nitrate transport in the Slapton Wood catchment using SHETRAN. *Journal of hydrology*, 230(1-2):18–33, 2000.

B. Bolker, S. Pacala, and W. Parton Jr. Linear analysis of soil decomposition: insights from the CENTURY model. *Ecological Applications*, 8(2):425–439, 1998.

E. Boyer, R. Alexander, W. Parton, C. Li, K. Butterbach-Bahl, S. Donner, R. Skaggs, and S. Grosso. Modeling denitrification in terrestrial and aquatic ecosystems at regional scales. *Ecological Applications*, 16(6):2123–2142, 2006.

J. Braden, D. Brown, J. Dozier, P. Gober, S. Hughes, D. Maidment, S. Schneider, P. Schultz, J. Shortle, S. Swallow, et al. Social science in a water observing system. *Water Resour. Res*, 45, 2009.

N. Brady and R. Weil. The nature and property of soils. *Mac Millan, New York*, 1974.

A. Burgin and S. Hamilton. Have we overemphasized the role of denitrification in aquatic ecosystems? A review of nitrate removal pathways. *Frontiers in Ecology and the Environment*, 5(2):89–96, 2007.

K. Butterbach-Bahl, F. Stange, H. Papen, G. Grell, and C. Li. Impact of changes in temperature and precipitation on N2O and NO emissions from forest soils. In *Non-CO2 Greenhouse Gases: Scientific Understanding, Control, and Implementation: Proceedings of the Second International Symposium, Noordwijkerhout, The Netherlands, 8-10 September 1999*, page 165. Kluwer Academic Pub, 2000.

K. Butterbach-Bahl, G. Willibald, and H. Papen. Soil core method for direct simultaneous determination of N 2 and N 2 O emissions from forest soils. *Plant and Soil*, 240(1):105–116, 2002.

O. Cainelli. *Subsurface Flow Modelling at the HillSlope Scale: Numerical and Physical Anaylsis*. PhD thesis, University of Trento, Italy, 2007.

C. Cho. Oxygen consumption and denitrification kinetics in soil. *Soil Science Society of America Journal*, 46(4):756, 1982.

J. Clement, J. Shrestha, J. Ehrenfeld, and P. Jaffe. Ammonium oxidation coupled to dissimilatory reduction of iron under anaerobic conditions in wetland soils. *Soil Biology and Biochemistry*, 37(12):2323–2328, 2005.

T. Clough, R. Sherlock, and D. Rolston. A review of the movement and fate of N2O in the subsoil. *Nutrient Cycling in Agroecosystems*, 72(1):3–11, 2005.

B. Colman, N. Fierer, and J. Schimel. Abiotic nitrate incorporation, anaerobic microsites, and the ferrous wheel. *Biogeochemistry*, 91(2):223–227, 2008.

R. Conrad. Soil microorganisms as controllers of atmospheric trace gases (H2, CO, CH4, OCS, N2O, and NO). *Microbiology and Molecular Biology Reviews*, 60(4):609–640, 1996.

P. Crutzen, A. Mosier, K. Smith, and W. Winiwarter. N2O release from agrobiofuel production negates global warming reduction by replacing fossil fuels. *Atmospheric Chemistry and Physics Discussions*, 7:11191–11205, 2007.

E. Daly and A. Porporato. A review of soil moisture dynamics: from rainfall infiltration to ecosystem response. *Environmental engineering science*, 22(1):9–24, 2005.

E. Davidson. Fluxes of nitrous oxide and nitric oxide from terrestrial ecosystems. *Microbial production and consumption of greenhouse gases: methane, nitrogen oxides and halomethanes*, pages 219–235, 1991.

E. Davidson. Soil water content and the ratio of nitrous oxide and nitric oxide emitted from soil. In *Biogeochemistry of Global Change Radiatively Active Trace Gases: Selected Papers from the Tenth International Symposium on Environmental Biogeochemistry, San Francisco, August 19–24, 1991*, pages 369–86, 1993.

E. Davidson and S. Seitzinger. The enigma of progress in denitrification research. *Ecological Applications*, 16(6):2057–2063, 2006.

T. Davidsson and L. Leonardson. Seasonal dynamics of denitrification activity in two water meadows. *Hydrobiologia*, 364(2):189–198, 1997.

P. De Gennes, F. Brochard-Wyart, D. Quere, and A. Reisinger. *Capillarity and wetting phenomena: drops, bubbles, pearls, waves*. Springer Verlag, 2004.

S. Deverel and S. Rojstaczer. Subsidence of agricultural lands in the Sacramento-San Joaquin Delta, California: Role of aqueous and gaseous carbon fluxes. *Water Resources Research*, 32(8):2359–2367, 1996.

P. Dodorico, F. Laio, A. Porporato, and I. Rodriguez Iturbe. Hydrologic controls on soil carbon and nitrogen cycles. II. A case study. *Advances in Water Resources*, 26(1):59–70, 2003.

J. Drexler, C. de Fontaine, and S. Deverel. The Legacy of Wetland Drainage on the Remaining Peat in the Sacramento-San Joaquin Delta, California, USA. *Wetlands*, 29 (1):372–386, 2009.

EEA. Annual European Community greenhouse gas inventory 1990 to 2005 and inventory report, EEA 2007. Technical report, 2007.

G. Ekama, G. Marais, I. Siebritz, A. Pitman, G. Keay, L. Buchan, A. Gerber, and M. Smollen. Theory, design and operation of nutrient removal activated sludge processes. *Water Research Commission, Pretoria, South Africa*, 1984.

H. Flessa, P. Dorsch, and F. Beese. Seasonal variation of N2O and CH4 fluxes in differently managed arable soils in southern Germany (Paper 95JD02270). *Journal of Geophysical Research-Part D-Atmospheres-Printed Edition*, 100(11):23115–23124, 1995.

C. Francis, J. Beman, and M. Kuypers. New processes and players in the nitrogen cycle: the microbial ecology of anaerobic and archaeal ammonia oxidation. *Isme Journal*, 1 (1):19–27, 2007.

A. Franzluebbers. Water infiltration and soil structure related to organic matter and its stratification with depth. *Soil and Tillage Research*, 66(2):197–205, 2002.

S. Frolking, A. Mosier, D. Ojima, C. Li, W. Parton, C. Potter, E. Priesack, R. Stenger, C. Haberbosch, P. Dorsch, et al. Comparison of N 2 O emissions from soils at three temperate agricultural sites: simulations of year-round measurements by four models. *Nutrient Cycling in Agroecosystems*, 52(2):77–105, 1998.

J. Galloway, J. Aber, J. Erisman, S. Seitzinger, R. Howarth, E. Cowling, and B. Cosby. The nitrogen cascade. *BioScience*, 53(4):341–356, 2003.

J. Galloway, A. Townsend, J. Erisman, M. Bekunda, Z. Cai, J. Freney, L. Martinelli, S. Seitzinger, and M. Sutton. Transformation of the nitrogen cycle: Recent trends, questions, and potential solutions. *Science*, 320(5878):889, 2008.

J. Gilmour. The effects of soil properties on nitrification and nitrification inhibition. *Soil Science Society of America Journal*, 48(6):1262, 1984.

L. Goodroad and D. Keeney. Nitrous oxide emission from forest, marsh, and prairie ecosystems. *Journal of Environmental Quality*, 13(3):448, 1984.

T. Goreau, W. Kaplan, S. Wofsy, M. McElroy, F. Valois, and S. Watson. Production of NO2-and N2O by nitrifying bacteria at reduced concentrations of oxygen. *Applied and Environmental Microbiology*, 40(3):526, 1980.

E. Gorham. Northern peatlands: role in the carbon cycle and probable responses to climatic warming. *Ecological applications*, 1(2):182–195, 1991.

R. Grant, E. Pattey, T. Goddard, L. Kryzanowski, and H. Puurveen. Modeling the effects of fertilizer application rate on nitrous oxide emissions. *Soil Science Society of America Journal*, 70(1):235, 2006.

P. Groffman, K. Butterbach-Bahl, R. Fulweiler, A. Gold, J. Morse, E. Stander, C. Tague, C. Tonitto, and P. Vidon. Challenges to incorporating spatially and temporally explicit phenomena (hotspots and hot moments) in denitrification models. *Biogeochemistry*, 93 (1):49–77, 2009.

B. D. Guha A., Detto M. and G. A. H. Methane Fluxes in a Composite Landscape in the Sacramento-San Joaquin Delta. *Eos Trans. AGU*, 90-52, A51N-07, 2009.

A. Gusman and M. Marino. Analytical modeling of nitrogen dynamics in soils and ground water. *Journal of Irrigation and Drainage Engineering*, 125:330, 1999.

A. Guswa, M. Celia, and I. Rodriguez-Iturbe. Models of soil moisture dynamics in ecohydrology: A comparative study. *Water Resour. Res*, 38(9):1166, 2002.

T. Guthrie and J. Duxbury. Nitrogen mineralization and denitrification in organic soils. *Soil Science Society of America Journal*, 42(6):908, 1978.

R. Harris. Effect of water potential on microbial growth and activity. *Water potential relations in soil microbiology*, 9:23–97, 1981.

S. Hart, J. Stark, E. Davidson, and M. Firestone. Nitrogen mineralization, immobilization, and nitrification. *Methods of soil analysis. Part*, 2:985–1018, 1994.

M. Heincke and M. Kaupenjohann. Effects of soil solution on the dynamics of N2O emissions: a review. *Nutrient Cycling in Agroecosystems*, 55(2):133–157, 1999.

M. Heinen. Simplified denitrification models: Overview and properties. *Geoderma*, 133 (3-4):444–463, 2006.

M. Henze. *Activated sludge models ASM1, ASM2, ASM2d and ASM3.* Iwa Publishing, 2000.

D. Herman, P. Brooks, M. Ashraf, F. Azam, and R. Mulvaney. Evaluation of methods for nitrogen-15 analysis of inorganic nitrogen in soil extracts. II. Diffusion methods. *Communications in soil science and plant analysis (USA)*, 1995.

J. Hoefs. *Stable isotope geochemistry*. Springer, 2008.

J. Hunt, P. Holden, and M. Firestone. Coupling transport and biodegradation of VOCs in surface and subsurface soils. *Environmental Health Perspectives*, 103(Suppl 5):75, 1995.

IPCC. Climate change 2007: the physical science basis. *Summary for Policy Makers, Contribution of Working Group I to the Fourth Assessment Report of the Intergovernmental Panel on Climate Change*, 2007.

D. Jenkinson, S. Andrew, J. Lynch, M. Goss, and P. Tinker. The Turnover of Organic Carbon and Nitrogen in Soil [and Discussion]. *Philosophical Transactions: Biological Sciences*, 329(1255):361–368, 1990.

A. Kappler, C. Hohmann, E. Winkler, M. Muehe, and G. Morin. Immobilisation of arsenic by iron (II)-oxidizing bacteria. In *American Geophysical Union, Fall Meeting 2008, abstract: B21B-0353*, 2008.

A. Kasimir-Klemedtsson, L. Klemedtsson, K. Berglund, P. Martikainen, J. Silvola, and O. Oenema. Greenhouse gas emissions from farmed organic soils: a review. *Soil Use and Management*, 13(s4):245–250, 1997.

C. Kendall and J. McDonnell. *Isotope tracers in catchment hydrology*. Elsevier Amsterdam, 1998.

I. Khdyer and C. Cho. Nitrification and denitrification of nitrogen fertilizers in a soil column. *Soil Science Society of America Journal*, 47(6):1134, 1983.

D. Kirkham and W. Bartholomew. Equations for following nutrient transformations in soil, utilizing tracer data. *Soil Science Society of America Journal*, 18(1):33, 1954.

P. Kitanidis. *Introduction to geostatistics: applications to hydrogeology*. Cambridge Univ Pr, 1997.

J. Kjellin, S. Hallin, and A. Worman. Spatial variations in denitrification activity in wetland sediments explained by hydrology and denitrifying community structure. *Water Research*, 41(20):4710–4720, 2007.

L. Klemedtsson, A. Klemedtsson, F. Moldan, and P. Weslien. Nitrous oxide emission from Swedish forest soils in relation to liming and simulated increased N-deposition. *Biology and Fertility of Soils*, 25(3):290–295, 1997.

A. Kremen, J. Bear, U. Shavit, and A. Shaviv. Model demonstrating the potential for coupled nitrification denitrification in soil aggregates. *Environmental science and technology*, 39(11):4180–4188, 2005.

F. Laio, A. Porporato, L. Ridolfi, and I. Rodriguez-Iturbe. Plants in water-controlled ecosystems: active role in hydrologic processes and response to water stress II. Probabilistic soil moisture dynamics. *Advances in Water Resources*, 24(7):707–723, 2001.

G. Langergraber and J. Simunek. Modeling variably saturated water flow and multicomponent reactive transport in constructed wetlands. *Vadose Zone Journal*, 4(4):924, 2005.

P. Leffelaar and W. Wessel. Denitrification in a homogeneous, closed system: experiment and simulation. *Soil Science*, 146(5):335, 1988.

C. Li, S. Frolking, and T. Frolking. A model of nitrous oxide evolution from soil driven by rainfall events: 2 Model applications. *J. Geophys. Res*, 97:9777–9783, 1992.

R. Lowrance, L. Altier, J. Newbold, R. Schnabel, P. Groffman, J. Denver, D. Correll, J. Gilliam, J. Robinson, R. Brinsfield, et al. Water quality functions of riparian forest buffers in Chesapeake Bay watersheds. *Environmental Management*, 21(5):687–712, 1997.

M. Maag and F. Vinther. Nitrous oxide emission by nitrification and denitrification in different soil types and at different soil moisture contents and temperatures. *Applied Soil Ecology*, 4(1):5–14, 1996.

F. Maggi, C. Gu, W. Riley, G. Hornberger, R. Venterea, T. Xu, N. Spycher, C. Steefel, N. Miller, and C. Oldenburg. A mechanistic treatment of the dominant soil nitrogen cycling processes: Model development, testing, and application. *Journal of Geophysical Research-Biogeosciences*, 113(G2):G02016, 2008.

M. Maljanen, A. Liikanen, J. Silvola, and P. Martikainen. Nitrous oxide emissions from boreal organic soil under different land-use. *Soil Biology and Biochemistry*, 35(5):689–700, 2003.

M. Maljanen, B. Sigurdsson, J. Gumundsson, H. Oskarsson, J. Huttunen, and P. Martikainen. Land-use and greenhouse gas balances of peatlands in the Nordic countries–present knowledge and gaps. *Biogeosciences Discussions*, 6:6271–6338, 2009.

S. Manzoni and A. Porporato. A theoretical analysis of nonlinearities and feedbacks in soil carbon and nitrogen cycles. *Soil Biology and Biochemistry*, 39(7):1542–1556, 2007.

S. Manzoni and A. Porporato. Soil carbon and nitrogen mineralization: Theory and models across scales. *Soil Biology and Biochemistry*, 2009.

P. Martikainen, H. Nykanen, P. Crill, and J. Silvola. Effect of a lowered water table on nitrous oxide fluxes from northern peatlands. 1993.

A. Matthias, D. Yarger, and R. Weinbeck. A numerical evaluation of chamber methods for determining gas fluxes. *Geophysical Research Letters*, 5:765–768, 1978.

D. McKenney, C. Drury, and S. Wang. Effects of oxygen on denitrification inhibition, repression, and derepression in soil columns. *Soil Science Society of America Journal*, 65(1):126–132, 2001.

D. McKenney, S. Wang, and C. Drury. Reaction of nitric oxide with acetylene and oxygen: implications for denitrification assays. *Soil Science Society of America Journal*, 61(5): 1370, 1997.

F. Meixner, T. Fickinger, L. Marufu, D. Serca, F. Nathaus, E. Makina, L. Mukurumbira, and M. Andreae. Preliminary results on nitric oxide emission from a southern African savanna ecosystem. *Nutrient Cycling in Agroecosystems*, 48(1):123–138, 1997.

D. Moorhead, W. Currie, E. Rastetter, W. Parton, and M. Harmon. Climate and litter quality controls on decomposition: an analysis of modeling approaches. *Global Biogeochemical Cycles*, 13(2).

M. Muller, V. Sundman, and J. Skujins. Denitrification in low pH spodosols and peats determined with the acetylene inhibition method. *Applied and environmental microbiology*, 40(2):235, 1980.

D. Or, M. Tuller, and S. Jones. Liquid Behavior in Partially Saturated Porous Media under Variable Gravity. *Soil Science Society of America Journal*, 73(2):341, 2009.

Pachauri. Statment IPCCSummit on Climate Change, UN Headquarters, New York, USA, IPCC, 2009.

Y. Pachepsky and W. Rawls. Soil structure and pedotransfer functions. *European Journal of Soil Science*, 54(3):443–452, 2003.

W. Parton, M. Hartman, D. Ojima, and D. Schimel. DAYCENT and its land surface submodel: description and testing. *Global and Planetary Change*, 19(1):35–48, 1998.

W. Parton, D. Ojima, and D. Schimel. Models to evaluate soil organic matter storage and dynamics. *Structure and Organic Matter Storage in Agricultural Soils*, pages 421–448, 1996.

W. Parton and P. Rasmussen. Long-term effects of crop management in wheat-fallow: II. CENTURY model simulations. *Soil Science Society of America Journal*, 58(2):530, 1994.

J. Pett-Ridge, W. Silver, and M. Firestone. Redox fluctuations frame microbial community impacts on N-cycling rates in a humid tropical forest soil. *Biogeochemistry*, 81(1):95–110, 2006.

A. Porporato, E. Daly, and I. Rodriguez-Iturbe. Soil water balance and ecosystem response to climate change. *The American Naturalist*, 164(5):625–632, 2004.

A. Porporato, P. DOdorico, F. Laio, and I. Rodriguez-Iturbe. Hydrologic controls on soil carbon and nitrogen cycles. I. Modeling scheme. *Advances in water resources*, 26(1): 45–58, 2003.

C. Potter, E. Davidson, and L. Verchot. Estimation of global biogeochemical controls and seasonality in soil methane consumption. *Chemosphere*, 32(11):2219–2246, 1996.

M. Prather, D. Ehhalt, F. Dentener, R. Derwent, E. Dlugokencky, E. Holland, I. Isaksen, J. Katima, V. Kirchhoff, P. Matson, et al. Atmospheric chemistry and greenhouse gases. *Climate change*, pages 239–287, 2001.

V. Ramanathan. Scientific use of surface radiation budget data for climate studies. *Surface Radiation Budget for Climate Application*, pages 58–86, 1986.

S. Ramaswamy, P. Tamayo, R. Rifkin, S. Mukherjee, C. Yeang, M. Angelo, C. Ladd, M. Reich, E. Latulippe, J. Mesirov, et al. Multiclass cancer diagnosis using tumor gene expression signatures. *Proceedings of the National Academy of Sciences*, 98(26):15149, 2001.

D. Reay. Comment microbes as climate engineers. *Microbiology Today*, 2002.

D. Reay. Tackling diffuse nitrate pollution:swapping eutrophication for climate change? . *Managing Rural Diffuse Pollution*, page 238, 2003.

D. Reay, K. Smith, and A. Edwards. Nitrous oxide emission from agricultural drainage waters. *Global Change Biology*, 9(2):195–203, 2003.

K. Regina, J. Silvola, and P. Martikainen. Short-term effects of changing water table on N2O fluxes from peat monoliths from natural and drained boreal peatlands. *Global Change Biology*, 5(2):183–189, 1999.

M. Repo, S. Susiluoto, S. Lind, S. Jokinen, V. Elsakov, C. Biasi, T. Virtanen, and P. Martikainen. Large N2O emissions from cryoturbated peat soil in tundra. *Nature Geoscience*, 2(3):189–192, 2009.

L. Ridolfi, P. Dodorico, A. Porporato, and I. Rodriguez-Iturbe. Stochastic soil moisture dynamics along a hillslope. *Journal of Hydrology*, 272(1-4):264–275, 2003a.

L. Ridolfi, P. Dodorico, A. Porporato, and I. Rodriguez-Iturbe. The influence of stochastic soil moisture dynamics on gaseous emissions of NO, N2O, and N2. *Hydrol. Sci. J*, 48 (5):781–798, 2003b.

F. Riley, G. Xu, N. Miller, and C. Oldenburg. A mechanistic treatment of the dominant soil nitrogen cycling processes: Model development, testing, and application. *Journal of geophysical research*, 113(G2), 2008.

W. Riley and P. Matson. NLOSS: a mechanistic model of denitrified N2O and N2 evolution from soil. *Soil Science*, 165(3):237, 2000.

G. Robertson and K. Gross. Assessing the heterogeneity of belowground resources: quantifying pattern and scale. *Exploitation of environmental heterogeneity by plants. Academic Press, New York*, pages 237–252, 1994.

L. Robertson and J. Kuenen. Combined heterotrophic nitrification and aerobic denitrification in Thiosphaera pantotropha and other bacteria. *Antonie van Leeuwenhoek*, 57 (3):139–152, 1990.

C. Rostagno. Infiltration and sediment production as affected by soil surface conditions in a shrubland of Patagonia, Argentina. *Journal of Range Management*, 42(5):382–385, 1989.

B. Runkle. *Plant Water Use and Growth in Response to Soil Salinity in Irrigated Agriculture*. PhD thesis.

R. Ruser, H. Flessa, R. Russow, G. Schmidt, F. Buegger, and J. Munch. Emission of N2O, N2 and CO2 from soil fertilized with nitrate: effect of compaction, soil moisture and reletting. *Soil Biology and Biochemistry*, 38(2):263–274, 2006.

D. Russo and A. Fiori. Equivalent vadose zone steady state flow: An assessment of its capability to predict transport in a realistic combined vadose zone–groundwater flow system. *Water Resources Research*, 44(9):W09436, 2008.

D. Russo, J. Zaidel, A. Fiori, and A. Laufer. Numerical analysis of flow and transport from a multiple-source system in a partially saturated heterogeneous soil under cropped conditions. *Water Resources Research*, 42(6):W06415, 2006.

D. Ryu and J. Famiglietti. Multi-scale spatial correlation and scaling behavior of surface soil moisture. *Geophysical Research Letters*, 33(8):L08404, 2006.

M. Saquet. Greenhouse gas flux and budget from an experimentally flooded wetland using stable isotopes and geochemistry. 2003.

J. Schimel. Playing scales in the methane cycle: From microbial ecology to the globe. *Proceedings of the National Academy of Sciences*, 101(34):12400, 2004.

J. Schimel, T. Balser, and M. Wallenstein. Microbial stress-response physiology and its implications for ecosystem function. *Ecology*, 88(6):1386–1394, 2007.

A. Schindlbacher, S. Zechmeister-Boltenstern, and K. Butterbach-Bahl. Effects of soil moisture and temperature on NO, NO2, and N2O emissions from European forest soils. *J. Geophys. Res*, 109, 2004.

A. Schramm, C. Santegoeds, H. Nielsen, H. Ploug, M. Wagner, M. Pribyl, J. Wanner, R. Amann, and D. de Beer. On the occurrence of anoxic microniches, denitrification, and sulfate reduction in aerated activated sludge. *Applied and Environmental Microbiology*, 65(9):4189, 1999.

J. Shrestha, J. Rich, J. Ehrenfeld, and P. Jaffe. Oxidation of Ammonium to Nitrite Under Iron-Reducing Conditions in Wetland Soils: Laboratory, Field Demonstrations, and Push-Pull Rate Determination. *Soil Science*, 174(3):156, 2009.

W. Silver, D. Herman, and M. Firestone. Dissimilatory nitrate reduction to ammonium in upland tropical forest soils. *Ecology*, 82(9):2410–2416, 2001.

W. Silver, A. Lugo, and M. Keller. Soil oxygen availability and biogeochemistry along rainfall and topographic gradients in upland wet tropical forest soils. *Biogeochemistry*, 44(3):301–328, 1999.

W. Silver, A. Thompson, A. Reich, J. Ewel, and M. Firestone. Nitrogen cycling in tropical plantation forests: potential controls on nitrogen retention. *Ecological Applications*, 15 (5):1604–1614, 2005.

J. Simunek, M. Sejna, and M. Van Genuchten. The HYDRUS-2D software package for simulating two-dimensional movement of water, heat, and multiple solutes in variably saturated media. Version 2.0. *US Salinity Laboratory, Riverside, CA*, 1999.

U. Skiba, L. Sheppard, C. Pitcairn, S. van Duk, and M. Rossall. The effect of N deposition on nitrous oxide and nitric oxide emissions from temperate forest soils. *Water, Air and Soil Pollution*, 116(1):89–98, 1999.

J. Skopp, M. Jawson, J. Doran, and A. USDA. Steady-state aerobic microbial activity as a function of soil water content. 1990.

K. Smith, T. Ball, F. Conen, K. Dobbie, J. Massheder, and A. Rey. Exchange of greenhouse gases between soil and atmosphere: interactions of soil physical factors and biological processes. *European Journal of Soil Science*, 54(4):779–791, 2003.

M. Soares, C. Braester, S. Belkin, and A. Abeliovich. Denitrificationin laboratory sand columns: carbon regime, gas accumulation and hydraulic properties. *Water research, Oxford*, 25(3):325–332, 1991.

P. Squillace, J. Scott, M. Moran, B. Nolan, and D. Kolpin. VOCs, pesticides, nitrate, and their mixtures in groundwater used for drinking water in the United States. *Environ. Sci. Technol*, 36(9):1923–1930, 2002.

J. Stark and M. Firestone. Mechanisms for soil moisture effects on activity of nitrifying bacteria. *Applied and Environmental Microbiology*, 61(1):218, 1995.

E. Stehfest and L. Bouwman. summarizing available measurement data and modeling of global annual emissions. *Nutrient Cycling in Agroecosystems*, 74:207–228, 2006.

R. Stevens, R. Laughlin, L. Burns, J. Arah, and R. Hood. Measuring the contributions of nitrification and denitrification to the flux of nitrous oxide from soil. *Soil Biology and Biochemistry*, 29(2):139–151, 1997.

K. Straub, M. Benz, B. Schink, and F. Widdel. Anaerobic, nitrate-dependent microbial oxidation of ferrous iron. *Applied and Environmental Microbiology*, 62(4):1458, 1996.

M. Sutton, W. Asman, and J. Schjorring. Dry deposition of reduced nitrogen. *Tellus B*, 46(4):255–273, 1994.

D. Sylvia, J. Fuhrmann, P. Hartel, and D. Zuberer. *Principles and applications of soil microbiology*. Prentice Hall, New Yersey, 1998.

Y. Teh and W. Silver. Effects of soil structure destruction on methane production and carbon partitioning between methanogenic pathways in tropical rain forest soils. *Multi-Campus: Retrieved from: http://www. escholarship. org/uc/item/0zf3z7nw*, 2006.

Y. Teh, W. Silver, O. Sonnentag, M. Detto, N. Kelly, and D. Baldocchi. Large greenhouse gas emissions from agricultural peatlands driven by management. *In review*, 2010.

P. Templer, W. Silver, J. Pett-Ridge, K. M. DeAngelis, and M. Firestone. Plant and microbial controls on nitrogen retention and loss in a Humid Tropical Forest. *Ecology*, 89(11):3030–3040, 2008.

R. Terry, R. TATE III, and J. Duxbury. The effect of flooding on nitrous oxide emissions from an organic soil. *Soil Science*, 132(3):228, 1981.

M. Thullner, L. Mauclaire, M. Schroth, W. Kinzelbach, and J. Zeyer. Interaction between water flow and spatial distribution of microbial growth in a two-dimensional flow field in saturated porous media. *Journal of contaminant hydrology*, 58(3-4):169–189, 2002.

M. Thullner, P. Van Cappellen, and P. Regnier. Modeling the impact of microbial activity on redox dynamics in porous media. *Geochimica et Cosmochimica Acta*, 69(21):5005–5019, 2005.

J. Tiedje. Ecology of denitrification and dissimilatory nitrate reduction to ammonium. *Biology of anaerobic microorganisms*, 179:244, 1988.

J. Tiedje, A. Sexstone, T. Parkin, and N. Revsbech. Anaerobic processes in soil. *Plant and Soil*, 76(1):197–212, 1984.

S. van Dijk and F. Meixner. Production and Consumption of NO in Forest and Pasture Soils from the Amazon Basin. *Water, Air and Soil Pollution: Focus*, 1(5):119–130, 2001.

J. Van Loon. *Analytical atomic absorption spectroscopy: selected methods.* Academic Press, 1980.

R. Vargas and T. Hattori. Protozoan predation of bacterial cells in soil aggregates. *FEMS Microbiology Letters*, 38(4):233–242, 1986.

R. Venterea and D. Rolston. Nitric and nitrous oxide emissions following fertilizer application to agricultural soil: Biotic and abiotic mechanisms and kinetics. *Journal of Geophysical Research,Atmospheres*, 105(D12):15117–15129, 2000.

R. Venterea and A. USDA. Nitrite-driven nitrous oxide production under aerobic soil conditions: kinetics and biochemical controls. 2007.

H. Vereecken, R. Kasteel, J. Vanderborght, and T. Harter. Upscaling hydraulic properties and soil water flow processes in heterogeneous soils: A review. *Vadose Zone Journal*, 6 (1):1, 2007.

J. Verhoeven. Nutrient dynamics in minerotrophic peat mires. *Aquatic Botany*, 25(2), 1986.

K. Von Arnold, M. Nilsson, B. Haanell, P. Weslien, and L. Klemedtsson. Fluxes of CO2, CH4 and N2O from drained organic soils in deciduous forests. *Soil Biology and Biochemistry*, 37(6):1059–1071, 2005.

L. Wang, P. DOdorico, S. Manzoni, A. Porporato, and S. Macko. Soil carbon and nitrogen dynamics in southern African savannas: the effect of vegetation-induced patch-scale heterogeneities and large scale rainfall gradients. *Climatic Change*, 94(1):63–76, 2009.

C. Werner, K. Butterbach-Bahl, E. Haas, T. Hickler, and R. Kiese. A global inventory of N2O emissions from tropical rainforest soils using a detailed biogeochemical model. *Global Biogeochemical Cycles*, 21(3), 2007.

S. Whalen. Biogeochemistry of methane exchange between natural wetlands and the atmosphere. *Environmental Engineering Science*, 22(1):73–94, 2005.

L. Whendee, W. Yang, and K. Weber. Feammox: A novel pathway for ammonium oxidation and nitrogen loss from terrestrial ecosystems. In *The 94th ESA Annual Meeting*, 2009.

N. Wrage, D. Kool, O. Oenema, and J. Van Groenigen. Nitrifier Denitrification: What We Know, Don't Know and Thought We Knew. 2007.

N. Wrage, G. Velthof, M. Van Beusichem, and O. Oenema. Role of nitrifier denitrification in the production of nitrous oxide. *Soil Biology and Biochemistry*, 33(12-13):1723–1732, 2001.

R. Yarwood, M. Rockhold, M. Niemet, J. Selker, and P. Bottomley. Impact of microbial growth on water flow and solute transport in unsaturated porous media. *Water Resources Research*, 42(10):10405, 2006.

T. Zejun, L. Tingwu, Z. Qingwen, and Z. Jun. The sealing process and crust formation at soil surface under the impacts of raindrops and polyacrylamide. In *Proc. 12th Conf. ISCO, May*, pages 26–31, 2002.

T. Zimenko and A. Misnik. Effect of ground-water level on ammonification and nitrification in peat bog soils. *Microbiology*, 39:446–449, 1970.